Fall 1-31-1994

Aqueous absorption of nitrogen oxides induced by oxychlorine compounds : a process development study for flue gas treatment

Chen-Lu Yang
New Jersey Institute of Technology

Copyright Warning & Restrictions

The copyright law of the United States (Title 17, United States Code) governs the making of photocopies or other reproductions of copyrighted material.

Under certain conditions specified in the law, libraries and archives are authorized to furnish a photocopy or other reproduction. One of these specified conditions is that the photocopy or reproduction is not to be "used for any purpose other than private study, scholarship, or research." If a, user makes a request for, or later uses, a photocopy or reproduction for purposes in excess of "fair use" that user may be liable for copyright infringement,

This institution reserves the right to refuse to accept a copying order if, in its judgment, fulfillment of the order would involve violation of copyright law.

Please Note: The author retains the copyright while the New Jersey Institute of Technology reserves the right to distribute this thesis or dissertation

Printing note: If you do not wish to print this page, then select "Pages from: first page # to: last page #" on the print dialog screen

ABSTRACT

AQUEOUS ABSORPTION OF NITROGEN OXIDES INDUCED BY OXYCHLORINE COMPOUNDS: A PROCESS DEVELOPMENT STUDY FOR FLUE GAS TREATMENT

by
Chen-Lu Yang

The use of chlorine (Cl_2), sodium hypochlorite (NaClO), and sodium chlorite ($NaClO_2$) as oxidizing agents to promote the absorption of nitric oxide (NO) from gas streams has been investigated in the Gas Scrubbing Laboratory of New Jersey Institute of Technology since 1988. The first step of this project had been to screen out the best scrubbing medium for nitric oxide removal from flue gases. The most successful oxidizing agent was found to be sodium chlorite in acidic aqueous solution. The screening results have been accepted for publication in Chemical Engineering Communications. A sodium chlorite containing aqueous acid solution quantitatively absorbs nitric oxide in a 5.1 cm in diameter by 61 cm long bubble column scrubber. Under the same conditions, 90% removal were achieved with either chlorine gas or sodium hypochlorite aqueous scrubbing.

An analytical instrument train, consisting of a Thermoelectron model 10A NO_x analyzer, Beckman model 715 process oxygen monitor, and Rosemount model 890 UV SO_2 analyzer, was set up to measure the concentration changes of inlet and outlet flue gas components. A preparatory liquid chromatography equipped with UV/Visible range photodiode array detector was set up for scrubbing solution real time monitoring of oxychlorinated compounds. Chlorine dioxide was found to be the active ingredient in the sodium chlorite aqueous scrubbing, while hypochlorous acid was the key oxidant for both chlorine and sodium hypochlorite scrubbing processes. During the operation, nitric oxide

was oxidized to nitrate ion and sulfur dioxide to sulfate ion and were collected in the scrubbing solutions. At the same time, oxychlorine compounds were reduced to chloride ion, which was analyzed by ion chromatography.

To obtain the reaction rate of nitric oxide with sodium chlorite aqueous solution for process design consideration, a droplet surface reaction model was derived to correlate experimental data from spray tower scrubber. The model predicted conversion of NO very well but not absorption because the model does not predict breakthrough of nitrogen dioxide (NO_2). Therefore, a model of absorption with chemical reaction was used to study the absorption of NO in a packed bed scrubber to determine the feasibility of controlling all air pollutants in one scrubber. In the model, theoretical height of transfer unit (HTU) was used to evaluate the efficiency of scrubbing solutions. The influence of different variables such as temperature, pH, gas stream flow rate, concentration of sodium chlorite, and other components in the flue gas on height of transfer unit was evaluated.

AQUEOUS ABSORPTION OF NITROGEN OXIDES INDUCED BY OXYCHLORINE COMPOUNDS: A PROCESS DEVELOPMENT STUDY FOR FLUE GAS TREATMENT

by
Chen-Lu Yang

A Dissertation
Submitted to the Faculty of
New Jersey Institute of Technology
in Partial Fulfillment of the Requirements for the Degree of
Doctor of Philosophy

Department of Chemical Engineering,
Chemistry and Environmental Science

January 1994

APPROVAL PAGE

AQUEOUS ABSORPTION OF NITROGEN OXIDES INDUCED BY OXYCHLORINE COMPOUNDS - A PROCESS DEVELOPMENT STUDY FOR FLUE GAS TREATMENT

Chen-Lu Yang

Dr. Henry Shaw, Thesis Advisor — date
Professor of Chemical Engineering, NJIT

Dr. Edward C. Roche, Jr., Committee Member — date
Professor of Chemical Engineering, NJIT

Dr. Howard D. Perlmutter, Committee Member — date
Professor of Chemistry, NJIT

Dr. Barbara B. Kebbekus, Committee Member — date
Professor of Chemistry and Acting Chairperson
of the Department of Chemical Engineering,
Chemistry, and Environmental Science, NJIT

Dr. Norman Sweed, Committee Member — date
Exxon Research and Engineering Co.

BIOGRAPHICAL SKETCH

Author: Chen-Lu Yang

Degree: Doctor of Philosophy in Chemical Engineering

Date: January 1994

Undergraduate and Graduate Education:

- Doctor of Philosophy in Chemical Engineering,
  New Jersey Institute of Technology, Newark, NJ, 1994
- Master of Science in Environmental Science,
  New Jersey Institute of Technology, Newark, NJ, 1990
- Bachelor of Engineering in Chemical Engineering,
  Feng-Chia University, Taichung, Taiwan, 1984

Major: Chemical Engineering

Honors: Alan Goldstein Memorial Award for Outstanding Research, January 1990

Publications and Presentations:

Yang, Chen-Lu, Henry Shaw, and Howard D. Perlmutter, "Absorption of NO Promoted by Strong Oxidizing Agents: Inorganic Oxychlorides in Nitric Acid," accepted for publication by *Chemical Engineering Communications* (1993).

Yang, Chen-Lu, Gwen. C. San Agustin and Henry Shaw, "On-line Ultraviolet Measurement of Dissolved Oxychlorine Compounds and Ions Using a Photodiode Array Detector," Submitted to *Environmental Science and Technology*.

Li, Maosheng, Henry Shaw, Chen-Lu Yang, and Gwen C. San Agustin, "Investigation of Kinetics of HCl Reaction with CaO by FT-IR," Fourth Annual Mini-Tech Student Conference, sponsored by the American Institute of Chemical Engineers (North Jersey Section) and the Society for the Advancement of Materials and Process Engineering (NJ Chapter), Stevens Institute of Technology, Hoboken, NJ, April 16, 1993. (To be submitted to *Environmental Science and Technology* for publication).

Yang, Chen-Lu, Howard D. Perlmutter and Henry Shaw, "Absorption of NO_X Induced by Strong Oxidants," Proceedings of the 1992 International Conference on Hazardous Waste Management: Technology, Perception and Reality, Diplomat Hotel, Atlantic City, NJ, May 5-7, 1992.

Yang, C. L., H. Shaw, and J. J. Weir, "Aqueous Absorption of NO_X Promoted by Strong Oxidizing Agents," Symposium of Offgas from Municipal Waste Incineration, 1991 AIChE Summer National Meeting, Pittsburgh, PA, Paper No. 22nd, August 18-21, 1991.

Shaw, H., and Chen-Lu Yang, "Alkaline Absorption of NO_X Induced by Sodium Chlorite Oxidation," American Flame Research Committee, Spring Members Only Meeting on NO_X Control, Developments and Commercial Applications, in Hartford, CN on March 18-19, 1991.

Shaw, H., Chen-Lu Yang, and Chun-Chiao Chuo, "Alkaline Absorption of NO_X Induced by Sodium Chlorite Oxidation," First Hazardous Waste Treatment and Prevention Technologies Conference (Thermal Treatment/Destruction), Niagara Falls, NY, October 9-10, 1990.

Shaw, H., and Chen-Lu Yang, "Alkaline Absorption of NO_X Induced by Sodium Chlorite Oxidation," Civil Engineering Department Seminar Series of the Technion-Israel Institute of Technology, Haifa, 32000 Israel, June 11, 1990.

This dissertation is dedicated to
my parents

TABLE OF CONTENTS

TABLE OF CONTENTS
(Continued)

TABLE OF CONTENTS
(Continued)

LIST OF TABLES

LIST OF FIGURES

LIST OF FIGURES
(Continued)

Figure **Page**

LIST OF FIGURES
(Continued)

Figure **Page**

LIST OF FIGURES
(Continued)

LIST OF FIGURES
(Continued)

Figure **Page**

LIST OF FIGURES
(Continued)

Fugure **Page**

CHAPTER 1

AN OVERVIEW OF NO_X CONTROL

1.1 Introduction

Every industrial process is developed to perform a specific purpose through a succession of treatment steps. Typically, a process development can be divided into the unit process development and equipment design. Design of equipment for the physical treatment steps is studied in unit operation while the chemical treatment step of a process are concerned in reaction kinetics and reactor design. Both physical and chemical treatments are based on chemical reactions and mechanisms from the unit process study [Levenspiel, 1972]. The purpose of this research is to develop an economically competitive scrubbing for nitrogen oxides (NO_X) emission control.

The nitrogen oxides found in nature are N_2O, NO, NO_2, N_2O_3, N_2O_4, and N_2O_5. Among these nitrogen oxides, NO (nitric oxide) and NO_2 (nitrogen dioxide) are the two most important air pollutants because they are emitted in large quantities from high temperature air oxidation processes. The term NO_X is a short hand method to refer to all of the nitrogen oxides, but in air pollution work NO_X generally refers only to NO and NO_2. NO_X are emitted in the United States at a rate of about 20 million metric tons per year, about 40% of which is emitted from mobile sources. Among the other 12 million tons of NO_X that are emitted from stationary sources, about 30% is the result of fuel combustion of large industrial furnaces and 70% is from electric utility furnaces. Figure 1.1 shows the contributions of the major anthropogenic NO_X sources in the United States [US. EPA., 1982].

Successful control of NO_X emissions depends on understanding their formation and physical and chemical properties. A thorough review of the literature is presented in Chapters 1 and 2 of this thesis. It should be noted that NO_X control is a very active

research field, and detail mechanisms of NO_X formation and removal are still not well understood. NO_X has been the most difficult and expensive pollutant to control. Hopefully, the result present here will serve as one of the better alternatives for control of NO_X emissions.

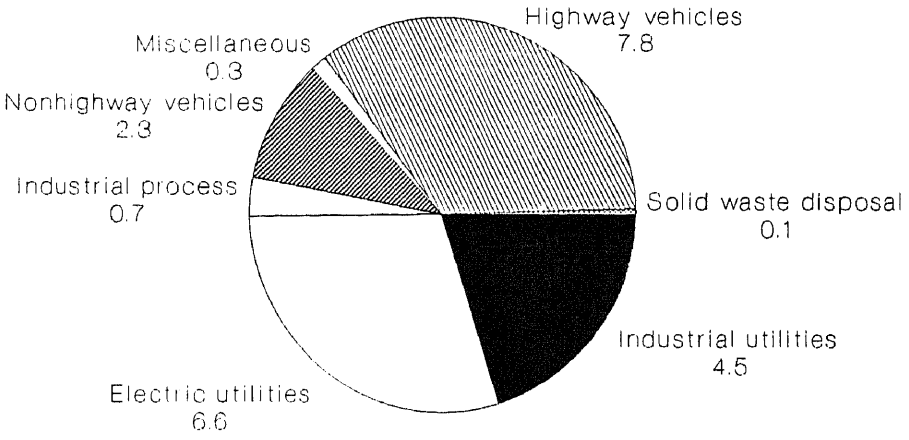

Figure 1.1 The anthropogenic sources of NO_X emission

Table 1.1 Sources of Nitrogen Oxides

Source	Nature of Source	Emissions (10^{12}g(N)/yr) US.	Global
Fossil fuel combustion	A	6.0	21
Biomass burning	A	0.1	12
Lightning	N	0.3	8
Biogenic production	N	0.3	8
From stratosphere	N	0.03	0.03
Total		6.8	50

A-anthropogenic; N-nature.
Global numbers are probably uncertain to 50%.

1.2 NO_X Sources

Nitrogen oxides are emitted primarily as nitric oxide (NO) from a variety of sources. The estimated emissions of NO_X have large uncertainties associated with them. Table 1.1 shows that 70% to 90% of NO_X emissions are from anthropogenic sources, which are contributed by fossil fuel combustion and biomass burning. The other 10% to 30% NO_X emissions are the result of natural sources consisting of lightning, microbial activity in soil and diffusion from the stratosphere [Singh, 1987].

1.2.1 Fossil Fuel Combustion and Biomass Burning

More than 95% of NO_X emitted from stationary sources is NO. Nitric oxide is formed in combustion due to high temperature air fixation (thermal NO_X) and nitrogen oxidation (fuel NO_X) [US. EPA., 1983]. Thermal NO_X formation is the process which NO is formed by the reaction of nitrogen with oxygen in the air used for combustion. The reaction rate of thermal NO_X formation is extremely temperature sensitive, and becomes important at flame temperature on the order of 1650 to 2000 ^{o}C (3000-3600 ^{o}F). Fuel NO_X results from the combustion of fuels that contain organic nitrogen. Fuel NO_X formation is dependent on local combustion conditions, oxygen concentration and mixing patterns, and the nitrogen content of the fuel or the biomass. There is another source of NO_X which is called "prompt NO_X" and is attributed to very fast reactions between atmosphere nitrogen, oxygen, and fuel. It is observed in kinetic studies where even at zero time the quantity of NO_X is greater than zero [Fennimore, 1971].

Thermal NO_X

Both thermodynamic (equilibrium) and kinetic (rate) information are important in the understanding of NO_X formation. The oxidation of N_2 by the O_2 in combustion air occurs primarily through the two reactions known as the Zeldovich mechanism 1946.

$$N_2 + O \rightarrow NO + N \qquad (1.1)$$

$$N + O_2 \rightarrow NO + O \quad (1.2)$$

The first reaction has a relative high activation energy, due to the need to break the strong N_2 bond. Because of the high activation energy, the first reaction is the rate limiting step for NO production and is highly temperature sensitive. Nitric oxide formed via this route is referred to as thermal NO_x. Reactions 1.1 and 1.2 are supplemented by the reaction in fossil fuel combustion systems.

$$N + OH \Leftrightarrow NO + H \quad (1.3)$$

In presenting Reactions 1.1-1.3, Assumptions can be made that the fuel combustion have reached equilibrium and the concentration of O, H, and OH can be described by equilibrium equations.

Considering only the thermodynamics of NO_x formation, the stoichiometric relationships are

$$N_2 + O_2 \Leftrightarrow 2\,NO \quad (1.4)$$

$$NO + 1/2\,O_2 \Leftrightarrow NO_2 \quad (1.5)$$

The equilibrium constants for Reactions 1.4 and 1.5 are

$$K_{p1} = \frac{Y_{NO}^2}{Y_{N_2} Y_{O_2}} \quad (1.6)$$

and

$$K_{p2} = \frac{P_T^{-1/2} Y_{NO_2}}{Y_{NO} Y_{O_2}^{1/2}} \quad (1.7)$$

Where,

K_p = equilibrium constant

Y_i = mole fraction of component i

P_T = total pressure, atm

Table 1.2 presents data for the equilibrium constants K_{p1} and K_{p2} for various temperatures at atmospheric pressure [JANAF., 1965].

Considering the Zeldovich mechanism and equilibrium constants in Table 1.2, equilibrium concentrations of NO and NO_2 at various temperatures in heated air and flue gas are calculated in Table 1.3 with the assumptions of 76% N_2 and 3.3% O_2 in the furnaces.

Table 1.2 Equilibrium Constants for the Formation of Nitric Oxide and Nitrogen Dioxide

Temperature		K_p	
^oK	^oF	K_{p1}	K_{p2}
300	80	10^{-30}	10^6
1000	1340	$7.5(10)^{-9}$	$1.2(10)^2$
1500	2240	$1.1(10)^{-5}$	$1.1(10)^{-2}$
2000	3140	$4.0(10)^{-4}$	$3.5(10)^{-3}$

[JANAF, 1965]

Table 1.3 Calculated Equilibrium Concentration (in ppm) of Nitric Oxide and Nitrogen Dioxide in Air and Flue Gas

Temperature		Air		Flue gas	
^oK	^oF	NO	NO_2	NO	NO_2
300	80	3.4(10)-4	2.1(10)-4	1.1(10)-10	3.3(10)-5
800	980	2.3	0.7	0.8	0.1
1400	2060	800	5.6	250	0.9
1873	2912	6100	12	2000	1.8

[US. EPA, 1970]

A review of Tables 1.2 and 1.3 leads to the conclusions that at flame zone temperatures, equilibrium concentrations of NO_x are 6,000 to 10,000 ppm, and the ratios of NO:NO_2 range from 500:1 to 1000:1, and at flue gas exiting temperatures, on the order of 150 to 320 ^oC (300 to 600 ^oF), equilibrium concentrations of NO_x are less than 1 ppm, and NO:NO_2 range from 1:10000 to 1:10. In actual furnaces, neither of the two cases is observed. Typical flue gas NO_x concentrations exiting from large coal-fire power

plants range from 300 to 1200 ppm, and the ratios of NO/NO_2 range from 10:1 to 20:1. Factors other than equilibrium must be considered to explain such behavior.

The rate of NO formation is the other major factor influencing the actual NO_x concentrations. Reaction 1.1 has an activation energy of 317 kJ/mole, and is the rate-controlling reaction [EPA., 1983]. Also, Reaction 1.3 is more important in fuel-rich flames and less so in lean or stoichiometric flames. Consideration of reactions 1.1 and 1.2 only, with the assumption that O and N atoms in the post-flame zone are at steady state concentrations, can lead to the development of a rate expression for NO formation [Fenimore, 1971]. The theoretical formation rate is a strong function of the temperature, as well as of nitrogen and oxygen concentration.

Experimental studies of heated mixtures of N_2, O_2, and Ar as well as air showed that below 1600 ^oC, concentrations of NO were less than 200 ppm. Above 1800 ^oC, concentrations of several thousand ppm NO were formed, and at 1950 ^oC, concentrations of NO could be as high as 12,000-13,000 ppm. A peak NO concentration was observed at 1990 ±26 ^oC. Above 2038 ^oC, the net formation of NO decreases. NO concentrations increased rapidly with time up to about 4 to 5 seconds, after which no further increases were observed. A global model was proposed to predict of NO as a function of temperature, nitrogen and oxygen concentrations, and time [Mackinnon, 1974]. At 1 atm, the model is

$$C_{NO} = 5.2(10)^{17} \exp[-72{,}300/T] Y_{N_2} Y_{O_2}^{0.5} t \qquad (1.8)$$

where,

C_{NO} = NO concentration, ppm

Y_i = mole fraction of component i

T = absolute temperature, ^oK

t = time, s

In actual flame system, the presence of H, C, OH, S, and other atoms and radicals can significant affect the NO formation rate. Typically, gases only stay in the flame zone for 0.5 second or less. Although actual concentrations do not reach equilibrium concentrations, an appreciable amount of NO_X is formed owing to the very rapid rates of the reactions. When the gases leave the flame zone, the concentration of NO and NO_2 freeze at the high levels.

Consideration of Equation 1.8 can provide some insight into the strategies for thermal NO_X control. Thus, to minimize NO_X, one needs to reduce the peak temperature, resident time, and oxygen concentration.

Fuel NO_X

When a fuel contains organically bound nitrogen, the contribution of the fuel-bound nitrogen to the total NO_X production is significant. The N-C bond is considerably weaker than N-N bound in molecular nitrogen, so the fuel can be oxidized to NO in the combustion. Both laboratory [Pershing, 1975] and full-scale experiment [Thompson, 1976] have shown that fuel-bound nitrogen can account for over 50% of the total NO_X. Roughly, over 90% of fuel-bound nitrogen can be converted to NO_X. The kinetic mechanisms of fuel nitrogen oxidation are currently an area of active research.

The nitrogen content of most US. coals ranges from 0.5% to 2%, whereas that of residual fuels ranges from 0.1% to 0.5%. Conversion efficiencies of fuel nitrogen to NO_X for coals and residual fuel oils have been observed between 10% to over 90% [Pohl and Sarofim, 1976, EPA., 1983].

Regardless of the detailed mechanisms, several general statements can be made for fuel nitrogen oxidation to NO. First, it is highly dependent on the air:fuel ratio. The air:fuel ratio primarily affects the oxidation of the R-N fraction, where R represents an organic fragment, rather than the nitrogen remaining in the char. Also, more R-N is converted to NO_X at low concentrations of fuel bound N than at high concentration. The

degree of fuel-air mixing also strongly affects the percent conversion of fuel nitrogen to NO, with greater mixing resulting in greater percent conversion.

Temperature changes do not affect production of NO_x from fuel nitrogen [Pershing, 1976]. This behavior is consistent with oxidizing R-N component in fuel which occur with relatively low activation energies.

1.2.2 Atmospheric Lightning

One of the most important natural sources of NO_x is atmospheric lightning. The temperature of a column of air exposed to atmospheric lightning is a function of the energy deposited by lightning. For a typical energy deposition of about 10^5 J/m, the column of air immediately surrounding the lightning is heated to temperatures on the order of 30,000 ^oC. At temperatures above 2000 ^oC, NO is in thermodynamic equilibrium with N_2 and O_2. As the temperature of the heated air parcel drops below 1700 ^oC, NO freezes out as a stable compound.

The total global production of NO due to atmospheric lightning is the product of two terms: (1) the yield or production of NO per energy input of lightning and (2) the total energy deposited by lightning or lightning flash frequency. Atmospheric chemistry experiments have been performed in the Langley Lightning Facility to identify and quantify the yield of trace compounds, including NO, N_2O, and CO. These research results were summarized in Table 1.4.

Inspection of this table indicates that theoretically calculated and experimentally determined values for the NO_x yield vary by a factor of ten from 2 to $17(10)^{16}$ NO_x molecule/J with a mean NO_x yield of about $6.5(10)^{16}$ molecule/J. On the other hand, the assumed values for the total energy deposited by lightning vary by two orders of magnitude from 10^{-9} to 10^{-7} J/cm^{2}s. Since the global production of NO_x is equal to the product of the NO_x yield and the total energy deposited by lightning, the latter term leads

to a large uncertainty in the determination of the global production of NO_x by lightning [Levine, 1984].

Table 1.4 Production of Nitric Oxides by Lightning

Researcher	NO_x/energy 10^{16}molc/J	NO_x/stroke 10^{25}molc/stk	Total energy J/cm^{2}s or Flash req.	Global MT(N)/yr
1. Atmospheric Measurement:				
Noxon		10-20 /stk	100 fl/ s	7
Drapcho		40 /fl	100 fl/s	30
2. Theoretical Calculation:				
Tuck		1.1 /stk	6(10)-8; 500 stk/s	4
Griffing		12-20 /fl	100 fl/s	8.8-14.7
Chameides	3-7		1.6(10)-7	30-40
Chameides	8-17		1.6(10)-7	35-90
Hill		6 /fl	(10)-9; 100 fl/s	4.5
3. Laboratory Experiments:				
Chameides	6, 8		1.6(10)-7	30-40
Levine	5		(10)-8-(10)-7	1.8-18
Peyrous	1.6-2.6		1.57(10)-7	9.25-15.5

Molc. indicates molecule, stk; stroke, fl; flash.
[Levine, 1984]

1.2.3 Biogenic Production: Other Major Natural Source of NO_x

In the early history of the Earth, oxygen was produced by photosynthetic organisms. Today, biogenic activity is a major source of several atmospheric gases. Recent field flux measurements by Galbally (1978) and laboratory experiments by Anderson (1983) indicate that soil microorganisms may also produce appreciable amounts of NO.

Two common bacteria, Nitrosomonas europaea (a nitrifier) and Alcaligenes faecalis (a denitrifier), were used to study the biogenic production of NO_x in soils. Nitrification is an aerobic process in which ammonium (NH_4^+) is oxidized to nitrite and nitrate. NO and N_2O are direct or indirect intermediates of this pathway. Denitrification is an anaerobic process in which nitrate is reduced to nitrite and eventually ammonia or nitrogen, with NO

and N_2O as intermediates. About 5 MT(N)/yr of N_2O was measured in the nitrification study. Using the measured ratio of 2 for NO to N_2O production at low oxygen levels, and 5 MT(N)/yr of N_2O produced by denitrification, a 10 MT(N)/yr of NO production was estimated. This estimate assumes that all NO produced by nitrifying bacteria is released to the atmosphere and not utilized by the biosphere.

1.3 Environmental Impacts of NO_X Emission

NO_X, once emitted to the atmosphere, becomes oxidized to nitrate through both gas and aqueous phase processes. In 1.5 days life time, it is transferred more than 1500 kilometers and removed by reaction with OH, dry deposition, or wet deposition. The phenomena of acid deposition appears to have been discovered as early as 1853 by Robert A. Smith. Little attention was paid until a Swedish soil scientist, Svante Odin, who defined the source and sink of the acidity of surface waters and soil in 1961. Since then, the true scope of the problem was appreciated in Europe. It was not until 1970s, both Canada and United States instituted their long-term programs for the chemical analysis of acid precipitation [Cowling, 1982]. Current studies categorized the environmental impacts of NO_X emission in four major fields, acid deposition, photochemical smog, ozone depletion in the stratosphere, and ozone formation in the troposphere.

1.3.1 Acid Deposition

Absolutely neutral precipitation would have a pH of 7. Even precipitation in areas totally free of local anthropogenic emissions, is presumed to be in equilibrium with atmospheric trace constituents at their background levels. Recognizing this, the natural acidity of rainwater is often taken to be at a pH of 5.6, which is that of pure water in equilibrium with the global atmospheric concentration of CO_2, 350 ppm, and this pH value has been used as the demarcation line for acidic precipitation. However, carbon dioxide is not the only background trace constituent of the atmosphere capable of influencing the pH of

rainwater. Charlson and Rodhe (1982) have shown that, in the absence of common basic compounds such as NH_3 and $CaCO_3$, rainwater pH values due to nature sulfur compounds alone could be expected to be about 5.0. Galloway et. al., (1982) have reported precipitation chemistry data from remote areas of the globe and have found background pH values of 5.0 or greater, with the relative contributions of H_2SO_4, HNO_3, and other acids HX (in which X is assumed to be a halogen atom F, Cl, Br, I.) to the acidity of the precipitation varying from site to site. Therefore, the conclusion is that rain of pH greater than 5.6 has not been influenced by man, or if it has, it has sufficient buffering capacity so that acidification does not occur. Rain with pH between 5.0 and 5.6 may have been influenced by man but not to an extent exceeding that of natural background sulfur species. If the pH of rain is less than 5.0, it is a given that man-made influences are present.

Table 1.5 Chemical Analysis of Acid Rain

Species	Concentration (μeq/L) Sjoangen Sweden 1973-1975	Hubbard Brook New Hampshire 1973-1974	Pasadena California 1978-1979
SO_4^{2-}	69	110	39
NO_3^-	31	50	31
Cl^-	18	12	28
NH_4^+	31	22	21
Na^+	15	6	24
K^+	3	2	2
Ca^{2+}	13	10	7
Mg^{2+}	7	32	7
H^+	2	114	39
pH	4.30	3.94	4.41

[Seinfeld, 1986]

Table 1.5 gives concentrations of constituent in rain at three locations where acid rain has been reported. It can often assumed that the predominant ions in acid rain are H^+, NH_4^+, Ca^{2+}, and SO_4^{2-} and NO_3^- [Gorham, 1984].

There are three major pathways, shown in Figure 1.2, by which nitrate can be incorporated into precipitation: (1) nucleation scavenging of nitrate-containing aerosols in cloud formation; (2) absorption of gaseous nitric acid by cloud droplets; and (3) below-cloud scavenging of nitrate-containing aerosols by rain. Note that aqueous phase formation of nitrate from absorbed NO and NO_2 was found to be too slow to be of atmospheric importance.

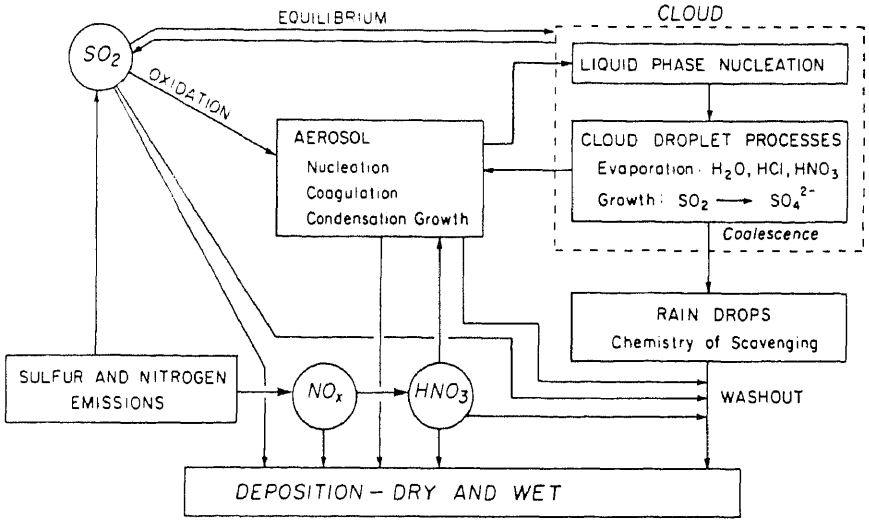

Figure 1.2 Atmospheric paths leading to acid deposition

The chemical reaction that converts NO_X to nitrate are central to the atmospheric processes that determine the relationship between the precursors and acidic deposition of nitrate. The reaction primarily responsible for the conversion in the gas phase involves the OH radical [Seinfeld, 1986],

$$NO_2 + OH \rightarrow HNO_3 \qquad (1.9)$$

Once the gaseous nitric acid is formed, rain drop washout becomes dominant in the acid deposition processes.

Acid deposition is a worldwide problem. Reports of high acid rain damage have come from Canada, England, Germany, France, Scandinavia, and the United States. Acid precipitation can cause damage in several different ways. Buildings and monuments are often made from materials that contain limestone, calcium carbonate. Nitric acid, one of the major components of acid rain, converts limestone to calcium nitrate, which is soluble and eroded over many years of contact with acid rain. Metal surfaces can also be attacked by acid rain [Enger, 1991].

The effects of acid rain on ecosystems are often more difficult to quantify. In many parts of the world, acid rain is suspected of causing the death of some forests and reducing the vigor and rate of growth of others. In Central Europe, many forests have declined significantly, resulting in the devastation of about 6 million hectares of trees. Northeastern North America has also seen significant tree death and reduction in vigor of tree growth, particularly at higher elevations. Some areas have experienced 50% mortality of red spruce trees [Johnson, 1986], a particularly susceptible tree.

The effects of acid rain on aquatic ecosystems are much more clear cut. Experiments shows that, as lakes become more acidic, there is a progressive loss of many kinds of organisms. The food web becomes less complicated, many organisms fail to reproduce, and many others die. At a pH of 5.5, many desirable species of fish have been eliminated; at a pH of 5, only a few starving fish may be found, and none are reproducing. Lakes with a pH of 4.5 are nearly sterile [Haines, 1986]. Various attempts have been made to assess changes in the acidity of surface waters that may have occurred over past 50 years. Results show that the extent to which lakes have been acidified is very large. About 14,000 lakes in Canada and 11,000 in the United States have been seriously altered by becoming acidic [Kramer, 1986]. However, it is not clear whether the acidity is due to acid precipitation or decay of organic matter producing organic acids.

1.3.2 Photochemical Smog

Secondary air pollutants are compounds that result from the interaction of various primary air pollutants with one another. Photochemical smog is a mixture of pollutants resulting from the interaction of NO_x with non-methane organic compounds (NMOC) in the presence of ultraviolet light. The two most destructive kinds of materials formed are ozone and peroxyacetylnitrates (PAN). Both compounds are excellent oxidizing agents, which means that they react readily with many other compounds, including those found in living things, causing destructive changes. Ozone is particularly harmful because it destroys chlorophyll and injures lung tissue. PAN, in addition to being oxidizing agents, are eye irritants.

A typical smog incident involves a serious events. As shown in Equations 1.10 and 1.11, when NO_x is present, ozone formation occurs as a result of the solar photolysis of NO_2,

$$NO_2 + h\nu \xrightarrow{\Phi I_a} NO + O \qquad (1.10)$$

$$O + O_2 + M \xrightarrow{k_2} O_3 + M \qquad (1.11)$$

Where,

Φ = quantum yield

I_a = absorbed radiation (photons/cm^2-s)

and, current studies show no other significant primary sources of ozone other than Reaction 1.11. Ozone, once formed, reacts rapidly with NO to regenerate NO_2, according to Reaction 1.12.

$$O_3 + NO \xrightarrow{k_3} NO_2 + O_2 \qquad (1.12)$$

In the absence of other compounds, a steady state is achieved in which the ozone concentration is given by the photostationary state relation

$$[O_3] = \frac{\Phi I_a [NO_2]}{k_3 [NO]} \tag{1.13}$$

The key to understanding the chemistry of NO_x in a organic containing atmosphere is the history of alkyl and acyl radicals in chain propagation reactions, which can be depicted as

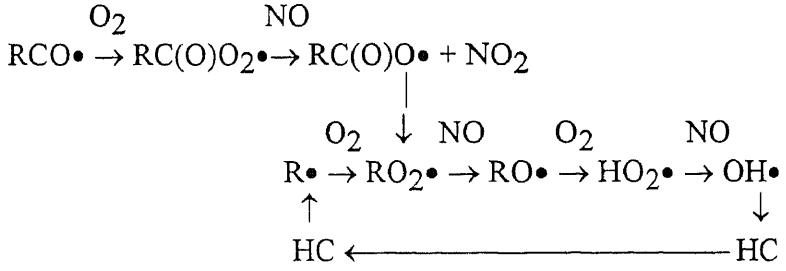

The chemistry of photochemical smog then can be summarized in a general way as follows. The major observed phenomena in the system are conversion of NO to NO_2, formation of a variety of nitrogen-containing compounds, such as nitric acid and peroxyacyl nitrates, and accumulation of O_3. NO_2 serve both as initiator and terminator of chain reactions that result in conversion of NO to NO_2 and build up O_3. Termination of the chain reactions leads to nitric acid and organic nitrates [Seinfeld, 1986].

1.3.3 Ozone Depletion

The most important trace constituent of the stratosphere is ozone. Although present only in a few ppm, ozone is responsible for shielding the earth from ultraviolet radiation that is harmful to life. Beside that, it also converts solar energy into heat, particularly in the upper stratosphere and produces the temperature inversion characteristic of that region.

In the 1970s, various sectors of the scientific community become concerned about the possible reduction of the ozone layer surrounding the earth in the upper atmosphere. In 1985, it was discovered that a significant thinning of the ozone layer over Antarctica occurred during the Southern Hemisphere spring. In some regions, the ozone layer

showed as much as 95% depletion. Ozone depletion also has been found to be occurring farther north than previously seen. Naturally, the amount of ozone in the stratosphere is maintained as the result of a dynamic balance between formation and destruction process. Formation occurs predominantly at altitudes above 30 km, where solar UV radiation with wavelengths less than 242 nm dissociates molecular oxygen into oxygen atoms,

$$O_2 + h\nu \rightarrow 2O \tag{1.14}$$

These oxygen atoms rapidly combine with O_2 to form ozone,

$$O + O_2 + M \rightarrow O_3 + M \tag{1.15}$$

the net effect being the conversion of three molecules of O_2 to two molecules of O_3.

Ozone itself absorbs solar radiation strongly in the wavelength region 240 to 320 nm,

$$O_3 + h\nu \rightarrow O_2 + O \tag{1.16}$$

It is this absorption that shields the earth from harmful UV radiation and produces heat in the upper stratosphere.

Balance the reverse of the formation processes, Reactions 1.14 and 1.15, are several pathways that destroy ozone. One example is the reaction of ozone and oxygen atoms to produce molecular oxygen,

$$O_3 + O \rightarrow O_2 + O_2 \tag{1.17}$$

The above scheme was suggested by Chapman (1930) and has provided the basis for analysis of stratospheric ozone ever since. However, it has been studied over the last 30 years that chemical processes other than Reaction 1.17 destroy large amounts of ozone [Johnston, 1975]. The original Chapman scheme given above accounts for about 20% of the total natural destruction rate for the stratosphere ozone, while transport of ozone to the troposphere contributes an additional 0.5%.

About 10% of the destruction is caused by catalytic cycles involving hydrogen-containing species: free hydrogen atoms (H), hydroxyl (OH), and hydroperoxyl (HO_2), which can achieve the same effect as Reaction 1.17 without being themselves removed.

$$O + HO_2\bullet \rightarrow OH\bullet + O_2 \quad (1.18)$$

$$OH\bullet + O_3 \rightarrow HO_2\bullet + O_2 \quad (1.19)$$

$$\text{NET} \quad O + O_3 \rightarrow O_2 + O_2 \quad (1.20)$$

A catalytic cycle involving NO and NO_2 provides the most important destruction process for ozone. This process accounts for most of the remaining 70% of the natural ozone destruction rate; there is also a small contribution from chlorine compounds. For the nitrogen oxides the dominant processes are

$$O + NO_2 \rightarrow NO + O_2 \quad (1.21)$$

$$NO + O_3 \rightarrow NO_2 + O_2 \quad (1.22)$$

$$\text{NET} \quad O + O_3 \rightarrow O_2 + O_2 \quad (1.23)$$

These processes again produce the same effect as Reaction 1.17 without the nitrogen oxides being consumed.

1.4 Legal Aspects of NO_X Emissions

The history of federal legislative efforts begins with the Air Pollution Control Act of 1955. This act provided funds only for federal research and technical assistance, and was effect only for five years. The Clean Air Act (CAA) of 1963, which was requested by the president, replace the 1955 act. Not only provided money for federal research, but also provided for grants to outside research agencies. This act also provided, for the first time, federal authority to address interstate air pollution problems.

The Clean Air Act Amendments of 1970 is widely recognized as a powerful and very important piece of environmental legislation. Along with the National Environmental Policy Act, which created the Environmental Protection Agency (EPA), it put some actions into air pollution control enforcement. The amendments of 1977 incorporated many modifications and additions to the 1970 act. However the 1977 amendments retained basic philosophy of federal management with state implementation. Likewise, the

Clean Air Act Amendments 1990 (CAAA 1990) promise to further refine and strengthen air pollution control.

1.4.1 The Clean Air Act and Amendments of 1990

With the 1990 Amendments, the updating Clean Air Act has a more direct and pervasive impact on our every-day lives than any other environmental law. This section provides a brief overview of the Clean Air Act's various air quality programs. It is a summary intended to provide a guideline for process development and design.

National Ambient Air Quality Standards

The US. Environmental Protection Agency (EPA) established primary and secondary National Ambient Air Quality Standards (NAAQS) for six pollutants, which are called criteria pollutants. The primary standards specify maximum concentrations of the pollutants necessary to protect the public health with an adequate margin of safety. Secondary standards are designed to protect the public welfare, such as soil, vegetation, and wildlife.

The pollutants for which a NAAQS has been adopted are carbon monoxide, lead, nitrogen oxides, ozone, sulfur dioxide, and fine particulate matter (that is, particles with an aerodynamic diameter less than or equal to a nominal 10 micrometers, designated PM-10). Table 1.6 summarizes the primary and secondary NAAQS for these pollutants.

Individual states are primarily responsible for achieving and maintaining the attainment of NAAQS. The state fulfills this responsibility by preparing a State Implementation Plan (SIP), which is subject to EPA approval. Areas that have not attained the air-quality standard for any pollutant subject to a NAAQS, called nonattainment areas, require additional controls designed to provide emission reductions leading to attainment of the standard.

Congress specifically addressed ozone nonattainment areas in the Clean Air Act Amendments of 1990 by classifying areas ranging from marginal to extreme as shown in Table 1.7, and by imposing increasingly stringent controls in these areas.

Table 1.6 National Ambient Air Quality Standards

	Averaging	NAAQS ($\mu g/m^3$)	
Pollutant	time	Primary	Secondary
Carbon monoxide	8-hour	10000	As primary
	1-hour	40000	As primary
lead	Calendar	1.5	As primary
	Quarter	1.5	As primary
Nitrogen oxide	Annual	100	As primary
ozone	1-hour	235	As primary
Sulfur dioxide	Annual	80	None
	24-hour	365	None
	3-hour	None	1300
PM-10	Annual	50	As primary
	24-hour	150	As primary

[Code of Federal Regulations, 40 CFR 50]

Table 1.7 Area Classification by Ambient Ozone Concentration

Area	Design value, ppmv
Marginal	0.121-0.138
Moderate	0.138-0.160
Serious	0.160-0.180
Severe	0.180-0.280
Extreme	0.280 and above

New Source Performance Standards

A variety of industrial companies have been identified as having a significant potential to emit criteria or other designated air pollutants. For those, EPA has established technology-based emission control standards called New Source Performance Standards (NSPS), Which are applicable to new, modified, or reconstructed stationary sources. NSPS must reflect the degree of emission limitation achievable through the application of

the best system of emission reduction. Taking cost into account, facilities that are subject to NSPS must comply with the standards regardless of the ambient air quality of the area. EPA has indicated that additional 189 pollutants for the equipment leaks of volatile organic compounds (VOC) emissions in the synthetic organic chemical manufacturing industry will be a priority under the Clean Air Act Amendments of 1990.

National Emission Standards for Hazardous Air Pollutants

With the passage of the Clean Air Act Amendments of 1990, Congress directed EPA to establish health-based emission standards for hazardous air pollutants (HAPs). National Emission Standards for Hazardous Air Pollutants (NESHAP) include control technology requirements, operational controls, and disposal requirements, and they apply to both new and existing emission sources.

To date, EPA has regulated only seven hazardous air pollutants they are asbestos, benzene, beryllium, inorganic arsenic, mercury, radionuclides, and vinyl chloride. Standards for an eighth HAP, coke oven emissions, are prepared now but have not yet issued.

Because relatively little progress toward regulating hazardous air pollutants had been made, Congress substantially revised the Clean Air Act Amendments of 1990. The 1990 Amendments direct EPA to identify major and area source of the 189 listed hazardous air pollutants and then develop regulations for those source categories within 10 years.

Prevention of Significant Deterioration

The final set of emission standards applicable to facilities are the standards adopted to protect clean air areas, the Prevention of Significant Deterioration (PSD) regulation. Clean air areas are divided into classes, with emission standards or technology-based requirements established to protect the air quality in the areas. The standards must be incorporated into the state's SIP.

Permitting

Under prior law, major sources were regulated independently under each particular program. A facility could have more than one permit under the SIP programs governing criteria pollutants if it had more than one major source of emissions. Any portion of the facility that did not qualify as major source of emissions was not required to obtain such a permit.

In the 1990 Amendments, Congress provided for a facility-wide permit system. Under this approach, if a facility has a source that is regulated under a NESHAP, a NSPS, or the SIP, all of the sources within the plant will be included under a single permit regardless of the size of the additional sources.

Enforcement

Civil penalties may be assessed at up to $25,000/day per violation. Criminal penalties include prison terms of one year for negligently releasing a hazardous air pollutant, two years for knowingly making a false report or failing to file a required report, five years for knowingly violating a SIP or NSPS, and fifteen years and up to $1 million in fines for knowingly releasing a hazardous air pollutant that places another person in imminent danger of death or serious bodily injury. Penalties for subsequent convictions are generally double the penalties for the initial offense.

The 1990 Clean Air Act Amendments increase the penalties for failure to comply with the Act. Citizen can sue to enforce the Act, if EPA fails to do so after being put on notice [Davenport, 1992].

1.4.2 NO_X Rules in 1990 Clean Air Act Amendments

The Clean Air Act Amendments (CAAA) of 1990 contained therein provide governmental agencies with well defined tasks to accomplish improvements in air quality. The first section of the amendments, identified as Title I, pertains to the attainment of air quality standards for three parameters that were either weakly addressed in the Clean Air Act, or

have been difficult to meet in certain regions. The parameter for which Title I has the most far reaching effect is surface ozone. More ozone nonattainment areas exist across the country than for any other criteria pollutant.

Title I addresses the ozone problem by subdividing areas by degree of nonattainment. The areas listing the types of nonattainment are summarized in Table 1.7, along with the ambient concentration which defines them. Each area, in turn, requires the performance of tasks that can cause reductions of ozone precursors until attainment can be demonstrated. A subtle implication of the ozone portion of Title I is the need for reductions of NO_X emissions. NO_X is itself determined to be an ozone precursor as reactions between VOC and NO_X in the presence of ultraviolet light produce surface level ozone [Kane, 1992].

Besides the ozone formation, new power plants have faced NO_X emission rules since the 1971 New Source Performance Standards (NSPS) were established. The 1990 Clean Air Act Amendments revised these under the acid rain provisions, Title IV. The legislation calls for a cut of 2 million tons in NO_X emissions by the year 2000. The EPA is has set emission limits for tangential fire and dry-bottom boilers in mid-1992 and will set emissions for all other boilers by 1997. Continuous emission monitors are required for NO_X emissions. January 1, 1995 is the NO_X compliance deadline for tangential-fired, or dry-bottom, wall-fire boilers in phase I. Suggested NO_X emissions levels are 0.45 and 0.5/MBtu, respectively. Actual levels were to be set by May 1992 and NO_X limits for cyclone, cell-burner wall-fired boilers and others are due by January 1997 [Rittenhouse, 1992].

1.5 NO_X Control Technologies

There are several types of control technologies available to reduce NO_X emissions from industrial boilers and furnaces. These technologies fall into two general categories, combustion modifications and flue gas treatment. Combustion modifications are used to limit the formation of NO_X during the combustion process. Flue gas treatment

technologies are used to remove NO_X from flue gas after the NO_X has been formed in combustion. Flue gas treatment systems are in wide commercial use in Japan [Parkinson, 1981] while observers in United states believe that combustion modification alone might be sufficient to meet current EPA regulations [Moore, 1984].

1.5.1 Combustion Modifications

There are several factors contributing to high NO_X formation. Combustion modifications reduce NO_X formation by one or more of the following strategies [Cooper, 1986]:

1. Reduce peak temperature of the flame zone by
   (a) using a fuel-rich primary flame zone
   (b) increasing the rate of flame cooling
   (c) dilution
2. Reduce gas residence time in the flame zone by
   (a) changing the shape of the flame zone
   (b) using steps in strategy 1
3. Reduce oxygen concentrations in the flame zone by
   (a) decreasing the overall excess air rates
   (b) controlling mixing of fuel and air
   (c) using a fuel-rich primary flame zone

These approaches can be implemented by either modifying the operating conditions in existing furnaces, or installing a low-NO_X burners.

Over the past few years, intensive research and development have led to the development of a number of technologies that can be used to control NO_X emissions. However, few technologies that can reduce NO_X by more than 80%.

Diluent injection (WI, SI)

This method involves injecting water (WI) or steam (SI) into the combustion zone. Water is injected into the combustion air stream at a water:fuel mass ratio of 0.2:1 to 1:1

through nozzles mounted on the windbox. water evaporates before entering the combustion chamber producing steam and consuming energy to reduce the flame temperature. If steam is injected directly, the diluent:fuel ratio is on the order of 1:1 to 2:1.

Diluent injection can reduce NO_X emissions by as much as 75%. In general, steam injection results in greater NO_X reduction than does water injection, and the decrease in NO_X emissions increases with the diluent to fuel ratio. For example, a water to fuel ratio of 0.5 will reduce thermal NO_X formation by about 40%; if the ratio is increased to 1.0, NO_X reduction will increase to between 60 and 70% [Crawford, 1977].

Great amounts of water or steam need to be injected to meet NO_X limits. At the same time, the more diluent injected, the lower the thermodynamic efficiency of the boiler. In addition, CO emissions increase as the diluent injection rate increases. However, for gas turbines part of the diluent effect is offset by greater mass throughput to the turbine and the efficiency is affected to a lesser extent.

Finally, as more water is injected into the combustion zone, flame stability may be affected; in the extreme case, the water may even extinguish the flame.

Flue Gas Recirculation (FGR)

Another way to reduce combustion zone temperature is by recirculating a portion of the exhaust gas to a point where it dilutes the inlet combustion air flow.

Advantages of flue gas recirculation are two fold: First, diluting the effluent with inert exhaust results in a lower flame temperature; therefore, reducing thermal NO_X formation. Second, the oxygen concentration in the flame is also decreased, which suppresses NO_X formation in the first place.

This technology can result in NO_X reductions of 15% for oil-fired boiler, and as 85% for gas-fired units. According to the report of EXXON research, 50% of flue gas recirculation reduces 60% thermal NO_X formation [Sommerlad, 1971].

In retrofit applications, FGR can be very expensive. In addition to requiring new large ducts, major modification to the fans, dampers, and controls might be required. The additional gas flow through the furnace and flues might cause operating and maintenance problems. FGR is usually better applied to new designs than retrofit in existing furnaces.

Low-excess-air Firing (LEA)

LEA is a very simple yet effective technique. Thirty years ago it was not uncommon to see furnaces operating with 50-100% excess air. As fuel price escalated, the percent of excess air was decreased to about 15-30% to save money. This level of excess air was considered a practical limit because it gave good combustion, but did not require extensive furnace monitoring. Owing to less than perfect mixing of air and fuel, there are some excess air percentages to ensure good fuel use and do not cause excessive smoke formation. In recent years, development of advanced instrumentation has allowed continuous automatic furnace monitoring and control of excess air, and the percent excess air can now be reduced below the 15-30% limit. Results of tests on various boiler with various fuels reported by the EPA [Lim, 1980] indicate an 19% reduction of NO_X by reducing the percent of excess air from an average of 20% to an average of 14%.

Staged Combustion (SC)

Staged combustion, also called off-stoichiometric combustion (OSC), which combusts the fuel in two or more steps. The initial flame zone is fuel rich , and the secondary and following zones are fuel lean. Without retrofitting with specially designed burners, OSC can be accomplished by firing some of the burners fuel rich and the rest fuel lean, or by taking some of the burners out of service (BOOS), and allowing them only to admit air to the furnace or by firing all of the burners fuel rich and admitting the remaining air over the top of the flame zone. Incomplete combustion in the first stage lowers thermal NO_X formation. The second stage uses excess air to complete the combustion, reduce the combustion temperature and lower the thermal NO_X formation [Bienstock, 1972]. This method requires some form of interstage cooling in order to avoid a large temperature

increase as the system goes through stoichiometric combustion. In a test of 31 boilers burning coal, oil, or gas, NO_X emissions were reduced an average of 34% using the preceding methods [Lim, 1980]. Careful monitoring of the flue gas is necessary with this method to protect against CO and smoke.

Reduced Air Preheat

Reduced air preheat lowers peak temperature in the flame zone thus reducing thermal NO_X. However, unless an alternative means of recovering heat is available, a substantial overall energy penalty results. A similar statement can be made for reduced firing rate. By reducing the firing rate, the heat release per unit volume is reduced. Reducing the firing rate generally reduces thermal NO_X formation, but creates several problems. Besides the obvious penalty of reducing unit capacity, low load operation usually requires increased excess air to control smoke and CO emissions. Also, operating flexibility is reduced.

Low-NO_X Burner (LNB)

New low NO_X burners represent the most common equipment design change for reducing NO_X formation. Low NO_X burners are not only effective on new power plants , but also can be readily applied to older facilities as retrofit technologies. Various burner designs have been proposed to lower the NO_X emission such as tangential fired boilers. The essential elements of a burner are a fuel introduction system and a burner throat to supply combustion air. Design variables used to achieve stable combustion and good fuel conversion efficiency include the fuel injector configuration and the rate of air mixing, controlled by the throat velocity, use of swirl, and design of the flame holder. The fuel and air mix initially in a primary reaction zone that may contain a wide range of stoichiometries from very rich to very lean. The balance of the combustion air is mixed with the primary zone products further downstream and combustion is completed. Also, relatively cool combustion products may recirculate in the combustion chamber and be entrain by the flame, leading to a diluent effect that reduces peak temperature. Entrained combustion gas recirculation burners have achieved thermal NO_X reductions in excess of

50% for clean fuels such as natural gas and distillate oil. In addition, several study of advanced burner designs for staged-air burners produce decreased NO_X emissions of about 40%, while staged-fuel burners can reduce emission by as much as 70% [Fusselman, 1992].

Alternate Fuels

Alternate fuels refers to fuels other than nature gas and fuel oil. If a boiler cannot meet mandated NO_X levels with its existing fuel, a switch to alternate fuel may prove worthwhile.

Methanol and ethanol can be a replacement for light fuel oils. Because these fuels burn with lower flame temperatures and contain no fuel nitrogen, baseline NO_X levels below 100 ppm may be achieved, as compared to a baseline level of 200 ppm for fuel oil No. 2. In conjunction with other NO_X reduction strategies, oxygenated fuels such as methanol and ethanol can achieve NO_X levels of 40 ppm or lower.

Natural gas is the most appropriate fuel for low NO_X situations. Most boilers are already equipped to burn both natural gas and fuel oil. Natural gas produces lower amounts of NO_X than does fuel oil, because it contains no nitrogen and burns at a lower flame temperature. Natural gas is often more expensive than fuel oils on a cost-to-energy basis. However, when maintenance and reliability are considered, natural gas is a comparable value.

Typically, propane and butane give baseline NO_X levels slightly higher than natural gas, due to an increased peak flame temperature. However, when diluted to 1,400 Btu/ft^3 with air upstream of the burner, they behave much like natural gas and allow existing natural gas burners to be used without modification [Colannino, 1993].

1.5.2 Flue Gas Treatment Technologies (FGT)

Flue gas treatment to remove NO_X is useful in cases where higher removal efficiencies are required than can be achieved with combustion controls and also is used where

combustion controls are not applicable such as controlling NO_2 emissions from HNO_3 plants. FGT technologies are broadly categorized as dry and wet techniques, and the dry techniques are further classified as selective catalytic reduction (SCR), selective non-catalytic reduction (SNCR), adsorption, and electron beam irradiation.

A. Flue Gas Denitrification (FGDN)

FGDN systems use common wet scrubbing techniques to dissolve NO into the scrubbing solutions. The wet scrubbing processes usually remove SO_X as well as NO_X. However, because NO is basically insoluble in water, additional chemicals are added first to bring the NO into the solution, followed by oxidation or reduction reaction. Chemicals used for this purpose are water-soluble ferrous-chelating agents [Chang, 1988], hydrogen peroxide (H_2O_2) [Robinson, 1993], organic hydroperoxides [Perlmutter, 1993], ozone (O_3) [Rhoads, 1990], chlorine (Cl_2) [Hixson, 1990], sodium chlorite ($NaClO_2$) [Sada, 1977, 1979], Chlorine dioxide (ClO_2) [Rhoads, 1990], potassium permanganate ($KMnO_4$) [Shaw, 1977], and sodium hypochlorite NaClO [Yang, 1992].

The major drawbacks to the use of an FGDN process include expensive chemical additives, high water usage, undesired products, and variable SO_2 levels with some fuels such as municipal solid waste (MSW). Some recent pilot studies with metal chelates (particularly iron EDTA) have indicated NO_X removals of 70% to 90%, using techniques such as an electrolytic cell to maintain reactivity or high temperature regeneration [Tsai, 1989]. Comparable simultaneous SO_2 removal can be achieved. So that if wet SO_X scrubbing is practiced at a particular location, it might be practical to consider simultaneous NO_X scrubbing as well.

B. Selective Catalytic Reduction (SCR)

One of the most advanced FGT technique is selective catalytic reduction. There are more than 70 full-scale SCR units operating in Japan [US. EPA, 1983]. SCR process use a catalytic bed and anhydrous ammonia (NH_3) for removal of NO_X emissions. NH_3 is injected into the flue gas upstream of the catalyst. Intimate mixing occurs between the

injected ammonia and flue gas NO_X. This mixture then passes over the catalyst bed and reacts to form diatomic nitrogen and water, provided the reaction temperature is approximately 320 ^oC (600 ^oF) to 370 ^oC (700 ^oF). With a suitable catalyst, NH_3, H_2, CO, or even H_2S could be used as the reducing gas, but the most commonly used material is NH_3. Some of the catalysts are a mixture of titanium and vanadium oxides, Pt, or molecular sieves (Zeolites), and are formulated in pellets for gas fired unit and honeycomb shapes for coal or oil fired units, which might have particulate in the flue gas.

Most SCR experience is in Japan and Western Europe where NO_X removal has ranged from 85% to 90%. SCR has been used with success on gas turbines and is planned for fluidized bed cogeneration facilities in the United States [Rhoads, 1990]. However, in the US., SCR has not yet been used for coal firing or MSW. Experience with European coal fired installations suggests that transfer of the Japanese technology to United States design and operating practices may not be straightforward [Cichanowicz, 1988]. Domestic coal and MSW present other problems to available catalysts. For example, catalyst attack by acid gases requires the use of innovative special acid resistant catalysts. The catalysts presently available on a commercial basis are sensitive to particulate and sulfur compound. Thus catalysts would have to be installed downstream of acid gas and particulate controls. As a result, the flue gas stream needs to be reheated prior to NO_X removal.

C. Selective Non-catalyst Reduction (SNCR)

SNCR involves the reduction of NO_X with NH_3 or urea at temperatures of 900-1000 ^oC without a catalyst. At NH_3:NO_X molar ratios of 1:1 to 2:1, about 40% to 60% NO_X reduction can be achieved [EPA, 1983]. Two major SNCR systems are commercially available: the EXXON Thermal $DeNO_X$ ammonia injection system and the Fuel Tech NO_XOUT urea injection system. A third system, the Emcotek Two-Stage $DeNO_X$ urea/methanol injection system, has undergone extensive pilot testing and full scale demonstration, but has not been commercialized.

Ammonia Injection

The EXXON Thermal $DeNO_X$ ammonia injection uses the NO_X/ammonia reaction to convert no to molecular nitrogen. However, without catalyst use or supplemental hydrogen injection, NO_X reduction reaction temperatures must be tightly controlled between 870 ^oC (1600 ^oF) and 1200 ^oC (2200 ^oF). Below 980 ^oC (1800 ^oF) and without hydrogen also being injected, ammonia will not fully react, resulting in ammonia breakthrough. If the temperature rises above 980 ^oC (1800 ^oF), the rate of ammonia oxidation to NO_X begins to contribute resulting in increased NO_X emissions. Therefore, the region where ammonia is injected must be maintained at optimum reduction reaction temperature.

Thermal $DeNO_X$ is an available technology which has been used primarily on gas fired boilers and gas turbines and may achieve NO_X reduction to 70% to 80% within the temperature range 1600 ^oF and 1800 ^oF. Thermal $DeNO_X$ has also attained 40% to 60% removals on commercial oil and coal fired installations.

The major disadvantages of this process are the narrow temperature window, mixing requirements, and possibility of NH_3 breakthrough which can cause odors, fouling, and a visible plume. Besides that, Thermal $DeNO_X$ has an additional disadvantage in that the storage and handling of anhydrous ammonia may pose safety problems.

Urea Injection

The process NO_XOUT urea ($CO[NH_2]_2$) injection has been developed and marketed by Fuel Tech, Inc. Urea alone injected has a high NO_X reduction activity between 925 ^oC (1700 ^oF) and 1035 ^oC (1900 ^oF). With process enhancers and adjusted concentrations, the NO_XOUT process is effective from 815 ^oC (1500 ^oF) to 1150 ^oC (2100 ^oF). Enhancers alone are used between 538 ^oC (1000 ^oF) and 815 ^oC (1500 ^oF). The NO_XOUT process can be utilized at temperatures above 1150 ^oC (2100 ^oF) by introducing dilution water to cool the gas stream to within desired temperature ranges. A 50% urea solution is typical but solutions as low as 10% may be used. To optimize NO_X

reduction, different urea and chemical enhancer solutions may be injected at different temperature levels.

Major drawbacks of NO_XOUT process include: ammonia may be formed in this process and react with sulfur compounds to form ammonia salts and foul the heat recovery equipment. Also, this process is impractical for controlling NO_X sources with large load variations and gas turbines. The applicability to turbines and other sources may be feasible in the future, pending development of new chemical enhancers and commercial demonstration experience.

Commercial applications employing NO_XOUT process for post-combustion NO_X control have been made at a pulverized brown coal-fired boiler, a refinery gas-fired CO boiler, and a pulverized coal utility boiler. These applications have demonstrated NO_X reductions of 35% to 70% [Rhoads, 1990].

Urea/Methanol Injection

A two-stage DeNO_X process has been developed and patented by Emcotek. This process utilizes both urea and methanol as the reducing agents. Emcotek initial pilot studies on a 1 MW crude oil boiler used methanol alone to remove NO_X. The final patent both urea and methanol alone with a special designed nozzle. The methanol is used to prevent the ammonia slip and provide heat for air preheater.

The Two-Stage DeNO_X system has been installed, operated, and tested at a 24 year old MSW incinerator, which has heat recovery [Jones, 1989]. 65% to 80% NO_X reduction were achieved with 160 ppm uncontrolled level at flue gas temperatures between 815 ^{o}C (1500 ^{o}F) and 1040 ^{o}C (1900 ^{o}F). Ammonia slip was below 5 ppm for flue gas temperatures greater than 1600 ^{o}F and can be maintained below 1 ppm. NO_X reductions of 78%, 65%, and 48% were achieved at urea to NO_X ratios of 0.8, 0.6, and 0.4, respectively.

D. Adsorption

A number of adsorbents have been proposed and demonstrated for simultaneous control of NO_x and SO_x. One type of system uses activated carbon with NH_3 injection to simultaneously reduce the NO_x to N_2 and oxidize the SO_2 to H_2SO_4. The carbon must be operated in the temperatures of 220 to 230 ^oC, and should be regenerated to remove the H_2SO_4. Washing is the best process for carbon regeneration to remove H_2SO_4 [EPA, 1983]. If there is no SO_2 in the flue gas, the carbon acts as a catalyst for NO_x reduction.

Copper oxide is also a effective adsorbent for NO_x removal. The copper oxide selectively adsorbs SO_2 to form copper sulfate. Both copper oxide and copper sulfate are good catalysts for the selective NO_x reduction with NH_3. The catalyst beds are regenerated with hydrogen to produce a rich stream of SO_2 which can be further processed to elemental sulfur or H_2SO_4. This process has been installed on a 40-MW oil fired boiler in Japan, and has shown 90% SO_x removal along with 70% NO_x reduction [EPA, 1983].

E. Electron Beam Irradiation

The Electron Beam irradiation is an advanced technique for NO_x removal that has been tested in pilot-scale in 1985 and 1986. Electron beam is applied to provide the activation energy for the reaction of NO_x and SO_2 with ammonia or lime. Addition of water to the flue gas produces solid NH_4NO_3 and $(NH_4)_2SO_4$, which can be separated and sold as fertilizers. In practice, the process would proceed as follows: First, most of the particulate matter is removed by electrostatic precipitator (ESP). Next, the flue gas is humidified and cooled down to 70-90 ^oC, and ammonia is injected into the flue gas. The gas stream is then bombarded by the electron beam, forming first nitrate and sulfate anions and then their respective ammonium salts. finally, the products are recovered by a baghouse [Chemical Week, 1983].

1.6 Cost Estimation of NO_X Control

Information on costs of NO_X control technologies are strongly affected by the specific applications and are difficult to generalized. However, one can show general trends for the technologies described above. Low-NO_X burners are cost effective, achieving 50% NO_X reductions on Coal-fired boilers at capital costs of about $5/kW [Moore, 1984]. However, for retrofit applications, costs are highly site-specific. Information in 1983 showed a $1/kW to $20/kW range for a coal-fired boiler, which is equal to $20 million for a 1000-MW plant. Annualized operating costs for several cases were reported in the range of $0.5/kW-year to $3.00/kW-year [EPA, 1983].

Selective Catalyst Reduction (SCR) requires much higher costs than those of Low-NO_X burner. In 1984, SCR system capital costs were about $100/kW for a new boiler, while retrofit costs were higher than that [Moore, 1984]. Maxwell [1980] reported preliminary capital investments for various NO_X and NO_X/SO_X removal systems. Jahnig and Shaw (1981) summarized much of the information available for flue gas treatment proceed on a consistent basis i.e., for the same conceptual 800 MW power plant burning high sulfur Illinois coal. their results indicate that NO_X control costs add 20 to 75% to FGD costs. The average of the estimated costs of three SCR systems was $140/kW, excluding the cost of the ESP. Shaw [Yang, 1992] showed that the reported economics for NO_X control grow exponentially as a function of percent removal for various technologies as shown in Figure (1.3).

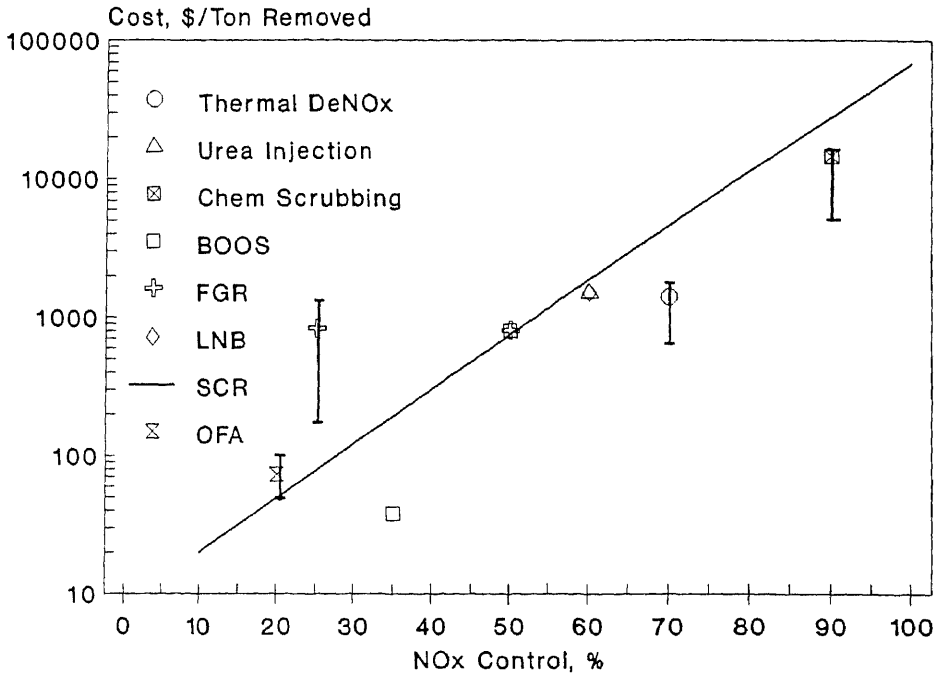

Figure 1.3 Cost estimation of NO_x control

CHAPTER 2

LITERATURE REVIEW OF NO_x ABSORPTION

2.1 Introduction

Absorption of NO_x from a flue gas is an important process in its control, and has received considerable R&D attention due to the stringent requirement of the recently enacted 1990 amendments to the Clean Air Act. During the past fifty years, substantial information has been accumulated on various aspects of NO_x absorption. However, it is an extremely complex example of an absorption operation for the following reasons:

(1) The NO_x gas can be a mixture of several components consisting of N_2O, NO, NO_2, N_2O_3, N_2O_4, and N_2O_5. The resulting products of NO_x absorption in water are oxyacids namely nitric acid and nitrous acid.

(2) More than forty equilibria reactions exist between NO_x and oxyacids.

(3) Absorption, desorption and chemical reactions occur simultaneously. Especially, the absorption and oxidation of NO induced by oxychlorine compounds which have a very complicate equilibrium with the following components in solution; Cl_2, HClO, ClO^-, ClO_2, and ClO_2^-.

(4) It is anticipated that the reaction kinetics involve simultaneously reversible, parallel and consecutive reactions in both gas and liquid phases.

(5) Data on physical and chemical properties such as diffusivity, solubility, equilibrium and rate constants are limited.

In aqueous absorption processes, nitric oxide is oxidized to more reactive nitrogen dioxide (NO_2). The oxidation reaction can occur in either the gas phase or the liquid phase. The resulting NO_2 is more soluble than NO in aqueous solutions, and is easily absorbed. The wet processes are operated at ambient conditions, as against very high temperatures required for dry process, and can be coupled with existing desulfurization

processes. It is, thus, desirable to review the published information on NO_X absorption before the new developments which are the subject of this thesis are described.

2.2 NO_X-Water Equilibrium

In the absorption of NO_X in aqueous solutions, every component in the system equilibrates with one or more of the other components present. The components in the gas phase equilibrate with those in the liquid phase. The following section, summarizes these equilibrium reactions.

2-2-1 Gas Phase Equilibrium

The following equilibria prevail in the gas phase:

$$2NO_{2(g)} \overset{K_{g1}}{\Leftrightarrow} N_2O_{4(g)} \tag{2.1}$$

$$NO_{(g)} + NO_{2(g)} \overset{K_{g2}}{\Leftrightarrow} N_2O_{3(g)} \tag{2.2}$$

$$NO_{(g)} + NO_{2(g)} + H_2O_{(g)} \overset{K_{g3}}{\Leftrightarrow} 2HNO_{2(g)} \tag{2.3}$$

where,

$$K_{g1} = \frac{P_{N_2O_4}}{P_{O_2}^2} \tag{2.4}$$

The value of K_{g1} in atm^{-1} is given by the following equation [Bronsted, 1922; JANAF, 1971]

$$\log K_{g1} = \frac{2993}{T} - 9.226 \tag{2.5}$$

In SI units $(kN/m^2)^{-1}$, K_{g1} is given by

$$\log K_{g1} = \frac{2993}{T} - 11.232 \tag{2.6}$$

The value of K_{g2} is given by [Beattie, 1963]

$$\log K_{g2} = \frac{2072}{T} - 7.234 \tag{2.7}$$

$$\log K_{g2} = \frac{2072}{T} - 9.240 \tag{2.8}$$

where,

$$K_{g2} = \frac{P_{N_2O_3}}{P_{NO} P_{NO_2}} \tag{2.9}$$

In addition to the equilibria represented by Equations 2.1-2.3, several other equilibria mare also attained in the gas phase. These are listed in Table 2.1.

Table 2.1 Gas Phase Equilibria Involving Nitrogen Oxides and Oxyacids

Equilibrium	Constant at 25 °C
$NO + NO_2 + H_2O \Leftrightarrow 2HNO_2$	$1.6(10)^{-2}$ $(kN/m^2)^{-1}$
$3NO_2 \Leftrightarrow N_2O_5 + NO$	$4.2(10)^{-11}$ $(kN/m^2)^{-1}$
$3HNO_2 \Leftrightarrow HNO_3 + 2NO + H_2O$	3.33 (kN/m^2)
$NO_2 + HNO_2 \Leftrightarrow HNO_3 + NO$	$5.59(10)^{-2}$
$2NO_2 + H_2O \Leftrightarrow HNO_2 + HNO_3$	$9.36(10)^{-4}$ $(kN/m^2)^{-1}$
$3NO_2 + H_2O \Leftrightarrow 2HNO_3 + NO$	$5.23(10)^{-5}$ $(kN/m^2)^{-1}$
$N_2O_4 + H_2O \Leftrightarrow HNO_2 + HNO_3$	$1.38(10)^{-2}$
$N_2O_3 + H_2O \Leftrightarrow 2HNO_2$	3.18
$N_2O_5 + H_2O \Leftrightarrow 2HNO_3$	$1.23(10)^{6}$

[Schwartz and White, 1981]

In the eleven equilibria listed, the first three are relatively important for absorption of NO_x gas. Further, only five of these eleven equilibria are independent and if the values of five equilibrium constants are known, the rest can be calculated.

2.2.2 Interphase Equilibrium

Consider the following equilibria:

$$NO_{(g)} + NO_{2(g)} + H_2O_{(g)} \Leftrightarrow 2HNO_{2(g)} \quad (2.3)$$

$$2HNO_{2(g)} \Leftrightarrow 2H^+_{(aq)} + 2NO_2^-{}_{(aq)} \quad (2.10)$$

Combining Equations 2.3 and 2.10 with the assumption that the activity of water is constant for dilute solutions, interphase equilibrium can be expressed as:

$$NO_{(g)} + NO_{2(g)} \underset{H_2O}{\overset{K_{i11}}{\Leftrightarrow}} 2H^+_{(aq)} + 2NO_2^-{}_{(aq)} \quad (2.11)$$

The interphase equilibrium constant, K_{i11} can be calculated in terms of K_{g3} and K_{i10} as:

$$K_{i11} = K'_{g3} K^2_{i10}$$

$$= 3.2(10)^{-5} \ [(kmole/m^3)/atm^2] \quad (2.12)$$

where K'_{g3} is the value of K_{g3} with activity of water equal to unity. Schwartz and White [1981] analyzed several interphase equilibria which are listed in Table 2.2. The symbol $\Leftarrow W \Rightarrow$ indicates that water takes part in these equilibria. It should be noted that all ions are assumed to be in solution although the qualifier, (aq), meaning aqueous is not included for brevity.

It must be pointed out that values for equilibrium constants given in Table 2.2 are for dilute aqueous solutions. These values have been selected by Schwartz and White [1981] on the basis of the ability to explain most of the reactions.

2.2.3 Aqueous Phase Equilibrium

Aqueous phase equilibria can be written in terms of gas phase and interphase equilibria. Consider the following reactions:

Table 2.2 Interphase Equilibria of NO_x and Oxyacids

Equilibrium	Constant
$2NO_{2(g)} \Leftarrow W \Rightarrow 2H+ + NO_2^- + NO_3^-$	$2.44(10)^2$ kmole/m$^3)^4$/atm^2
$NO_{(g)} + NO^2_{(g)} \Leftarrow W \Rightarrow 2H^+ + 2NO_2^-$	$3.28(10)^{-5}$kmole/m$^3)^4$/atm^2
$3NO_{2(g)} \Leftarrow W \Rightarrow 2H^+ + 2NO_3^- + NO_{(g)}$	$1.81(10)^9$ kmole/m$^3)^4$/atm^2
$N_2O_{4(g)} \Leftarrow W \Rightarrow 2H^+ + NO_2^- + NO_3^-$	$3.56(10)^1$ kmole/m$^3)^4$/atm
$N_2O_{3(g)} \Leftarrow W \Rightarrow 2H^+ + 2NO_2^-$	$6.14(10)^{-5}$kmole/m$^3)^4$/atm
$N_2O_{5(g)} \Leftarrow W \Rightarrow 2H^+ + 2NO_3^-$	$4.25(10)^{17}$kmole/m$^3)^4$/atm
$2H^+ + 3NO_2^- \Leftarrow W \Rightarrow NO_3^- + 2NO_{(g)}$	$2.27(10)^{11}$atm^2/kmole/m$^3)^4$
$NO_{2(g)} + NO_2^- \Leftrightarrow NO_3^- + NO_{(g)}$	$7.43(10)^6$
$2NO_{2(g)} \Leftarrow W \Rightarrow HNO_{2(aq)} + H^+ + NO_3^-$	$4.78(10)^5$ kmole/m$^3)^3$/atm^2
$NO_{(g)} + NO_{2(g)} \Leftarrow W \Rightarrow 2HNO_{2(aq)}$	$1.26(10)^2$ kmole/m$^3)^2$/atm^2
$N_2O_{4(g)} \Leftarrow W \Rightarrow HNO_{2(aq)} + H^+ + NO_3^-$	$6.98(10)^4$ kmole/m$^3)^3$/atm
$N_2O_{3(g)} \Leftarrow W \Rightarrow 2HNO_{2(aq)}$	$2.38(10)^2$ kmole/m$^3)^2$/atm
$3HNO_{2(aq)} \Leftarrow W \Rightarrow H^+ + NO_3^- + 2NO_{(g)}$	$3.01(10)^1$ atm^2/kmole/m^3)
$NO_{2(g)} + HNO_{2(aq)} \Leftarrow W \Rightarrow H^+ + NO_3^- + NO_{(g)}$	$3.79(10)^3$ kmole/m^3

[Schwartz and White, 1981]

$$2NO_{2(g)} \overset{K_{i13}}{\Leftarrow W \Rightarrow} HNO_{2(aq)} + H^+ + NO_3^- \tag{2.13}$$

$$NO_{(g)} + NO_{2(g)} \overset{K_{i14}}{\Leftarrow W \Rightarrow} 2HNO_{2(aq)} \tag{2.14}$$

$$2NO_{(g)} \Leftrightarrow 2NO_{(aq)} \tag{2.15}$$

Simplification of Equations 2.13-2.15 gives:

$$2HNO_{2(aq)} \overset{K_{a16}}{\Leftarrow W \Rightarrow} H^+_{(aq)} + NO_3^-(aq) + 2NO_{(aq)} \tag{2.16}$$

where,

$$K_{a16} = \frac{K_{i13}}{K^2_{i14}} H^2_{NO} \tag{2.17}$$

Similarly, for the following aqueous phase equilibrium:

$$2NO_{2(aq)} \overset{K_{a18}}{\Leftarrow W \Rightarrow} 2H^{+}_{(aq)} + NO_2^{-}(aq) + NO_3^{-}(aq) \tag{2.18}$$

where,

$$K_{a18} = \frac{K_{i13}}{H^2_{NO_2}} \tag{2.19}$$

Schwartz and White [1981] have reviewed the experimental data on liquid phase equilibria. The results are summarized in Table 2.3.

Table 2.3 Aqueous Phase Equilibria Involving NO_x and Oxyacids

Equilibrium	Constant
$3HNO_{2(aq)} \Leftarrow W \Rightarrow H^+ + NO_3^- + 2NO_{(aq)}$	$1.12(10)^{-4}$ (kmole/m^3)
$2H^+ + 3NO_2^- \Leftarrow W \Rightarrow NO_3^- + 2NO_{(aq)}$	$8.46(10)^5$ (kmole/m^3)$^{-2}$
$2NO_{2(aq)} \Leftrightarrow N_2O_{4(aq)}$	$6.54(10)^4$ (kmole/m^3)$^{-1}$
$NO_{(aq)} + NO_{2(aq)} \Leftrightarrow N_2O_{3(aq)}$	$1.37(10)^4$ (kmole/m^3)$^{-1}$
$2NO_{2(aq)} \Leftarrow W \Rightarrow HNO_{2(aq)} + H^+ + NO_3^-$	$3.8(10)^9$ (kmole/m^3)
$N_2O_{3(aq)} \Leftarrow W \Rightarrow 2HNO_{2(aq)}$	$3.3(10)^2$ (kmole/m^3)
$NO_{(aq)} + NO_{2(aq)} \Leftarrow W \Rightarrow 2HNO_{2(aq)}$	$4.52(10)^6$

[Schwartz and White, 1981]

2.2.4 Solubility

Solubility can be expressed in terms of partial pressure through Henry's law as

$$[A] = Hp \tag{2.20}$$

where,

H = Henry's law constant, kmole/m^3-kN/m^2

partial pressure, kN/m^2

[A] = saturation concentration of A in liquid phase, kmole/m3.

The solubility of nitric oxide (NO) in water with respect to temperature has been reported in the International Critical Tables [1928], Handbook of Chemistry and Physics [1963], and by Seidell [1965]. The value of Henry's law constants can be correlated by the following equation:

$$\log H_{NO} = \frac{-1463.32}{T} + 2.178 \tag{2.21}$$

where H is in kmole/m^3-Pa. Armor [1974] has measured the solubility of NO as a function of pH (2-13) which shows no significant change in the value of solubility.

The determination of solubility of nitrogen dioxide (NO_2) in water is difficult because NO_2 reacts with water. Komiyama and Inoue [1980] found the solubility of NO_2 in water using the theory of absorption followed by pseudo chemical reaction with m^{th} order. The value of H_{NO_2} was found to be 0.024 kmole/m^3-atm at 15 ^oC and 0.04 kmole/m^3-atm at 25 ^oC [Andrew, 1961].

Garcdel [1975] obtained a preliminary estimate of H_{NO_2} on the basis of following equation:

$$\frac{H_{NO_2}}{H_{NO}} = \frac{H_{CO_2}}{H_{CO}} \tag{2.22}$$

The value H_{NO_2} works out to be 0.07 kmole/m^3-atm at 25 ^oC. Schwartz and White [1981] have correlated the solubility of gases in water with their boiling points. They obtained a good relation for nitrogen, oxygen, carbon monoxide, nitric oxide, and carbon dioxide. Using this correlation the value of H_{NO_2} = 0.02 kmole/m^3-atm was estimated at 25 ^oC.

Perry [1984] collected solubility in a different form of Henry's law as

$$p = H_a[A] \tag{2.23}$$

where,

p = partial pressure, Pa

H_a = Henry's law constant, Pa-m^3/mol

[A] = saturation concentration of A in liquid phase, mol/m^3.

H_a values for nitrogen oxides along with those for some other air pollutants shown in Table 2.4.

Table 2.4 Henry's Law Constant

Gas	H_a (Pa-m^3/mol)	Temperature ^oC
NO	$4.42(10)^4$	15
	$5.24(10)^4$	25
NO_2	$1.90(10)^3$	15
	$2.48(10)^3$	25
N_2O	$1.10(10)^3$	20
N_2O_3	4.08	25
N_2O_4	41	15
	61	25
SO_2	21	20
Air	$3.64(10)^4$	20
NH_3	1.7	25
CO	$2.9(10)^4$	20
CO_2	778	20
HCl	$4.0(10)^{-3}$	20

[Perry, 1984]

2.3 Absorption of NO Followed by Oxidation

Oxidation of NO is the most important step of wet scrubbing process for NO_x emission control. The reaction rate of NO to NO_2 is relatively slow and thus, becomes the rate limiting step in the absorption of NO. This is especially true when low concentration of NO are to be absorbed or reacted as NO_2 to meet environmental regulations. Oxidation of NO in solution is very attractive under this condition. The common oxidizing agents are summarized in this section.

Ozone

When the concentration of nitric oxide is less than 50 ppm, it is desirable to use strong oxidizing agents to get reasonable rates of reaction.

The gas phase reaction of NO with ozone is given by the following equation:

$$NO + O_3 \rightarrow NO_2 + O_2 \qquad (2.24)$$

The resulting NO_2 can conveniently be scrubbed in alkaline solutions even at low ppm values. The mechanism of Reaction 2.24 has been studied by Harcourt [1972] and Bhatia and Hall [1980]. The kinetics have been investigated by Borders [1982]. Substantial amount of information is available in the patent literature regarding ozone treatment of nitric oxide. The amount of ozone required is generally in excess of the stoichiometric requirement to compensate to the decomposition of ozone. In some cases, in situ generation of ozone was made by electric discharge.

Sulfuric Acid

Topol et al., [1968] used sulfuric acid as the oxidizing agent for NO oxidation. The reaction is represented by:

$$4NO + 3H_2SO_4 \Leftrightarrow 2NO^+ + N_2O + H_3O^+ + 3HSO_4^- \qquad (2.25)$$

$$2NO + 5H_2SO_4 \Leftrightarrow 2NO^+ + SO_2 + 2H_3O^+ + 4HSO_4^- \qquad (2.26)$$

The values of equilibrium constants for these two reactions were found to be $2(10)^{50}$ $(kmole/m^3)^3$ and $4(10)^{12}$ $(kmole/m^3)^7$, respectively. The rate of the second reaction is second order in NO and the rate constant is found to be 0.2 m^3/kmole-s.

Hydrogen Peroxide

Takahashi et. al. [1979] carried out gas phase NO oxidation using hydrogen peroxide. Nitric oxide and hydrogen peroxide were taken in the ratio of 1:1.3 and oxidation was carried out at a temperature more than 400 ^oC. The extent of NO oxidation was greater than 95%.

Kinetics of liquid phase oxidation of nitric oxide in hydrogen peroxide solutions has been studied by Baveja et al., [1979] and Robinson [1993]. The absorption experiments were carried out using 101.5 mm i.d. stirred cell [Ladhabhoy, 1969]. The gas phase reaction between NO and H_2O_2 is given by the following equation

$$NO + H_2O_2 \rightarrow NO_2 + H_2O \quad \text{[Baveja, 1979]} \tag{2.27}$$

$$2NO + 3H_2O_2 \rightarrow 2HNO_3 + 2H_2O \quad \text{[Robinson, 1993]} \tag{2.28}$$

$$2NO_2 + H_2O_2 \rightarrow 2HNO_3 \quad \text{[Robinson, 1993]} \tag{2.29}$$

The reaction rate was found to be the first order in both reactants. Absorption of NO is accompanied by fast pseudo- first order chemical reaction. The value of reaction rate constant at 30°C was found to be $8.42(10)^2$ m^3/kmole-s with an activation energy of 13.7 kcal/mole.

Potassium Permanganate

Potassium permanganate was used for the oxidation of nitric oxide by Kann [1976]. Conversion of NO exceeding 80% has been reported by Kann for a mixture of H_3PO_4-H_2SO_4-H_2O in the ratio of (6:1:3).

Sada [1977] studied the oxidation of NO using aqueous solutions of $KMnO_4$ and aqueous solutions of $KMnO_4$ mixed with NaOH. In the absence of NaOH, the reaction between NO and $KMnO_4$ can be represented by the following equation:

$$NO + MnO_4^- \rightarrow NO_3^- + MnO_2 \tag{2.30}$$

The NO oxidation with aqueous solution of $KMnO_4$ was found to be first order with respect to NO and half order with respect to $KMnO_4$. The absorption of NO is accompanied by a fast oxidation reaction and the rate is given by the following equation:

$$R_A = P_{NO} H_{NO} (k_{NO} D_{NO} [KMnO_4])^{0.5} \tag{2.31}$$

Where,

P_{NO} = partial pressure of NO

H_{NO} = Henry's Law constant of NO

k_{NO} = reaction rate constant

D_{NO} = diffusivity of NO in water.

The value of reaction rate constant at 25°C was found to be $7(10)^5$ m^3/kmole-s. Uchida [1983] showed that the product of reaction MnO_2 has some inhibiting effect on the rate of reaction. Shaw [1977] reported that a deposit of MnO_2 plated out on the wall of the scrubber. The experiment was stopped in ten minutes in order to prevent plugging of the liquid spray nozzle.

In the presence of NaOH, the oxidation reaction is enhanced. The reaction between NO and $KMnO_4$ in a strong aqueous alkaline solution is given by:

$$NO + MnO_4^- + 2OH^- \rightarrow NO_2^- + MnO_4^{-2} + H_2O \qquad (2.32)$$

Uchida [1983] found that the reaction rate was first order in NO and first order in $KMnO_4$. The following reaction rate constant was proposed at a concentration of NaOH of 1 kmole/m^3:

$$k_{NO} = 8.51(10)^{14}\exp(-708/RT) \qquad (2.33)$$

The value of k_{NO} was found to be independent of NaOH concentration below 1 kmole/m^3 and increases with an increase in the NaOH concentration.

Sodium Chlorite

The absorption of NO in aqueous solutions of $NaClO_2$ and NaOH has been studied by Teramoto [1976] and Sada [1978]. Oxidation of NO with $NaClO_2$ in the presence of NaOH can be represented by:

$$4NO + 3ClO_2^- + 4OH^- \rightarrow 4NO_3^- + 3Cl^- + 2H_2O \qquad (2.34)$$

The specific rate of absorption is given by the following equation:

$$R_A = P_{NO} H_{NO} \left(\frac{2}{3} k_{NO} D_{NO} [NO][ClO_2^-]\right)^{0.5} \quad (2.35)$$

The third order global rate constant is given by the following equation:

$$k_{NO} = k_o \exp(-3.73[NaOH]) \quad (2.36)$$

Equation 2.36 shows that the value of third order rate constant decreases with an increase in the concentration of sodium hydroxide.

Chlorine Dioxide

Two Japanese patents claim the use of chlorine dioxide for NO oxidation, [Kushiro, 1976] and [Hayashi, 1976]. The process was applied for the removal of NO from flue gas. Fairly large flow rates of flue gas (300 m^3/hr and 70,000 m^3/hr of flue gas containing 100 ppm NO) were used to investigate the oxidation with chlorine dioxide. In both cases, the conversion of NO was about 90%.

Chlorine

Chlorine injection for the removal of nitric oxide from gas stream was patented by Dow Company [Hixson, 1990]. This process consists of injection of gaseous chlorine into a NO-laden gas stream followed by rigorous scrubbing using an acidic aqueous solution. The chemical reaction by which the process is carried out is proposed as:

$$2NO + Cl_2 \Leftrightarrow 2NOCl \quad (2.37)$$

$$NOCl + H_2O \Leftrightarrow HNO_2 + HCl \quad (2.38)$$

Also competing with Cl_2 for NO consumption was O_2 for the formation of NO_2. Much more water soluble than NO, NO_2 dissolves and reacts with HOCl in water to form HNO_3.

$$2NO_2 + H_2O + HOCl \rightarrow 2HNO_3 + HCl \quad (2.39)$$

The removal was found to be highly dependent upon gas stream Cl_2:NO ratio, temperature and pH. More than 90% NO removal were reported in laboratory experiments.

Sodium Sulfite/Ferric Sulfate

Takeuchi [1977, 1978] systematically studied the absorption of NO (100-800 ppm) in aqueous solutions of sodium sulfite at 25 ^oC using a stirred cell and mechanically agitated contactor. The absorption of NO in Na_2SO_3 solution was accompanied by a fast pseudo second order reaction with respect to NO and zero order in sulfite. The rate of absorption is given by the following equation:

$$R_A = [k_{NO}D_{NO}(H_{NO}P_{NO})^3(2/3)]^{0.5} \quad (2.40)$$

Where

k_{NO} = rate constant

D_{NO} = diffusivity of NO in water

P_{NO} = partial pressure of NO.

The rate constant was found to be 109 m^3/kmole-s at 25 ^oC.

Uchida [1983] studied absorption of NO in $Na_2SO_3/FeSO_4$ solutions. With the concentration of $FeSO_4$ held constant, the rate of NO absorption initially increases with Na_2SO_3 concentration, attains a maximum when $[Na_2SO_3]$ is 0.1 kmole/m^3 and then decrease with a further increase in Na_2SO_3 concentration. The kinetics of NO absorption was found below the critical concentration. The specific rate of absorption is given by the following equation:

$$R_A = P_{NO}H_{NO}(k_{NO}D_{NO}[Na_2SO_3]^{1.3}[FeSO_4]^{1.3})^{0.5} \quad (2.41)$$

where, the rate constant k_{NO} is given by

$$k_{NO} = 1.37(10)^{22}\exp(-1920/RT) \quad (2.42)$$

R is in (kJ/kmole-^oK). The fractional powers in Equation 2.41 indicates that the absorption operation follows some complex mechanism.

Sodium Dithionite/Sodium Sulfide

Lahiri [1981] measured specific rates of NO absorption in aqueous alkaline solutions of sodium dithionite ($Na_2S_2O_4$) and sodium sulfide (Na_2S) at 31 ^oC and 27 ^oC, respectively, using an agitated vessel with a flat gas-liquid interface. In both cases, absorption of NO was accompanied by fast reaction in the diffusion film. The reaction between NO and aqueous alkaline solution of $Na_2S_2O_4$ was found to be first order with respect to NO and zero order in $Na_2S_2O_4$. The first order rate constant was found to be $2.3(10)^3$ s^{-1} at 3 1^oC. The reaction can be represented by the following equation:

$$6NO + Na_2S_2O_4 + 2NaOH \rightarrow Na_2SO_3(NO)_2 + Na_2SO_4 + 2N_2O + H_2O \quad (2.43)$$

The reaction between NO and the aqueous alkaline solution of sodium sulfide was found to be zero order with respect to both NO and Na_2S. The rate constant was found to be $1.69(10)^{-4}$ kmole/m^3-s at 27 ^oC. The reaction is given by :

$$8NO + Na_2S \rightarrow Na_2SO_3(NO)_2 + 3N_2O \quad (2.44)$$

Organic Hydroperoxides

A method selectively remove nitric oxide from gas streams was investigated using 3,6-dimethyl-3-octyl hydroperoxide, p-menthanyl hydroperoxide, pinanyl hydroperoxide, and cumenyl hydroperoxide in solutions of n-hexadecane (cetane) [Perlmutter et al., 1993]. Fairly low flow rate (150 cm^3/min of helium containing 1500 ppm NO)were used to study the oxidation of NO with organic hydroperoxide. In an one inch diameter bubble column scrubber, the conversion with respect to NO was claimed to be more than 90%. The conversion was shown to be highly dependent on temperature, gas flow rate, and concentration of organic hydroperoxide. A hypothesis was proposed to explain the reaction between NO and organic hydroperoxide as following:

$$2ROOH + 2NO \rightarrow 2RONO_2 + H_2 \quad (2.45)$$

A promising technique has been reported to convert the scrubbing product, $RONO_2$, to useful nitrate or nitric acid and denitrated organic materials which can be recycled to regenerate hydroperoxide or commercially useful intermediates. The denitration can be expressed as:

$$RONO_2 + NH_4OH \rightarrow ROH + NH_4NO_3 \qquad (2.46)$$

2.4 Absorption of NO Followed by Complexation Reaction

Complexation reactions are another mechanism to remove nitric oxide from gas stream by wet scrubbing process. A limited number of publications were reviewed and summarized in this section.

Ferric Sulfate

Kustin [1966] has reported that the NO absorption into $FeSO_4$ aqueous solution is an equilibrium reaction:

$$NO + FeSO_4 \Leftrightarrow Fe(NO)SO_4 \qquad (2.47)$$

The forward reaction was found to be first order in both NO and $FeSO_4$. The reverse reaction was found to be first order in the complex $Fe(NO)SO_4$. The value of second order rate constant for the forward reaction was given by the following equation:

$$\log k_{NO} = 10.303 + 0.124I - \frac{1337}{T} \qquad (2.48)$$

where I is the ionic strength of the solution (k ions/m^3). The value of chemical equilibrium constant was also measured.

Sada [1978] has studied the kinetics of NO absorption in aqueous $FeSO_4$ solutions. The values of enhancement factor are reported and they are explained on the basis of theory of mass transfer with reversible complex reaction.

Fe-EDTA

The absorption of lean NO in aqueous solutions of Fe^{+3}-EDTA (ethylenediame tetraceteate) and aqueous slurries of $MgSO_3$ with Fe^{+2}-EDTA was carried out by Sada [1981]. For the determination of kinetics at 25°C, the authors used a stirred cell with a plane gas liquid interface. The forward complexation reaction was represented by:

$$NO + Fe^{+3}\text{-EDTA} \rightarrow Fe^{+3}\text{-(NO)(EDTA)} \qquad (2.49)$$

The reaction was found to be first order in NO and 1.5^{th} order in Fe^{+3}-EDTA at pH of 7.0. The value of the rate constant was found to be $1.5(10)^8$ $(m^3/kmole)^{1.5}s^{-1}$ at 25 °C. The effect of coexisting SO_2 on the absorption rate of NO and the role of $MgSO_3$ slurry have been discussed.

2.5 Absorption of NO Followed by Reduction Reaction

Reduction reaction is the new approach of NO absorption. One publication and one US. patent have claimed the potential for NO removal. No undesirable nitrates or complex compounds in the spent scrubbing solution makes these processes attractive. Both information have been reviewed and summarized in this section.

Sodium Chlorite/Bromic Acid

A US. patent [Patent 5,063,034, 1991] was issued to a reducing wet process for flue gas denitrification using the mixture of sodium chlorite and bromic acid. By the wet scrubbing, nitric oxide is oxidized by $NaClO_2$ into nitrogen dioxide which is then reduced to nitrogen by using the reducing properties of SO_2 present in the gas stream. The reduction is effective with the aid of an intermediate agent, HBr, which prevents the oxidation of nitric oxide into nitrates in the scrubbing solution.

Ferrous Cysteine/Cystine

Aqueous ferrous cysteine/cystine system has been reported to be useful for NO removal from gas stream [Chang, 1988]. The coupling chemistry of ferrous cysteine has

been proposed as a 1:2 complex in the alkaline solution. Ferrous cysteine is easily oxidized in air via the formation of ferric cysteine complex. Rapid intramolecular electron transfer from the coordinated cysteine to Fe^{3+} results in the regeneration of Fe^{2+} and the formation of cystine.

The absorption of NO in alkaline ferrous cysteine solution was proposed as:

$$2[Fe^{+2}(cys)^{2}] + 4NO + 3H_2O \rightarrow 2[Fe(OH)^{3}] + \text{cys-scy} + N_2 + N_2O \qquad (2.50)$$

Temperature and pH were found to be the most important factors. Conversion of NO exceeding 80% was reported.

CHAPTER 3

GAS ABSORPTION

3.1 General Concepts

This chapter deals with the specific application of mass transfer principles to gas absorption of NO_X from flue gas. Gas absorption is defined as a physical process where a soluble vapor or gas is preferentially dissolved into a liquid in which the solute gas is more soluble than the other gases in the mixture. The absorption of ammonia from a mixture of ammonia and air by means of liquid water is a typical example. In many pollution control applications, the absorbing liquid is water, and the process is referred to as scrubbing. This operation has been effectively developed for flue gas desulfurization. But applications for NO_X removal are still under investigated because of the low solubility of NO.

Absorption is a unit operation that is enhanced by all the factors which normally increase the rate of mass transfer. Desirable attributes for absorption are high interfacial area, turbulent contact between two phases, increased residence time, repetitive contact, high solubility, high diffusion coefficients, low liquid viscosity, and large negative Gibb's free energy changes in the case of reactive scrubbing (Scrubbing where a chemical reaction takes place with the target gas in order to get it into solution). These factors influence the rate of mass transfer because they directly affect the concentration gradient. For best operation, the contaminants should be readily soluble in the liquid phase and, if possible, undergo an irreversible reaction with the scrubbing reagent. This will allow removal of contaminants completely without fear of secondary release during spent liquid cleanup, pH adjustment, and recycle.

3.2 Absorption Equipment

A well-designed absorber performs many functions. The primary one is removal of the undesirable gas or contaminants by either physical or physico-chemical reaction processes. As a side benefit, particulate removal can also be accomplished with absorption equipment, but the mechanism depends on impingement or other physical interaction between the solid and the liquid. Absorbers are often used to cool, condense heavy components, or humidify the gas stream under treatment. Implicit in the design of a gas absorber for air pollution control service are low energy utilization, long contact time, and high turbulence as those characteristics promote rapid, effective mass transfer and low operating cost.

Gas absorbers and reactive scrubbers are flexible devices that are very dependable and effective. Figure 3.1 shows examples of the variety of commercial equipment used for gas absorption with or without chemical reaction. The selection of the particular scrubber configuration required for a given control problem is not simple. Almost any type of scrubber will be effective if the pollutants are easily absorbed. In these cases, local costs and availability dictate the type of scrubber. However, as indicated above, the design of a scrubber which needs to absorb gases that have low solubility must be designed carefully and may be expensive to operate because of special reagent requirements.

In the case of slow reaction or low contaminant solubility, either the packed bed or plate tower should be selected as it will give adequate residence time for mass transfer. If solids are also present in the gas stream, the selected scrubber must be able to handle them as well. For these, spray chambers or ejectors might be adequate. They can be used as prescrubbers or preconditioners for fluidized beds and cross-flow-type scrubbers.

Cross-flow scrubbers operate at lower pressure drops than counter-current packed beds for the same application. The flooding potential is considerably reduced in the cross-flow design. They are suitable, as opposed to static packed beds which are not, for handling gas streams with high particulate loading.

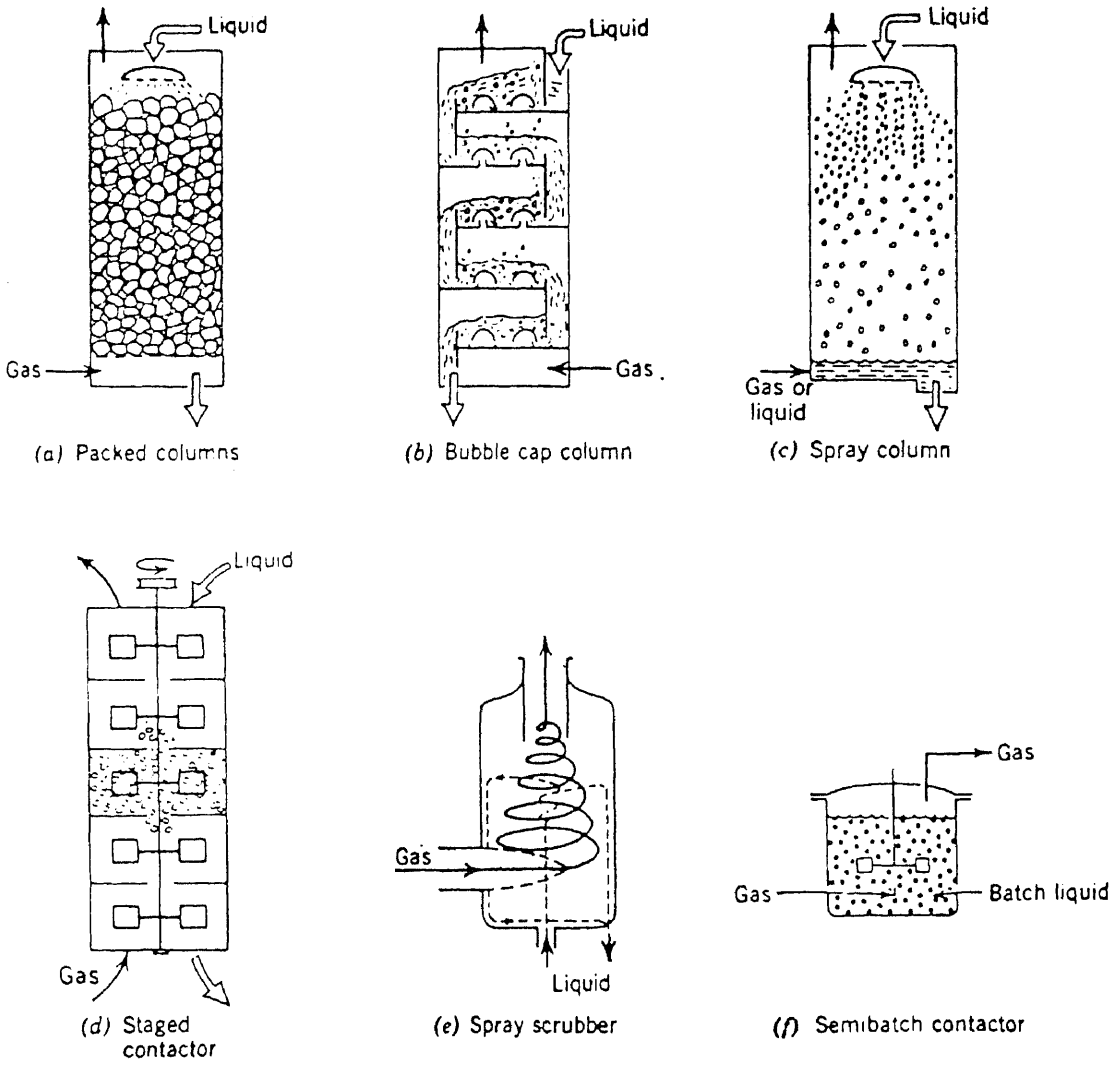

Figure 3.1 Equipment used (Some) commercially for gas absorption

Table 3.1 presents typical data for various scrubbers, from these data we see that spray or plate columns are efficient devices for systems with fast reaction, while bubble contactors are efficient for slow reactions. It should be noted that bubble columns are often used for feasibility and utilization evaluation while spray chamber and packed bed are used to derive process design and scale-up parameters.

Table 3.1 Equipment Characteristics for Gas-Liquid Contactors

Type of Contactor	Interfacial Surface / Volume of Liquid	Interfacial Surface / Volume of Reactor	Volume Fraction of Liquid	Volume of Liquid / Volume of Film
Spray Column	$\cong 200 m^2/m^3$	$\cong 60\ m^2/m^3$	$\cong 0.05$	$\cong 2\text{-}10$
Packed Column	1200	100	0.08	10-100
Plate Column	1000	150	0.15	40-100
Agitated Bubble Contactor	200	200	0.9	150-800
Bubble Contactor	20	20	0.98	4000-10000

Kramers and Westerterp [1964]

Packed Towers

Packed towers are used for continuous, countercurrent or concurrent, contact of liquid and gases in absorption operations. A counter current packed tower usually consists of a cylindrical column equipped with a gas inlet and distributing space at the bottom, a liquid inlet and distributor at the top, and liquid and gas outlets at the bottom and top, respectively. The column is packed with of inert solids called packing which provide relatively large surface area per unit volume. An example of a packed tower is shown in Figure 3.2.

In order to be useful, absorption packing should have the following properties. It should have large effective area, low mass, strong materials of construction, large free cross section when dumped, chemically inertness, small liquid hold-up, and low cost.

There are many types of packing, some of them are made of coke, wood, rocks, or ceramics, metals, or plastics. The most commonly used packing types in the chemical industry are Raschig rings, Berl and Intalox saddles, Spiral rings and miscellaneous types such as Pall rings, Tellerettes, grid blocks, etc. Typical packing are indicated in Figure 3.3. An open space or mechanical distributor at the bottom of the tower is necessary for even distribution of gas into the packing.

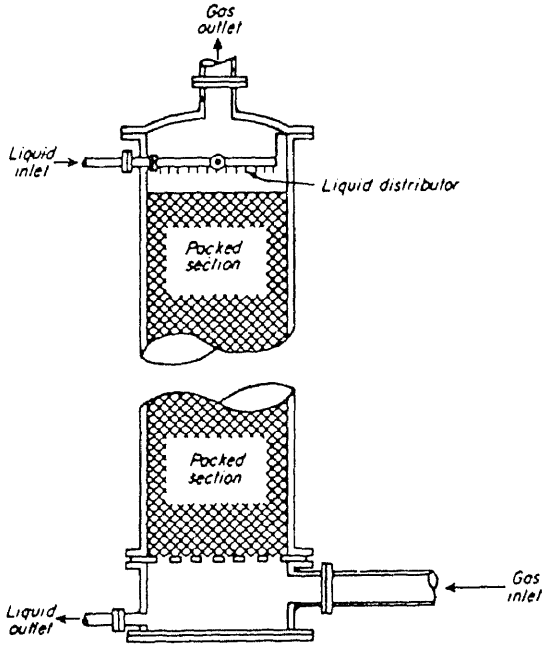

Figure 3.2 Packed tower

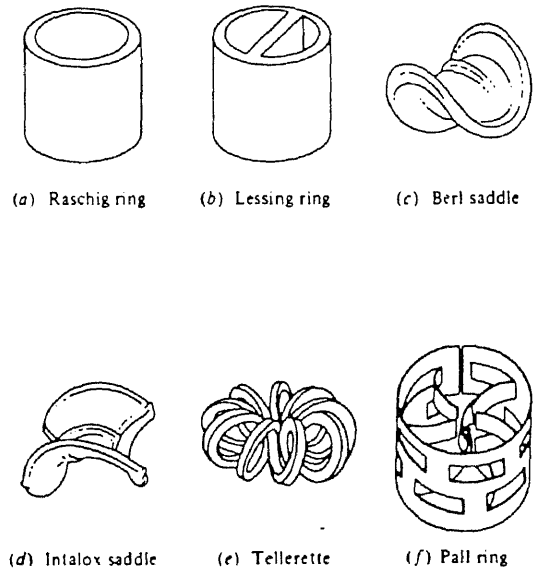

Figure 3.3 Typical dumped-type packing elements

This requires a packing support above the open space. It must be strong enough to support the packing and have enough free area to allow the fluids to flow with a minimum pressure drop. To prevent premature flooding, the net free area should be at least equal to that of the packing itself.

The requirement of good contact between the liquid and the gas is often difficult to attain. Ideally, the liquid flows in a thin film over all the packing surface along the total length of the tower. In reality, liquid tends to collect in small channels and flows in these localized paths through the packing. This effect is known as channeling and it is important to minimize this effect in order to obtain good performance of a packed tower. The tendency of channeling to occur is greatly reduced when the diameter of the individual packing units is less than 1/8 the diameter of the tower. It is generally recommended that redistributors should be installed at intervals varying from three to ten time the tower diameter, but at least every six meters.

The wetted surface may be as low as 30% of the dry packing surface. The wetted fraction is a very weak function of the gas flow rate, but depends very much on the liquid flow rate. As the liquid rate is increased, the wetted fraction of the packing increases until a point at which all the packing becomes completely wet. This critical liquid flow rate is usually high and is termed the minimum wetting rate. Generally, it is desirable to use a liquid mass velocity of at least 1.1 (kg/m^2-s) based on the empty cross section of the tower.

The pressure drop of the flowing gas is a function of the liquid and gas flow rates and the packing characteristics. At a fixed gas flow rate, the pressure drop increases with increasing liquid flow rate. At a fixed liquid flow rate, the liquid holdup can be estimated by the dimensionless equation of Buchanan [1967].

$$h = 2.2\left(\frac{u_l \ \mu_l}{\rho_l \ d_p^2}\right)^{1/3} + 1.8\left(\frac{u_l^2}{g \ d_p}\right)^{1/2} \qquad (3.1)$$

where,

h = liquid hold-up (dimensionless)

μ_l = liquid viscosity (kg/m-s)

u_l = liquid superficial velocity (m/s)

g = 9.81 (m/s^2)

ρ_l = liquid density (kg/m^3)

d_p = nominal packing size (m)

Upon further increase in the gas flow rate, a point is reached at which the gas begins impeding the downward flow of the liquid. This is known as the loading point.

The limiting gas velocity for a given tower is known as the flooding velocity. At flooding, the following changes in operation can be observed. A layer of liquid may appear at the top through which the gas bubbles. Liquid may fill the tower.

Flooding and loading velocities are well correlated for the stacked and the dumped packing as functions of the properties of the fluids processed, flow rates and the packing properties. It is desirable to design the column to operate at flow rates less than the loading points. These conditions are ordinarily met by designing the tower for gas velocities of forty to seventy percent of the flooding velocity. Figure 3.4 may be used to calculate flooding mass flow rates and pressure drop [Perry, 1984]. The pressure drop at the flooding point is independent of the liquid-gas ratio (L/G) and is dependent only on the physical properties of the gas-liquid system and the size and type of packing.

Where,

L = mass velocity of liquid, (lb/ft^2-s)

G = mass velocity of gas, (lb/ft^2-s)

F_p = packing factor, (ft^{-1})

ρ_l = density of liquid, (lb/ft^3)

ρ_g = density of gas, (lb/ft^3)

μ_l = viscosity of liquid, (cp)

g = Newton's law factor, 32.174 (ft-lb/lb$_f$-s)

ψ = the ratio of density of water to the density of liquid

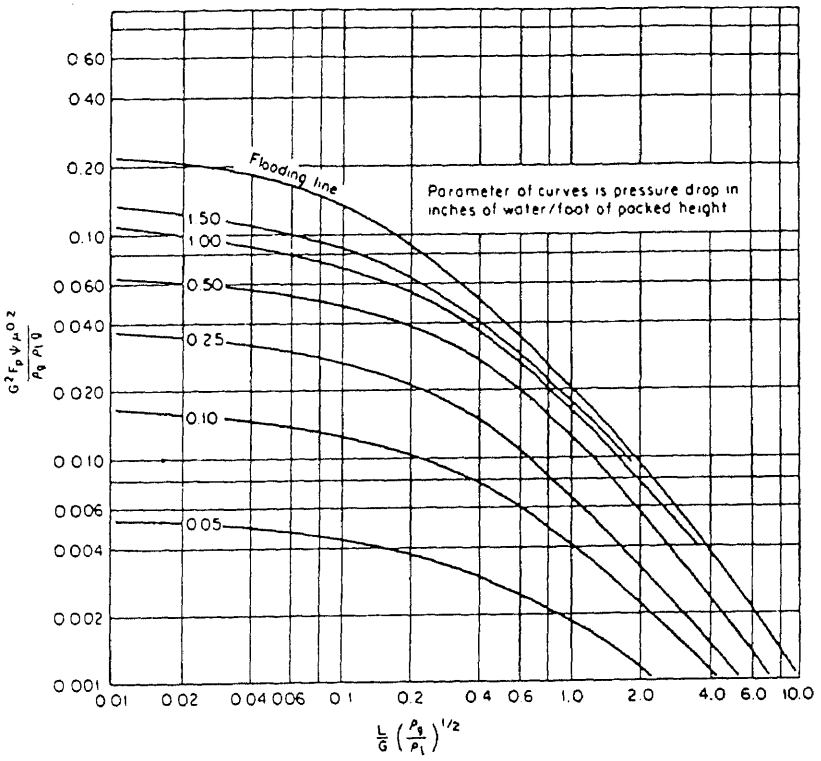

Figure 3.4 Generalized correlation for flooding and pressure drop in packed column

Spray Chambers

Another contacting device used for the study of gas liquid reaction is the spray chamber. In a countercurrent spray tower, drops of liquid are introduced by spray nozzles or shower sprayer and are allowed to fall due to gravity through a rising stream of gas stream. In order not to be entrained by the gas stream, the droplets must be large enough to have a falling speed greater than the upward velocity of the gas stream, which is usually in the range of 0.6 to 1 m/s.

Droplets smaller than 1 mm tend to be approximately spherical, and their falling speeds can be estimated by known methods. The droplets used in spray towers are on the

order of 0.1 to 1 mm in diameter. Under these conditions, its interfacial area has been correlated by Mehta [1970], according to Equation 3.2.

$$A_V = \alpha(\frac{L\rho_p}{\Omega})^{\beta} u_{sg}^{0.28} Z^{-0.38} \tag{3.2}$$

where, A_V is the interfacial surface area, α and β are empirical constants, Ω is cross section area of the column, u_{sg} is the superficial velocity, L is liquid phase mass flow rate, ρ_l is density of liquid, and Z is the effective height of spray chamber.

These units are also used to reduce the gas temperature in an economical fashion. Spray chamber are often used for gas conditioning and gross particulate removal upstream of the primary collector. They are not used extensively for gas absorption because they have a very low efficiency due to the limited amount of interfacial contact area. One can visualize a spray chamber being used as a prescrubber to convert 50% of incoming NO to NO_2. The effluent containing NO, NO_2 and SO_2 then can be treated with lime slurry.

The spray chambers operate essentially in a once-through mode. The pressure drop through spray absorbers is 1/2 to 3/2 in. of water. Superficial gas velocities can approach 2 ft/s. Because these devices are completely open, they are not subject to particulate plugging, which makes a spray chamber a good option for a prescrubber in an air pollution control process.

3.3 Physical Absorption

Experiments show that during absorption of a gas in a turbulent liquid, The mass flux, N, may be expressed as a driving force multiplied by a mass transfer coefficient k_l.

$$N = k_l(dC) \tag{3.3}$$

The basic equation describing the process of mass transfer is:

$$\frac{\partial C}{\partial t} + v\nabla C = D\nabla^2 C + R \tag{3.4}$$

where C is the molar concentration of the solute A, t is time, v the velocity of the liquid, D the diffusion coefficient of A in the liquid and R is the molar rate of disappearance of A by a chemical reaction, if significant.

Three models were proposed to explain the interfacial mass transfer mechanism. They are the thin film model by Whitman [1923], the penetration model by Higbie [1935], and the random surface renewal model by Danckwerts [1951]. All of them assume that diffusion of A takes place in a stagnant liquid, and as a consequence, the velocity term in Equation 3.3 becomes zero. From this point of view, all of the models belong to the same class called stagnant liquid models.

The film model was first proposed by Whitman. Instead of considering a progressive decrease of the turbulence as the interface is approached, he assumed a sharp change in the hydrodynamic conditions of the liquid, so that from the interface up to a depth d_f the liquid is frozen, forming a stagnant film, while after d_f the liquid is perfectly mixed.

From the formulation of the model, it follows that mass transfer is eventually in a steady state and mass transfer only occur in a stagnant liquid film. Both terms in the left-hand side of Equation 3.4 are zero. If physical absorption predominates, then R approaches zero.

$$D\frac{d^2C}{dx^2} = 0 \tag{3.5}$$

Now the boundary conditions can be stated as follows:

$$\text{At } x = 0 \qquad C = C_o \tag{3.6}$$

$$\text{At } x = d_f \qquad C = C_l \tag{3.7}$$

Integration of Equation 3.5 gives a linear dependence of concentration on x as follows:

$$C = -(C_o - C_l)\left(\frac{x}{d_f}\right) + C_o \tag{3.8}$$

The flux of A is given by:

$$N_A = -D\left(\frac{dC_A}{dx}\right)_{x=0} = \left(\frac{D}{d_f}\right)(C_{Ao} - C_{Al}) = 0 \qquad (3.9)$$

and since N has already been defined in Equation 3.3, k_l can be expressed as

$$k_l = D/d_f \qquad (3.10)$$

Equation 3.9 states that the mass transfer flux per unit driving force, that is k_l, is a function of two variable. The diffusivity of the gas in the liquid which is a physical property of the system, and d_f, which represents the hydrodynamics of the system.

The overall gas phase mass transfer coefficient K_{og} multiplied by the overall interface area, a, can be expressed in terms of the two localized film coefficients as shown in Equation 3.11.

$$K_{og}a = \frac{1}{\frac{1}{k_g a} + \frac{m}{k_l a}} \qquad (3.11)$$

where,

a = total interfacial contact area, (ft^2)

K_{og} = overall volumetric mass transfer coefficient, (lb mole/hr ft^2 atm)

k_g = local gas phase mass transfer coefficient, (lb mole/hr ft^2 atm)

k_l = local liquid phase mass transfer coefficient, (lb mole/hr ft^2 atm)

m = slope of equilibrium distribution, (mole gas/mole liquid), or Henry's law constant for gas-water system.

If the value of the Henry's law constant H is < 3 (atm ft^3/lb mole), the gas phase controls the rate of mass transfer. If H > 3000 (atm ft^3/lb mole), the liquid phase is controlling [Bethea, 1978].

3.4 Chemical Absorption

When a scrubbing solution contains a compound B, which can react with compound A, the contaminant in gas phase, then removal of A is referred as chemical absorption. compound B will prevent the concentration of A to build up in the bulk liquid. The overall rate expression for the reaction will have to account for mass transfer resistance, to bring reactants together, and the resistance due to the chemical reaction rate. The relative magnitude of these two resistance can vary greatly and each situation requires its own analysis. The first problem is to identify these time dependent regimes and to select the one which matches the given physical situation.

Depending on the relative rates of diffusion and reaction, the absorption systems are classified into five different regions and shown in Figure 3.5 [Levenspiel, 1972]. The rate equations for absorption with instantaneous reaction and fast reaction will be developed for their applicable to reactive scrubbing.

Rate Equation for Instantaneous Reaction

Consider an infinitive fast reaction of any order:

$$aA_{\text{(from gas)}} + bB_{\text{(liquid)}} \rightarrow \text{product} \tag{3.12}$$

If C_B is not too large, the situation is illustrated in Figure 3.6. At steady state, the flow rate of B toward the reaction zone will be b times the flow rate of A toward the reaction zone. Thus, the rate of disappearance of A and B are given by

$$-r''_A = -\frac{r''_B}{b} = k_{Ag}(p_A - p_{Ai}) = k_{Al}(C_{Ai} - 0)\frac{x_o}{x_o - x} \tag{3.13}$$

where r" is the rate of disappearance per unit interface area, k_{Ag} and k_{Al} are the mass transfer coefficients in gas and liquid phases.

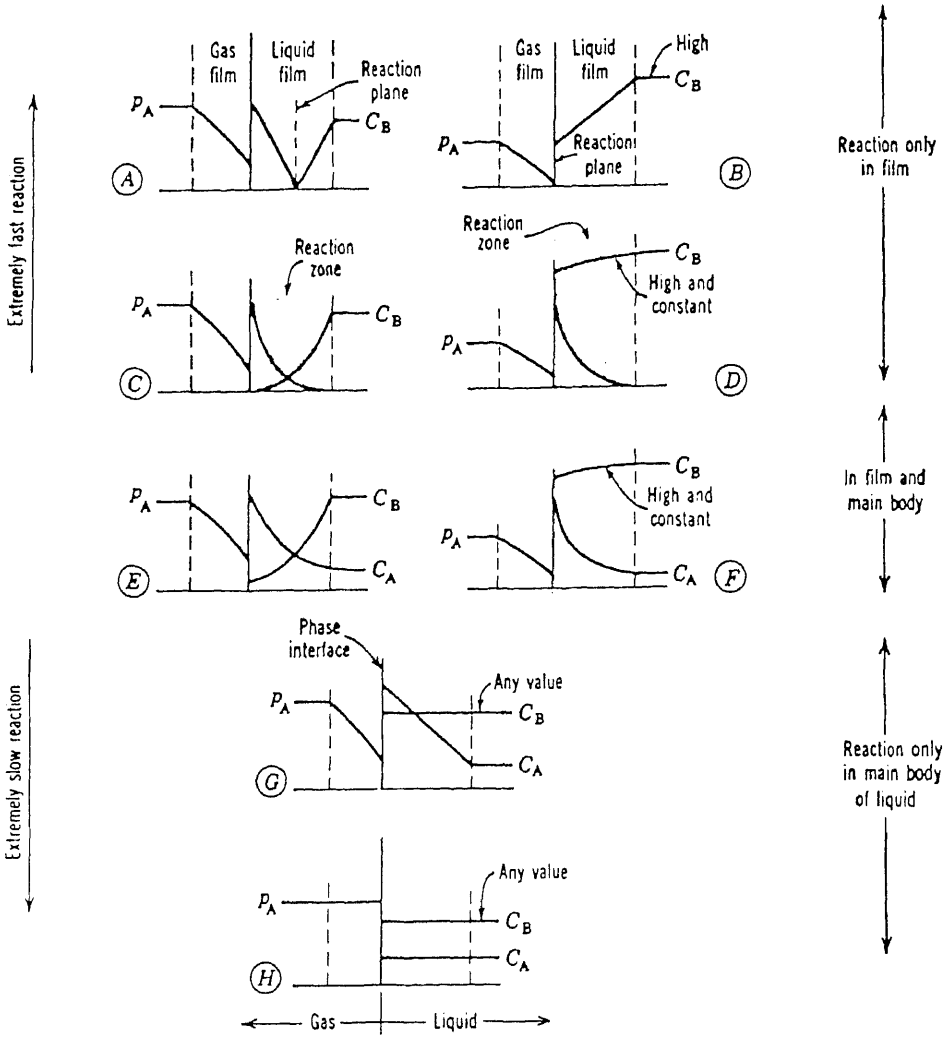

Figure 3.5 Interfacial behavior for the liquid phase reaction, Eq. 3.11, for the complete range of rates of the reaction rate and the mass transfer rate.

At the interface, the relationship between P_A and C_A is given by Henry's law constant for gas liquid systems. Thus

$$P_{Ai} = H_A C_{Ai} \tag{3.14}$$

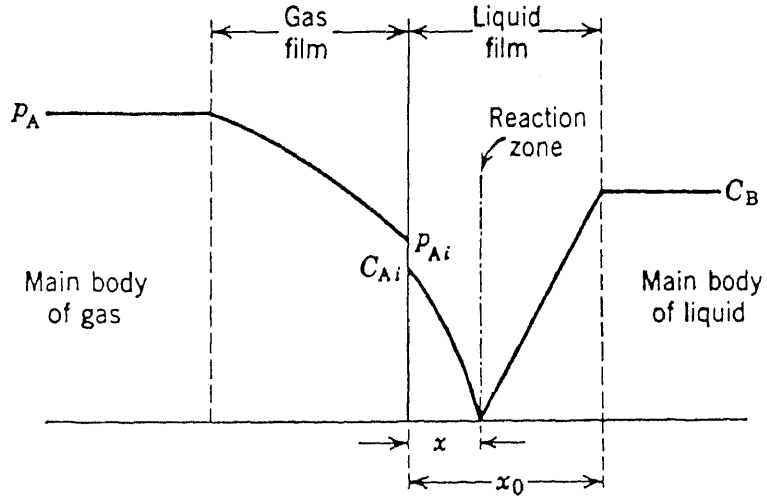

Figure 3.6 Concentrations of reactants as visualized by the two film theory.

Since the movement of material within the film is visualized to occur by diffusion alone, the transfer coefficients for A and B are related by

$$\frac{k_{Al}}{k_{Bl}} = \frac{\dfrac{D_{Al}}{x_o}}{\dfrac{D_{Bl}}{x_o}} = \frac{D_{Al}}{D_{Bl}} \tag{3.15}$$

Eliminating the unknowns in Equations 3.13, 3.14, and 3.15, we obtain

$$-r''_A = -\frac{1}{s}\frac{dN_A}{dt} = \frac{\dfrac{D_{Bl}}{D_{Al}}\dfrac{C_B}{b} + \dfrac{P_A}{H_A}}{\dfrac{1}{H_A k_{Ag}} + \dfrac{1}{k_{Al}}} \tag{3.16}$$

For the special case of negligible gas phase resistance, k_{Ag} is infinitive, and $P_A = P_{Ai}$, Equation 3.16 reduces to

$$-r''_A = k_{Al} C_{Ai}\left(1 + \frac{D_{Bl} C_B}{b D_{Al} C_{Ai}}\right) \tag{3.17}$$

Comparing Equation 3.17 with the expression for the maximum rate of mass transfer, or

$$-r''_A = k_{Al} C_{Ai} \tag{3.18}$$

it is found that the term in brackets represents the increase in rate of absorption of A resulting from adding reactant B to the liquid. Thus a enhancement factor is defined as

$$E = \left(\frac{\text{Rate with reaction}}{\text{Rate for mass transfer}}\right) \tag{3.19}$$

For the case of infinitely fast reaction rate and no gas phase resistance

$$-r''_A = k_{Al} C_{Ai} E \tag{3.20}$$

where,

$$E = 1 + \left(\frac{D_{Bl} C_B}{b D_{Al} C_{Ai}}\right) \tag{3.21}$$

For the special case of high C_B, or if

$$k_{Al} \leq \frac{k_{Bl}}{b} C_B \tag{3.22}$$

then this condition, requires that the reaction zone move to and remain at the interface. When this happens, the resistance of the gas phase controls, and the rate is not affected by any further increase in concentration of B. Equation 3.15 simplifies to

$$-r''_A = \frac{1}{S}\frac{dN_A}{dt} = k_{Ag} p_A \tag{3.23}$$

Note that the reaction rate constant does not enter into either Equation 3.15 or 3.22, showing that the rate is completely mass transfer controlled. Also, even though the resistance of liquid film may normally control, when C_B is raised sufficiently, then the resistance always shifts to gas phase control.

Rate Equations for Fast Reaction

For a second order reaction between A and B

$$-r_{Al} = \frac{1}{V}\frac{dN_A}{dt} = k C_A C_B \tag{3.24}$$

In the gas and liquid films

$$-r''_A = k_{Ag}(p_A - p_{Ai}) = k_{Al} C_{Ai} E \tag{3.25}$$

Eliminating C_{Ai} and P_{Ai} with Equation 3.14 gives

$$-r''_A = \frac{1}{\frac{1}{k_{Ag}} \frac{H_A}{k_{Ai} E}} p_A \tag{3.26}$$

For the special case where C_B is sufficiently high to be considered constant the reaction in the liquid becomes pseudo-first order, or

$$-r_A = k C_A C_B = (k C_B) C_A = k_1 C_A \tag{3.27}$$

in which case the enhancement factor is a simple expression, as follows:

$$E = \frac{\sqrt{D_{Al} k C_B}}{k_{Al}} = \frac{\sqrt{D_{Al} k_1}}{k_{Al}} \tag{3.28}$$

For a special case of high C_B, intermediate concentrations can be eliminated. The rate equation becomes

$$-r''_A = \frac{1}{\frac{1}{k_{Ag}} + \frac{H_A}{\sqrt{D_{Al} k C_B}}} \tag{3.29}$$

Note that film thickness does not enter into this expression since reactant A does not penetrate and uses the whole film.

3.5 Surface Reaction in a Spray Chamber

In order to estimate the potential use a spray chamber as a pre-scrubber, a droplet surface reaction model was derived from the surface area correlation of a shower sprayer [Metha,

1970], given in Equation 3.1. The mathematical model for estimating the height of a scrubber, a key scale-up parameter, is obtained by conducting a material balance around a differential element of volune in the absorption chamber. At steady state, the amount of A reacting with B will disappear from the gas phase. In this case, A is NO and B is $NaClO_2$.

$$-r''_A = \frac{dC_A}{dt} = k' C_A^m C_B^n \tag{3.30}$$

where k' is the reaction rate constant per unit interfacial area. Equation 3.30 can be rewritten as

$$-\frac{dC_A}{dt} = k A_V C_A^m C_B^n \tag{3.31}$$

where A_V is the interfacial surface area in the spray chamber. Eliminating A_V with Equation 3.2 gives

$$-\frac{dC_A}{dt} = k\alpha\left(\frac{L\rho_l}{\Omega}\right)^{\beta} u_{sg}^{0.28} Z^{-0.32} C_A^m C_B^n \tag{3.32}$$

$$t = \frac{V}{v_o} = \frac{Z\Omega}{v_o} = \frac{Z}{\left(\frac{v_o}{\Omega}\right)} = \frac{Z}{u_{sg}} \tag{3.33}$$

where V is the effective volume of absorber and v_o is the volumetric flow rate of gas.

For each run, u_{sg} is a constant. Differentiating Equation 3.33, one obtains

$$dt = \frac{1}{u_{sg}} dZ \tag{3.34}$$

Substituting Equation 3.34 into Equation 3.32 and rearranging, we get

$$-\frac{dC_A}{C_A^m} = k\alpha\left(\frac{L\rho_l}{\Omega}\right)^{\beta} u_{sg}^{0.28} Z^{-0.38} C_B^n dt \tag{3.35}$$

For the special case where C_B is large enough to be considered constant and first order with respect to C_A, integration of Equation 3.35 gives

$$X_A = 1 - \exp[-K(\frac{L^{\beta}}{u_{sg}^{0.72}})] \tag{3.36}$$

where, X_A is the conversion of A and is defined as

$$X_A = 1 - \frac{C_A}{C_{Ao}} \tag{3.37}$$

K is a lumped constant

$$K = \alpha' k(\frac{\rho_l}{\Omega})^{\beta} Z^{0.62} C_B^n \tag{3.38}$$

where

$$\alpha' = \frac{\alpha}{0.62} \tag{3.39}$$

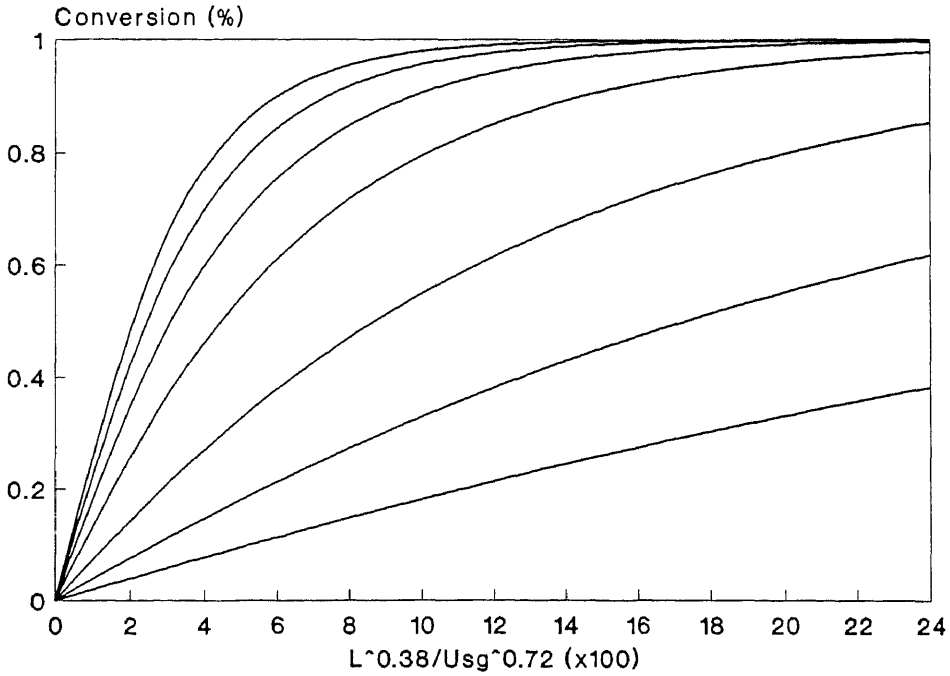

Figure 3.7 Model calculation of NO conversion in a shower spray chamber with a first order reaction in NO

For shower sprayer, α and β are $2.46(10)^{-2}$ and 0.38 respectively. The results of calculations are shown in Figure 3.7.

For the special case of excess C_B and zero order in C_A, integration of Equation 3.35 gives

$$\frac{C_A}{C_{Ao}} = 1 - K'\left(\frac{L^{0.38}}{u_{sg}^{0.72}}\right) \tag{3.40}$$

where,

$$K' = \alpha' k\left(\frac{\rho_l}{\Omega}\right)^{\beta} Z^{0.62} C_{Ao} C_B^n \tag{3.41}$$

The calculated results are shown in Figure 3.8.

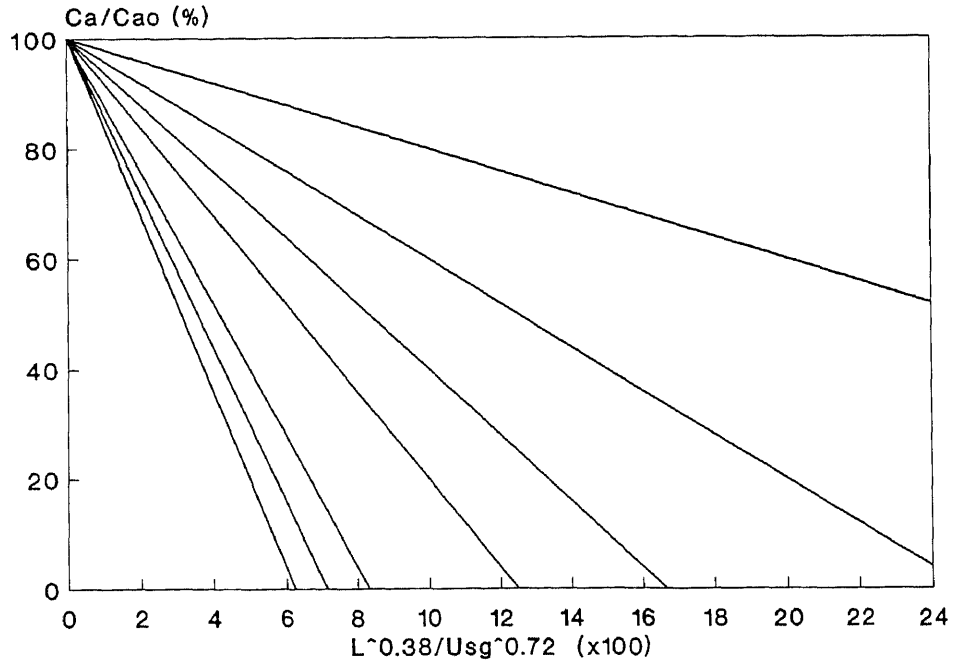

Figure 3.8 Model calculation of NO conversion in a shower spray chamber with a zero order reaction rate in NO

Using Figures 3.7 and 3.8, one can correlate the experimental data. It should be noted that this model is based on the surface area correlation of Mehta and Sharma [1970].

3.6 Chemical Absorption in a Packed Bed

Rate of absorption can be expressed in four different ways by using individual or overall mass transfer coefficients based on the gas or liquid phases. The rate of absorption per unit volume of a packed column is given by any of the following equations, where y and x are the mole fraction of the components which are absorbed in gas and liquid phases respectively.

$$r = k_y a(y - y_i) \tag{3.42}$$

$$r = k_x a(x_i - x) \tag{3.43}$$

$$r = K_y(y - y^*) \tag{3.44}$$

$$r = K_x a(x^* - x) \tag{3.45}$$

An absorber can be designed using any of the four basic rate equations, but the gas film coefficients are most common. Consider the packed bed shown in Figure 3.2. The cross section is Ω and the differential volume in height dZ is ΩdZ. If the change in molar flow rate F is neglected, the amount absorbed in section dZ is -Fdy, which equals the absorption rate times the differential volume:

$$-Fdy = K_y a(y - y^*)\Omega dZ \tag{3.46}$$

This equation is rearranged for integration, grouping the constant factors F, Ω, and $K_y a$ with dZ.

$$\frac{K_y a\Omega}{F}\int_0^{Z_T} dZ = \frac{K_y a\Omega Z_T}{F} = \int_b^a \frac{dy}{y - y^*} \tag{3.47}$$

The equation for column height can be written as follows:

$$Z_T = [\frac{(\frac{F}{\Omega})}{K_y a}]\int_b^a \frac{dy}{y - y^*} \tag{3.48}$$

The integral in Equation 3.48 represents the change in vapor concentration divided by the average driving force and is called the number of transfer units (NTU) or N_{oy}. The

other part of Equation 3.48 has the unit of length and is called the height of transfer unit (HTU) or H_{oy}.

Reaction in the liquid phase reduces the equilibrium partial pressure of the solute over the solution, which greatly increases the driving force for mass transfer. If the reaction is essentially irreversible at absorption conditions, the equilibrium partial pressure is zero, and Noy can be calculated just from the change in gas composition. For $y^* = 0$,

$$N_{oy} = \int_b^a \frac{dy}{y} = \ln\left(\frac{y_a}{y_b}\right) \tag{3.49}$$

A large part of the research described in this thesis is directed at obtaining the H_{oy} for NO absorption with $NaClO_2$ oxidation in a packed bed. Other parts of this research are designed to evaluate the effects of key parameters such as temperature, concentration, pH, etc. on NO absorption using H_{oy} as an index.

Notation

Ω, cross sectional area of tower (ft^2 or m^2).

α, correlation constant.

β, correlation constant.

μ_l, liquid viscosity (kg/m-s).

a, area of interface per unit packed volume (ft^2/ft^3 or m^2/m^3).

A_V, interfacial surface area (m^2 or ft^2).

C_i, concentration of component i ($kmole/m^3$).

D, diffusivity (ft^2/hr).

d_f, thickness of the stagnant liquid film (ft or m).

d_l, density of liquid phase (kg/m^3 or lb/ft^3).

d_p, nominal packing size (m).

E, enhancement factor, ratio of mass transfer flux with and without chemical reaction (dimensionless).

F, molar flow rate of gas phase

F_p, packing factor (ft^{-1}).

g, 9.81 (m/s^2)

G, mass velocity based on cross section area (lb/ft^2-s or kg/m^2-s).

g_c, Newton's law factor, 32.174 ($ft\text{-}lb/lb_f\text{-}s^2$).

G_x, G of liquid stream.

G_y, G of gas stream.

h, liquid hold-up

H_{oy}, height of a transfer unit based on overall gas phase driving force (m).

HTU, height of a transfer unit (m).

k", surface reaction constant (m/hr-kmole).

$K_x a$, overall mass transfer coefficient based on liquid phase driving force ($kmole/m^3$-hr-unit molarity difference).

$K_y a$, overall mass transfer coefficient based on gas phase driving force($kmole/m^3$-hr-atm).

L, molar flow rate of liquid (mole/hr).

L_m, liquid phase mass flow rate (lb/s or kg/s).

m, slope of equilibrium distribution (mole gas/mole liquid), Henry's law constant for gas-water system.

N, mass flux (lb/ft^2-hr or kg/m^2-hr).

N_{oy}, number of transfer units based on overall gas phase driving force.

P_i, partial pressure of component i (atm).

r, reaction rate (mole/s).

t, time (sec or hr).

u_l, liquid superficial velocity (m/s).

U_{sg}, superficial velocity (m/hr).

V, effective volume of an absorber (m^3).

v_o, volumetric flow rate (ft^3/hr or m^3/hr)

y, mole fraction of solute in gas (dimensionless).

y_a, y at gas inlet.

y_b, y in gas outlet.

Z_T, total height of packed section (m).

CHAPTER 4

ANALYTICAL METHODS DEVELOPMENT

4.1 Introduction

In the broadest sense, chemical analysis provides information about the composition of a sample. Qualitative results yield useful clues from which compositions, structural features, or even functional groups can be deduced. On the other hand, quantitative analysis results take the form of numerical data in units such as percent, ppm, or moles per liter. In both types of analysis, the required information is obtained by measuring one of the physical or chemical properties of the component of interest.

Properties that are useful for determining chemical compositions are called analytical chemistry. Analytical chemistry uses that signals include intensity of emitted or absorbed light such as IR, UV, or chemiluminescence, electrical or thermal conductivity, weight, volume, refractive index etc. None of these signals is unique to a given species. Therefore, almost all analysis require separations or calibrations.

4.2 Gas Phase Monitoring of NO, NO_2, O_2, and SO_2

During scrubbing, concentration change of NO, NO_2, O_2, and SO_2 in the gas phase were determined by NO/NO_X analyzer, process O_2 monitor, and UV SO_2 analyzer.

Chemiluminescent NO/NO_X Analysis

The chemiluminescent producing reaction of NO and O_3 provides the analysis signal for this technique. Specifically,

$$NO + O_3 \rightarrow NO_2^* + O_2 \qquad (4.1)$$

$$NO_2^* \rightarrow NO_2 + h\nu \qquad (4.2)$$

Light emission results when electronically excited NO_2 molecules revert to their ground state.

To measure NO concentrations, the gas sample to be analyzed is blended with O_3 in a reaction chamber. The O_3 is generated in situ by a high voltage arc ozone generator. The resulting chemiluminescence is monitored through an optical filter by a high sensitivity photomultiplier positioned at one end of the chamber. The filter/photomultiplier combination responds to light in a narrow wavelength band unique to Reaction 4.2. The output from the photomultiplier is linearly proportional to the NO concentration.

Basically, chemiluminescent analysis is only sensitive to NO, to measure NO_X concentrations, NO plus NO_2, the sample gas flow is diverted through a high temperature NO_2 to NO converter. A temperature controller is used to maintain the proper temperature for NO_2 thermal conversion to NO which is 670 ^oC. The chemiluminescent response in the reaction chamber to the converter effluent is linearly proportional to the NO_X concentration entering the converter.

Both concentrations of NO and NO_2 were analyzed by Thermoelectron model 10A NO/NO_X analyzer and Beckman model 955 NO/NO_X analyzer independently to double check the results.

Both instruments were calibrated with an analyzed mixture of 307 ppm NO and 320 ppm NO_2 in nitrogen. In all runs, the agreement between both measurements are better than 10%. The output signal from both analyzers were continuously recorded. A strip chart of a breakthrough test is shown in Figure 4.1.

Electrical Conductance O_2 Analysis

The oxygen concentration is determined with Beckman model 715 process oxygen monitor. This instrument has an amperometric oxygen sensor, which contains a metallic cathode and anode. The two electrodes are separately mounted within the polyethylene body and are electrically connected by a potassium chloride electrolyte. A constant potential is impressed across the two electrodes. A gas-permeable Teflon membrane separates the electrodes from the process sample and fits firmly against the cathode. Oxygen from the sample diffuses through the membrane and is reduced at the cathode.

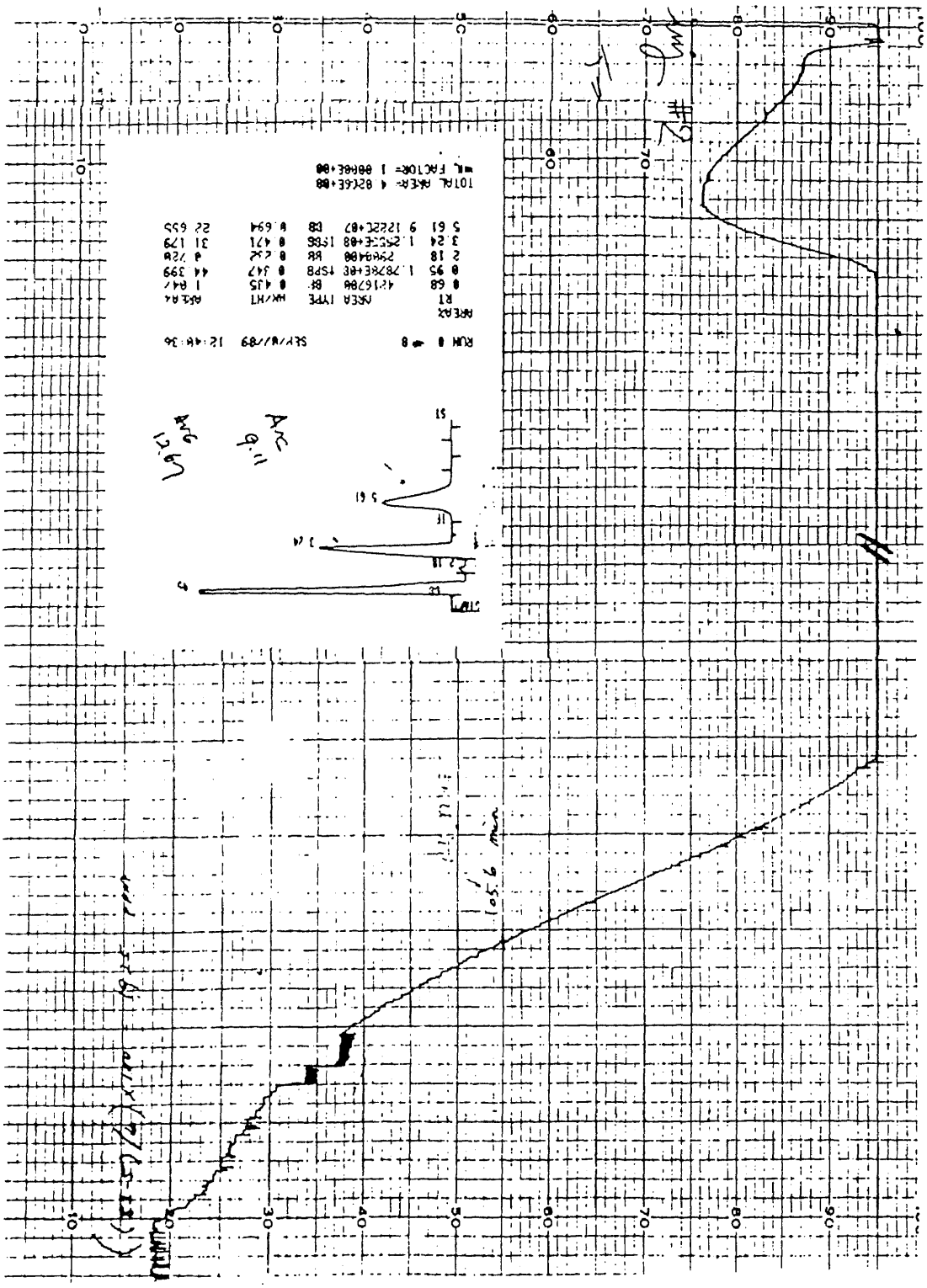

Figure 4.1 The strip chart of NO/NO_X analyzer for a breakthrough test of NO absorption with $NaClO_2$ oxidation

The resultant electrical current flow between the anode and cathode is proportional to the partial pressure of oxygen in the sample.

The sensor is calibrated with an analyzed 5% oxygen in nitrogen mixture and an air sample assumed to be 21% oxygen. Signal from the monitor is recorded continuously.

A Beckman model 7005 oxygen monitor is used to double check the results from model 715. The agreement between these two instruments is always better than 10%.

Ultraviolet SO_2 Analysis

The Rosemount Model 890 UV analyzer is designed to determine continuously the concentration of SO_2 in a flowing gaseous mixture. This instrument is capable of measurement in the 50 to 5,000 ppm range.

The ultraviolet source emits a pulsed beam of energy. This energy is split by a beam splitter, each beam being directed to pairs of detectors before and after the sample cell.

Four detectors are used in this system, two before the sample cell, sample before [S_b] and reference before [R_b], and two after, sample after [S_a] and reference after [R_a]. S_b and S_a receive energy in the 265 to 310 nm wavelength region, R_b and R_a in the 310 to 355 nm region.

These four detectors measure SO_2 concentration and correct for NO_2 interference and UV lamp fluctuations. The difference between detector determinations is the SO_2 concentration, following this equation:

$$SO_2 = [f(R_b) - S_b] - [f(R_a) - S_a] \qquad (4.3)$$

where f is the attenuation factor for the reference signal, adjusted to compensate for NO_2 interference.

This instrument was calibrated with analyzed mixture of 495 ppm SO_2 in nitrogen. signal from the analyzer is recorded continuously.

4.3 On-line Determination of Oxychlorine Compounds, Cl_2, HClO, ClO^-, ClO_2, and ClO_2^-

A Waters preparatory liquid chromatography (prep. LC) with no separation column and equipped with a UV/Visible range photodiode array detector was used to obtain all spectra reported in this thesis. A NEC AT personal computer with Waters PDA 990 Data Acquisition System was employed to collect and treat all analytical data. Samples were diluted and buffered by the eluent pumping system of the prep. LC and was pumped into the flow cell where light could pass through the solution and reach the photodiode array after reflecting from a flat-focus holographic grating. The physical width of the slit is 0.25 mm. However, there are a variety of slit widths available ranging from 0.05 mm to 0.25 mm. The Waters PDA consists of 512 photodiodes, each with a dynamic range from ultraviolet to near infrared, 190 to 800 nm.

Concentration distributions of the hypochlorite system containing Cl_2, HClO, ClO^-, and the chlorite system containing Cl^-, ClO_2^-, and ClO_2 were obtained from three dimensional plots of intensity, wave length, and time. Figure 4.2 shows the real time monitoring of ClO_2^- at 259 nm and ClO_2 at 358 nm.

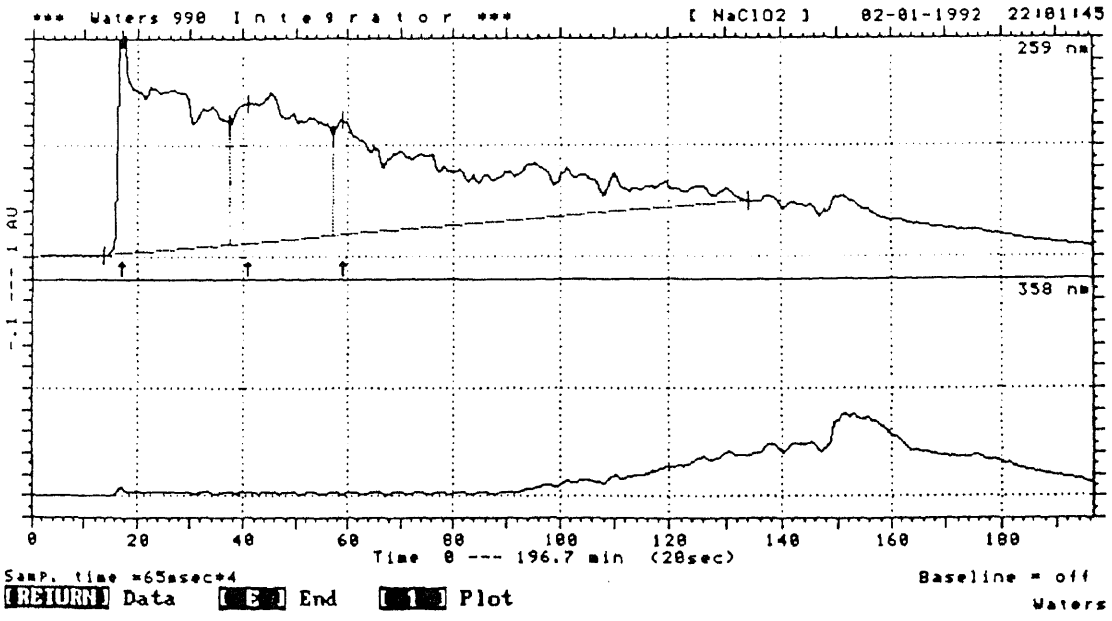

Figure 4.2 $NaClO_2$ depletion and ClO_2 formation during the NO scrubbing

The method for calibrating the system for ClO_2^-, ClO^-, HClO and ClO_2 is described below.

Chlorite (ClO_2^-)

An appropriate concentration of sodium chlorite in aqueous solution was prepared to obtain an absorbance of about 2 absorbance unit (AU) at a wavelength of 260 nm. The spectrum of aqueous sodium chlorite as a function of concentration is shown in Figure 4.3. Programmed pumping was used to dilute the inlet sample of 330 ppmw Cl by 1/10, 2/10, and so on of the original concentration with deionized water. Each composition was scanned for 30 minutes in order to obtain 6 data points which were used to derive the calibration curve shown in Figure 4.4. To explore the accuracy of the lower detection limit, the scale was changed to 0.05 AU. The resulting low concentration calibration curve for sodium chlorite is shown in Figure 4.5 which has a multiple coefficient of determination R^2 (Variations explained by the data fit out of total variations of the data) better than 0.999. Consequently, the linearity of the calibration between 0 and 330 ppmw Cl for $NaClO_2$ is demonstrated.

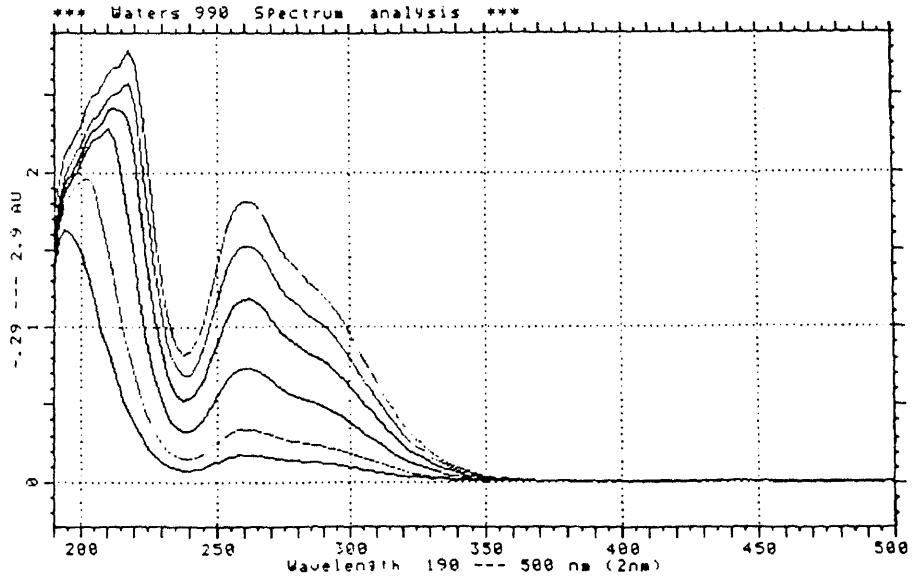

Figure 4.3 The UV/Visible spectrum of $NaClO_2$ as a function of wavelength and concentrations of 330, 264, 198, 132, 66, and 33 ppm Cl (contained in $NaClO_2$).

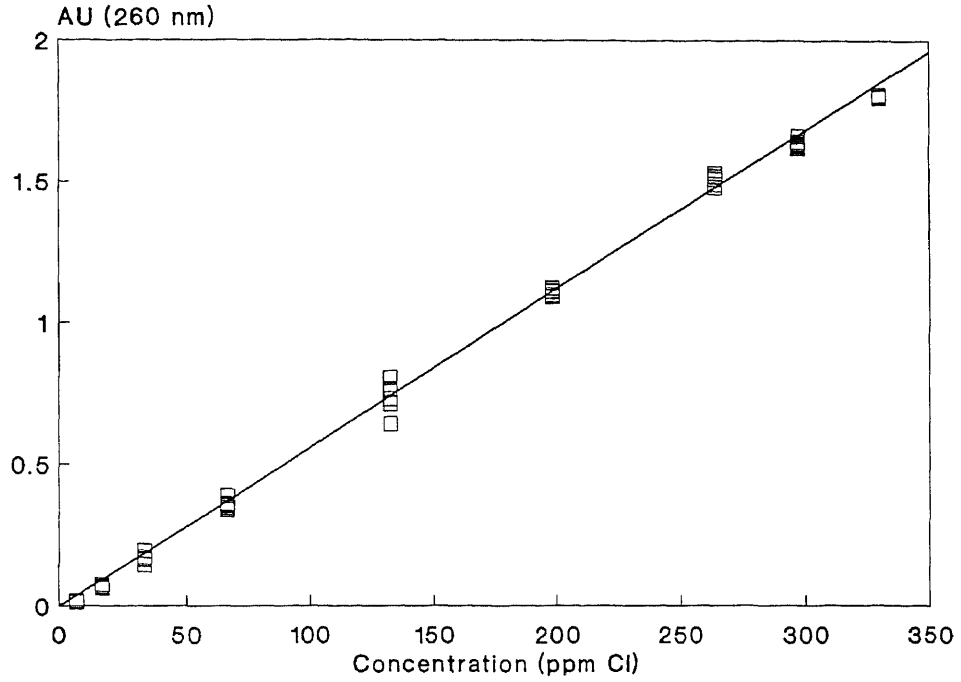

Figure 4.4 Calibration curve of high concentration of $NaClO_2$ diluted with the eluent pumping system of the Waters preparatory liquid chromatography.

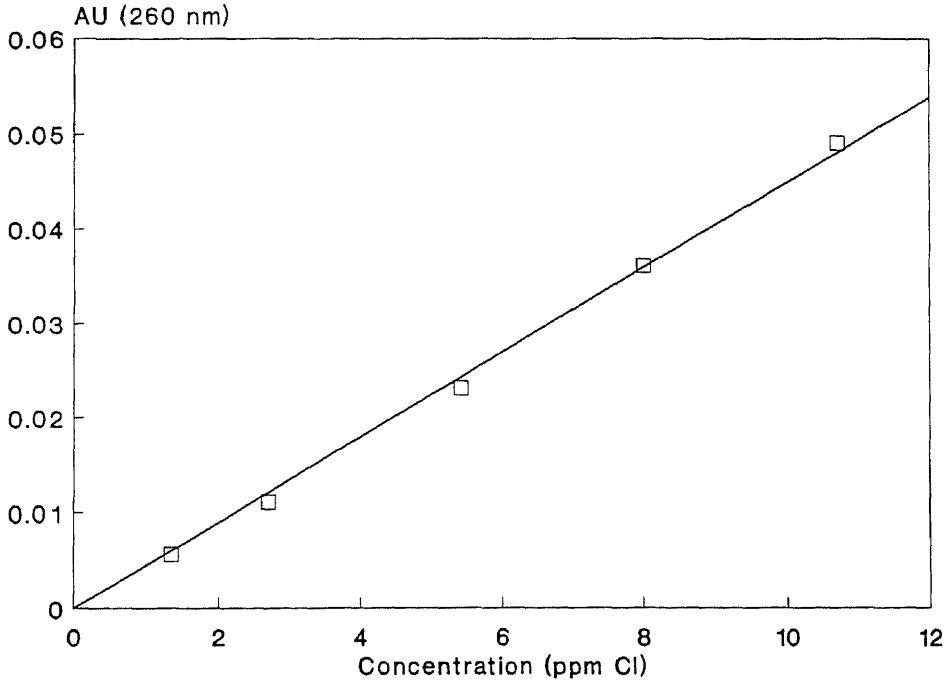

Figure 4.5 Calibration curve of very low concentration $NaClO_2$ diluted with the eluent pumping system of the Waters preparatory liquid chromatography.

Chlorine Dioxide ClO_2

According to the stoichiometric equation for the formation of chlorine dioxide from sodium chlorite, hydrochloric acid was titrated with aqueous sodium chlorite in an ice bath to produce an appropriate concentration of chlorine dioxide with absorbance about 2 AU. A UV spectrum for ClO_2 was obtained as shown in Figure 4.6, this spectrum, which was not independently confirmed, is in agreement with the data of W. Finkelnburg [Calvert, 1966].

The calibration curve shown in Figure 4.7 was obtained by diluting the ClO_2 with the eluent pumping system of the prep. LC. The multiple coefficient of determination R^2 was better than 0.998 for 36 data points.

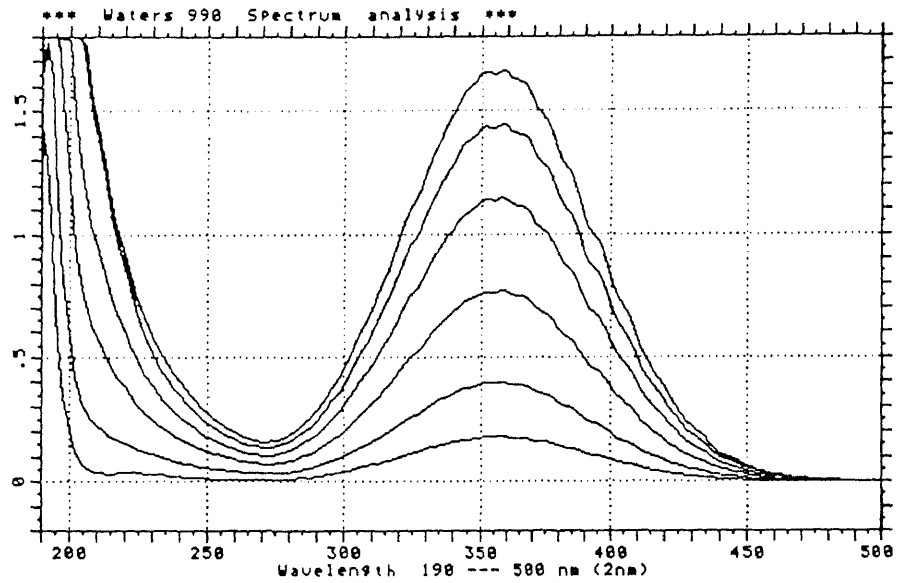

Figure 4.6 The UV/Visible spectrum of ClO_2 as a function of wave length and concentrations of 190, 152, 114, 76, 38, and 19 ppmw Cl.

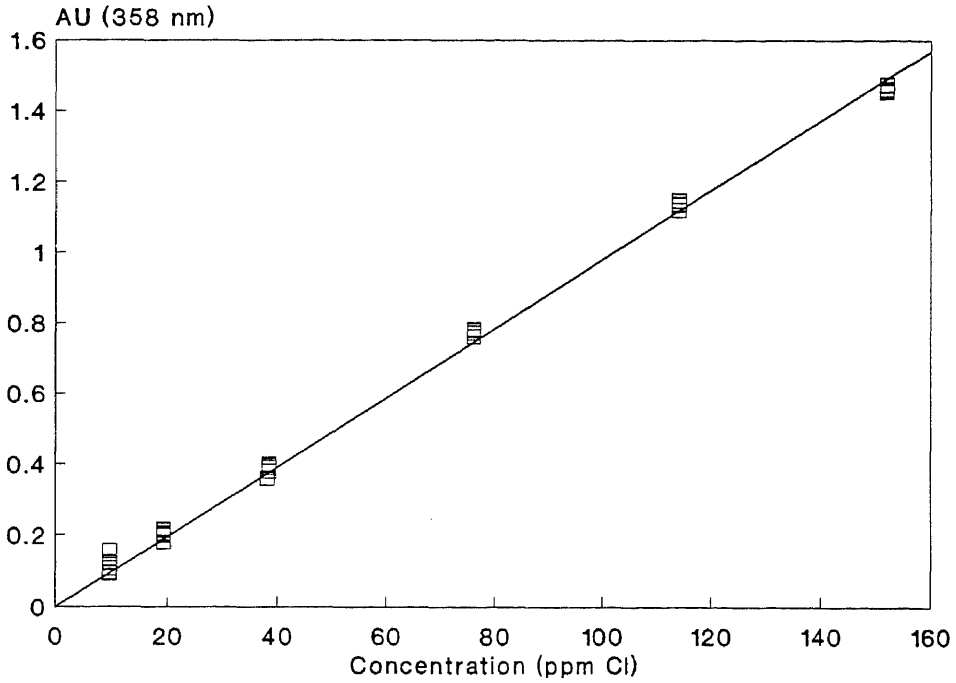

Figure 4.7 Calibration curve of an aqueous solution ClO_2 diluted with the eluent pumping system of the Waters preparatory liquid chromatography.

Hypochlorite (ClO^-)

Chlorine, when dissolved in water, produces hypochlorous acid, hypochlorite and chloride ions, which equilibrate rapidly to reproducible concentrations as a function of pH. Monitoring both OCl^- and HClO levels is necessary to establish the disinfecting power of chlorine gas.

Figure 4.8 shows the complete equilibrium spectrum for water chlorination at pH 6.5 as a function of chlorine concentration based on the absorbance of Cl^- at 190 nm, HClO at 238, ClO^- at 293 nm and Cl_2 at 330 nm. White [1986] summarized previous studies showing the composition of the various chlorine components at equilibrium as a function of pH. We confirmed White's data as shown in Figure 4.9.

To calibrate for free available chlorine, commercial bleach containing 5.25 (w)% NaClO was diluted to have an absorbance of about 2 AU. The standard solution was diluted and pumped into the PDA system. Dilution with a borax buffered solution at pH 10.5 quantitatively converts free available chlorine to ClO^-.

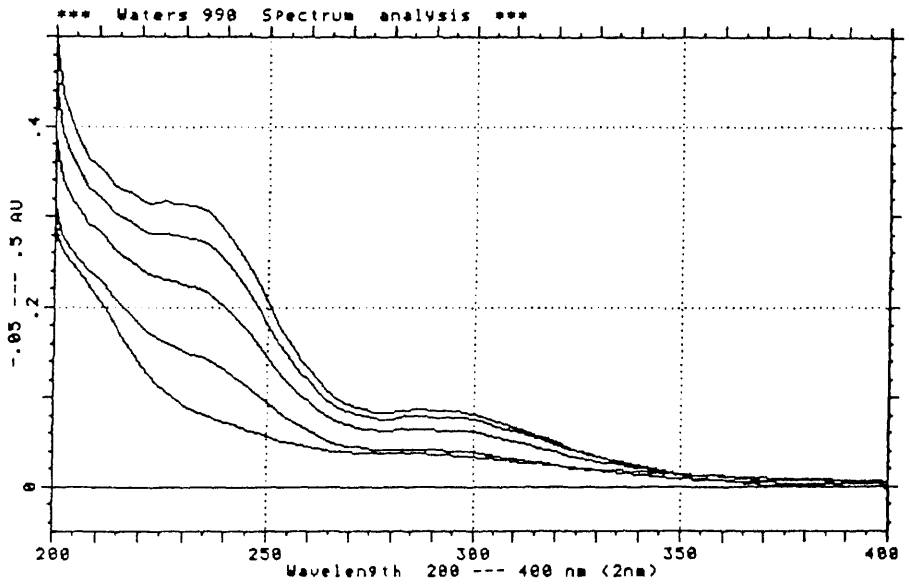

Figure 4.8 The UV/Visible spectrum of chlorinated water based on the absorbance of Cl^- at 190 nm, HClO at 238 nm, ClO^- at 293 nm, and Cl_2 at 330 nm.

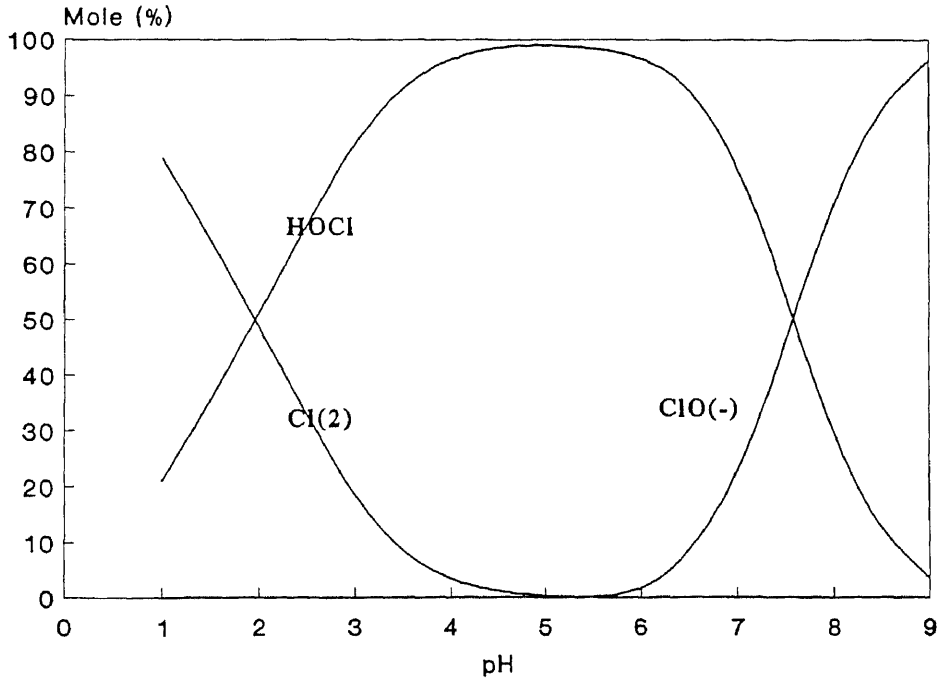

Figure 4.9 Equilibrium concentrations of Cl_2, HClO and ClO^- in NaClO aqueous solution as a function of pH.

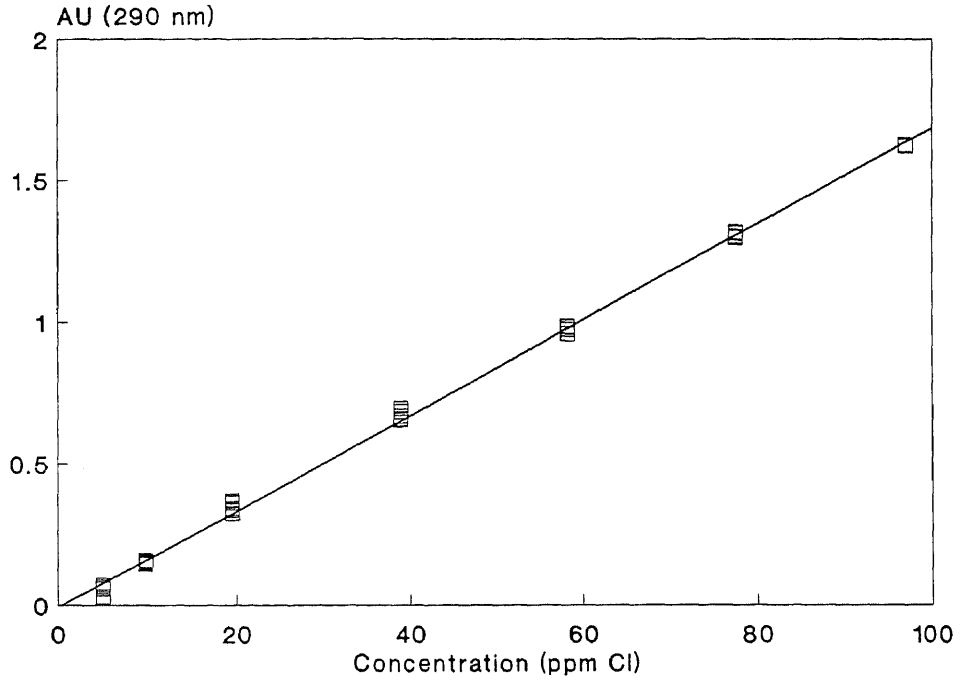

Figure 4.10 Calibration curve of high concentration of NaClO diluted with a borax buffered solution at pH 10.5.

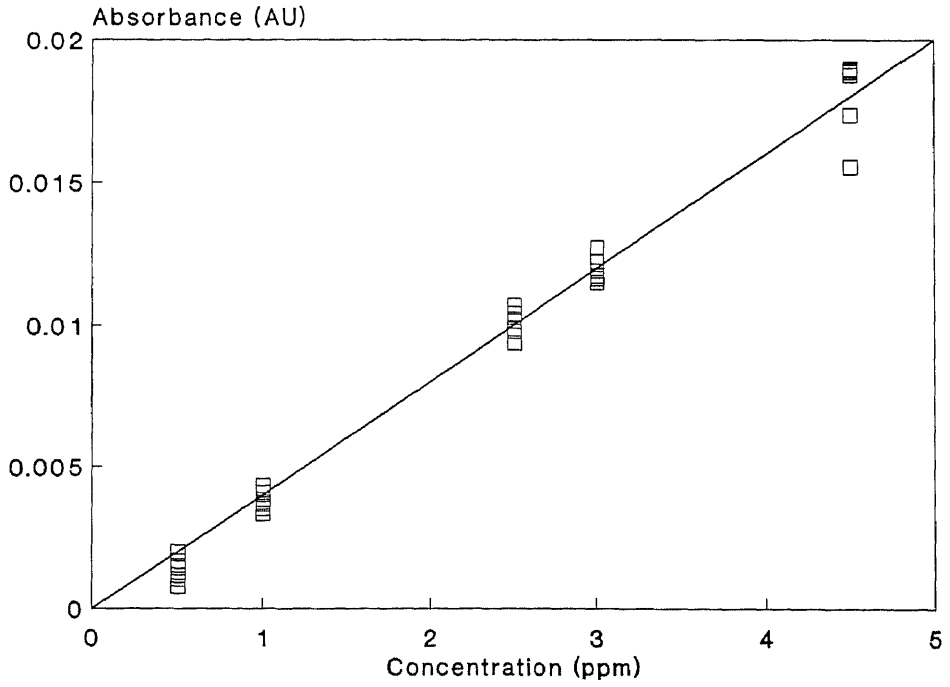

Figure 4.11 Calibration curve of low concentration of aqueous solution NaClO dilute with a borax buffered solution at pH 10.5.

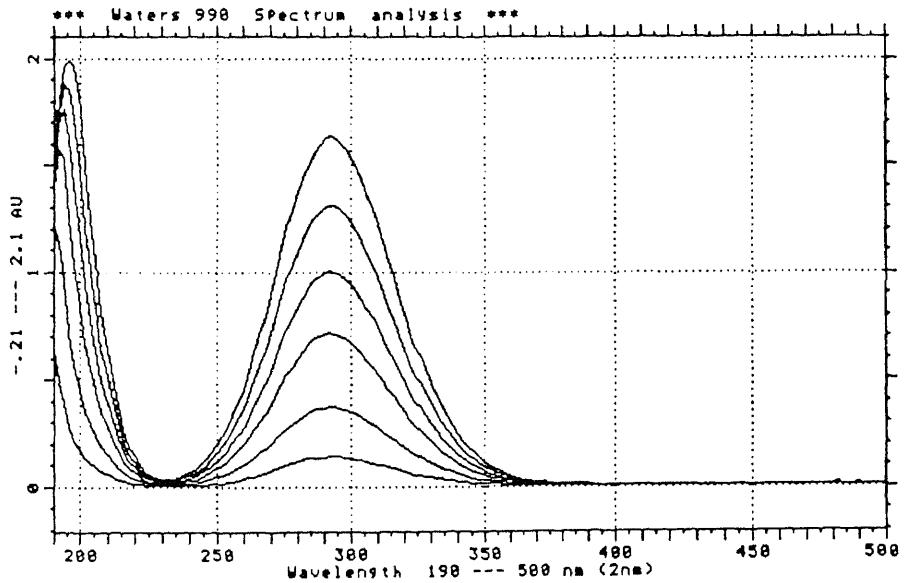

Figure 4.12 The UV/Visible spectrum of aqueous solution ClO^- as a function of wave length and concentrations of 97, 77.6, 58.2, 38.8, 19.4, 9.7, and 4.9 ppmw Cl.

The sensitivity of the measurement of ClO^- at 293 nm was greater than that of any other component in the aqueous solution. Calibration curves were obtained at different concentration ranges as shown in Figures 4.10 and 4.11 from measured spectra depicted in Figures 4.12 and 4.12. Both have R^2 better than 0.998.

Spectra of solutions of chlorine and oxychlorine compounds were obtained with a PDA system. Except for Cl^- which has maximum absorbance in the cut off range, 190 nm, and Cl_2 which has relative low extinsion coefficient at 330 nm, the other oxychlorine compounds were measured with great accuracy. It was found that HClO can be quantified by its absorbance at 238 nm, ClO^- at 293 nm, ClO_2^- at 258 nm, and ClO_2 at 358 nm.

Absorbance versus concentration curves were found to be linear when concentration was kept low enough so as exceed 2 absorbance units. To extend the range to higher concentration measurements, such as was used in the scrubbing work, the eluent pumping system of the prep. LC. was used to dilute the inlet sample. However, the samples were

not pumped back into the process. The mixing did not cause any disturbance, if the flow rate was kept below 3 cm^3/min.

For free available chlorine measurement, the pH of incoming sample was controlled at 10.5 by borax buffer solution with the eluent pumping system of the prep. LC. As a function of pH, free available chlorine can be quantified by measuring the ClO^- at 293 nm.

For pH control, the background scan must be carefully taken by sending the buffer solution into the PDA system. If the background scan has an absorbance at 230 nm lower than 80% full scale, sampling time should be adjusted to meet this criteria of increasing sampling time in order to increase the absorbance to at least 80% of full scale.

The reaction rate of $NaClO_2$ with HCl to produce ClO_2 is not instantaneous. When preparing the solution of ClO_2 for PDA calibration, it is recommended that a scan of the HCl solution be taken as background, and then run the titration with $NaClO_2$ aqueous solution.

4.4 Product, NO_3^-, Cl^-, and SO_4^{-2}, Analysis

After the scrubbing, NO_3^-, Cl^-, and/or SO_4^{-2} were expected to be in the spent scrubbing solution and were analyzed by ion chromatography. Other ions such as NO_2^-, SO_3^{-2}, HSO_4^-, HSO_3^-, etc., were not found in effluent scrubbing solution.

A Waters ion chromatography system was used to conduct this analysis. The components of single column ion chromatography (SCIC) as practiced in this laboratory are:

1. Eluent pumping system: Waters 600E Multisolvent Delivery System
2. Injector: Waters 715 Ultra Wisp Sample Processor
3. Column: Waters IC-Pak A HC
4. Detectors:

   UV-VIS: Waters 484 Tunable Absorbance Detector

   Conductivity: Waters 431 Conductivity Detector

5. Chromatography data system: VG Data System Minichrom V.1.60.

The analysis of ions in actual samples is often complicated by the presence of interferences in the sample matrix. These matrices may contain major constituents that affects the quality of separation and detection of the components of interest. Generally, these problems are caused by pH, high or low ionic concentrations, presence of organic, coelution, or reactivity.

The effects of sample pH can be seen both in the chromatographic analysis, and in the sample itself. Without any sample preparation, high and low pH samples may cause perturbations and drift in the chromatographic baseline which may interfere with the analytes of interest. This is of particular concern in this study for the method analyze anions using standard Borate/Gluconate eluent.

This behavior is most easily explained by the use of pK tables. The pK is simply an emperical value. It is the pH at which the ion is half in one form and half in the other form. So at one pH unit above the pK_a, the predominant form of the ion is the less protonated form. One pH unit below, the predominant form is the more protonated form.

Without pH control, liquid samples of the spent scrubbing solution were at pH 1.8. The pH of samples were adjusted to around 7 before analysis.

One of the most common problems encountered in analyzing actual samples is extremes in ionic concentrations. Exceeding high levels of total ionic compounds may result in column overloading, and degradation of the analytical separation. The capacity of the separating column used in this research is 100 ppm. The total ionic concentration of the spent scrubbing is around 7,000 ppm, therefore dilution by a factor of 100 had to be accomplished before the sample was analyzed.

Many ionic compounds are reactive and undergo electrochemical reactions in solution. Care must be taken to ensure that these compounds remain unchanged throughout the sample preparation and analysis procedures. All of the oxychlorine compounds, ClO_2^-, ClO^-, HClO and ClO_2, used for this study are on the list of active compound table

recommended by Waters Company. Therefore the scrubbing samples were taken only after the NO breakthrough to make sure that there is no oxidizing agent left.

Liquid samples were taken from the scrubber after the NO breakthrough. Ionic concentrations were determined both qualitatively and quantitatively using Waters Ion Chromatography Method # A-102 under the following conditions:

Eluent: Borate/Gluconate

Flow rate: 2.0 cm^3/min

Injection: 100 μl of standard anion mix

Range: 500 μs

Temperature: On

Polatriy: +

Background: 274 μs.

The sample injection is pushed by buffer eluent through the analytical column, where ions are separated. After separation, the sample is carried to detectors, where both electrical conductivity and UV absorbance of the ions were taken.

At low concentrations, both analytical signals are linearly proportional to the concentration of conductive species in the solution. Figure 4.13 shows a chromatogram of standard solution of Cl^-, NO_2^-, NO_3^-, and $SO_4^{=}$. Figures 4.14, 4.15, 4.16 and 4.17 are calibration curves of them.

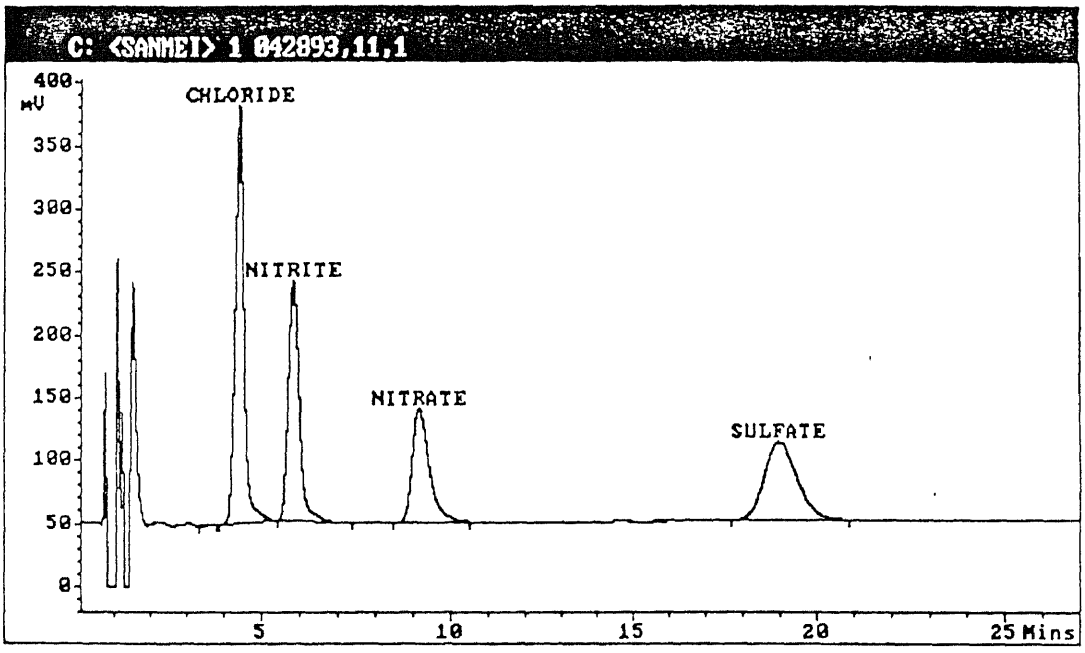

Figure 4.13 The chromatogram of standard aqueous solution of Cl^-, NO_3^-, and SO_4^{-2}

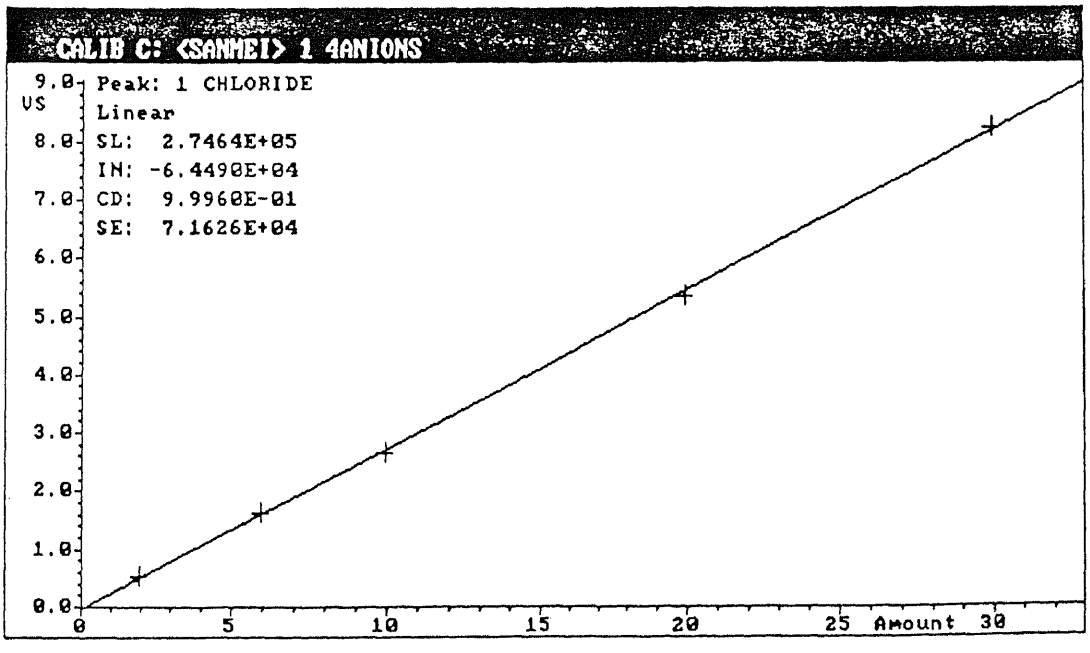

Figure 4.14 Calibration curve of aqueous solution chloride

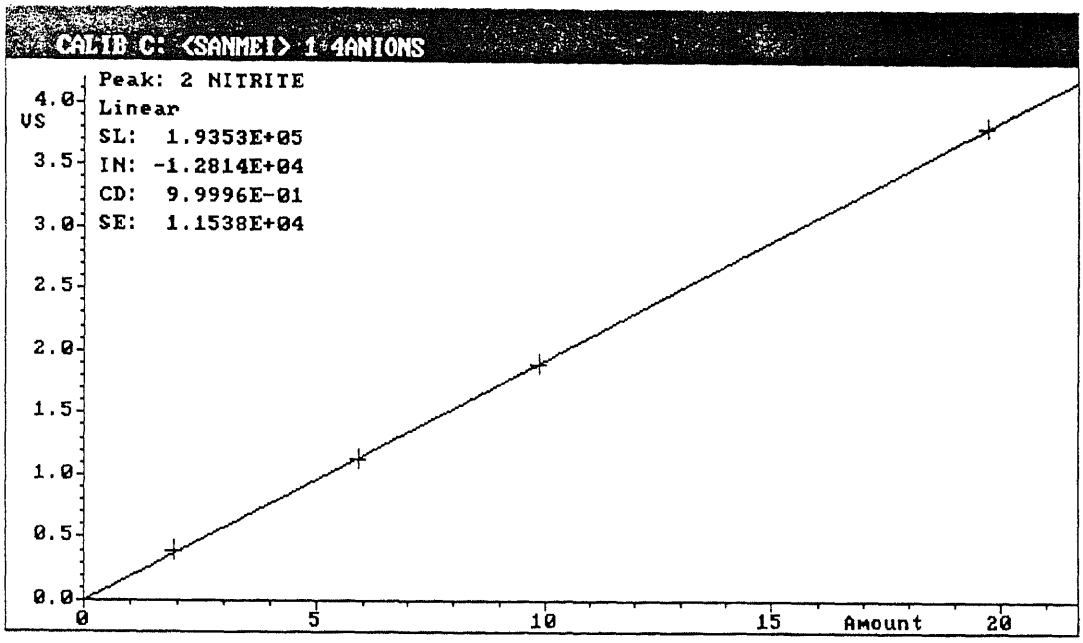

Figure 4.15 Calibration curve of aqueous solution nitrite

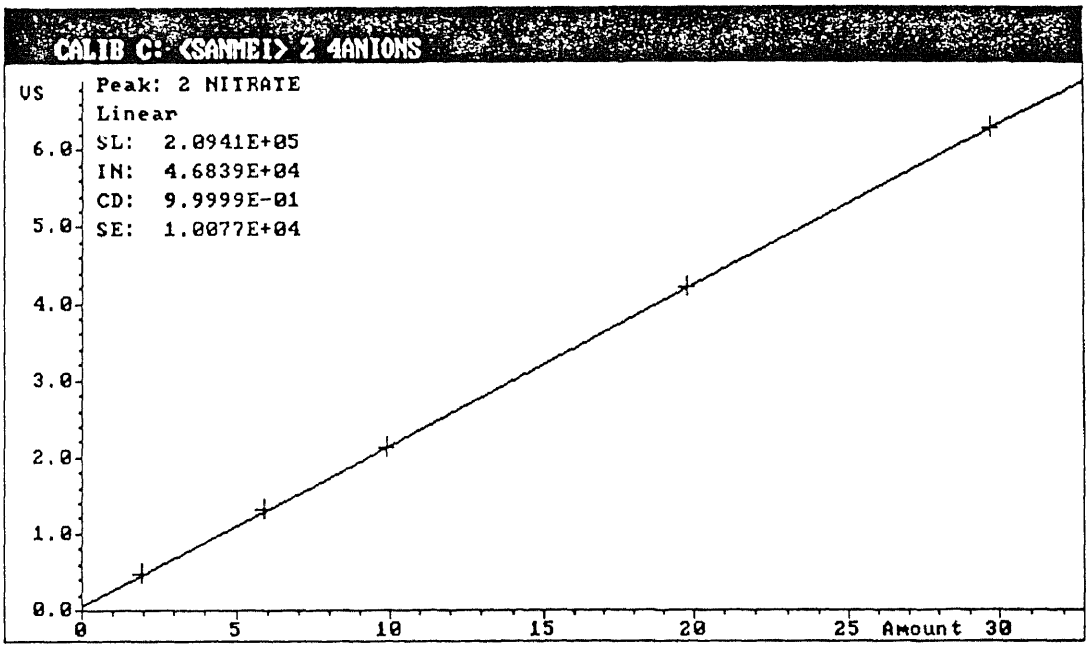

Figure 4.16 Calibration curve of aqueous solution nitrate

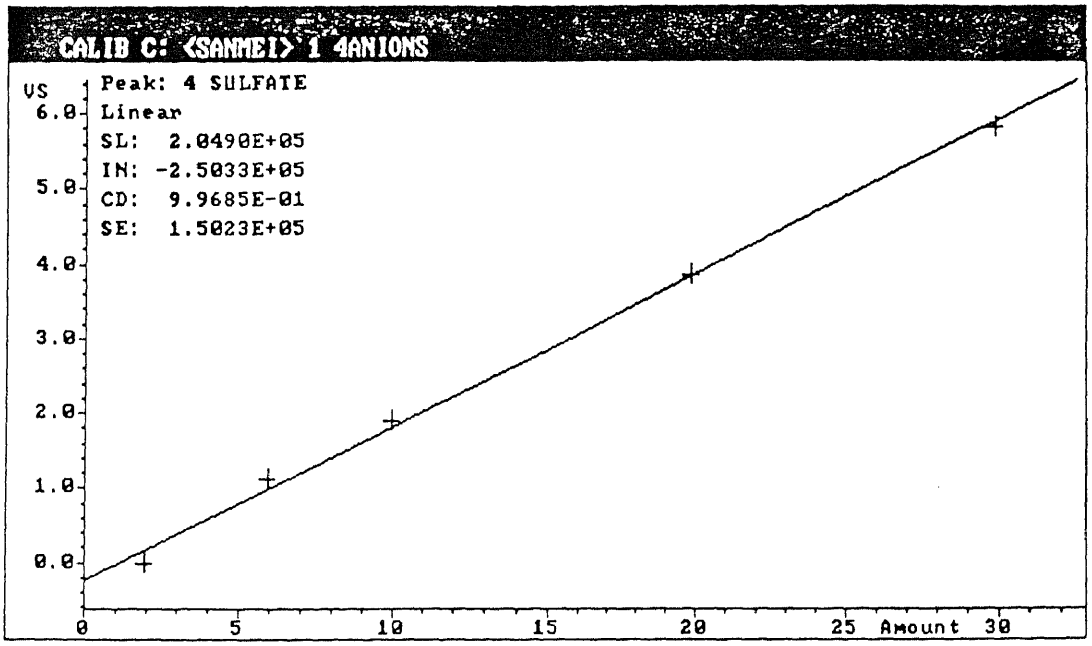

Figure 4.17 Calibration curve of aqueous solution sulfate

CHAPTER 5

FEASIBILITY AND UTILIZATION EVALUATION

5.0 Scope

This chapter describes the laboratory apparatus used to screen various aqueous solutions for NO_X scrubbing potential and to derive absorption data for mass transfer coefficient calculation. The experimental results of screening tests are contained in following sections of this chapter while the kinetic study and mass transfer coefficients are presented in the following chapters.

The research started with a series of screening tests in order to ascertain which compounds are capable of enhancing the absorption of NO_X. The experiments are conducted with absorption of NO in one liter scrubbing solution in a bubble column illustrates in Figure 5.1. Bubble column scrubbers have the advantage that they provides a large volume fraction of liquid which favor kinetically controlled systems. in addition, only small liquid volume are required and the experiments are fast and easy to perform. However it is difficult to estimate mass transfer coefficients and mass transfer area in bubble column scrubbers. Therefore, the experimental results presented in this chapter will serve as background for further investigation in spray chamber and packed bed scrubbers.

The following compounds were tested in a bubble column scrubber:

Sodium hydroxide (NaOH)

Hydrogen peroxide (H_2O_2)

Chlorine (Cl_2)

Sodium hypochlorite (NaClO)

Sodium chlorite ($NaClO_2$)

Sodium chlorate ($NaClO_3$).

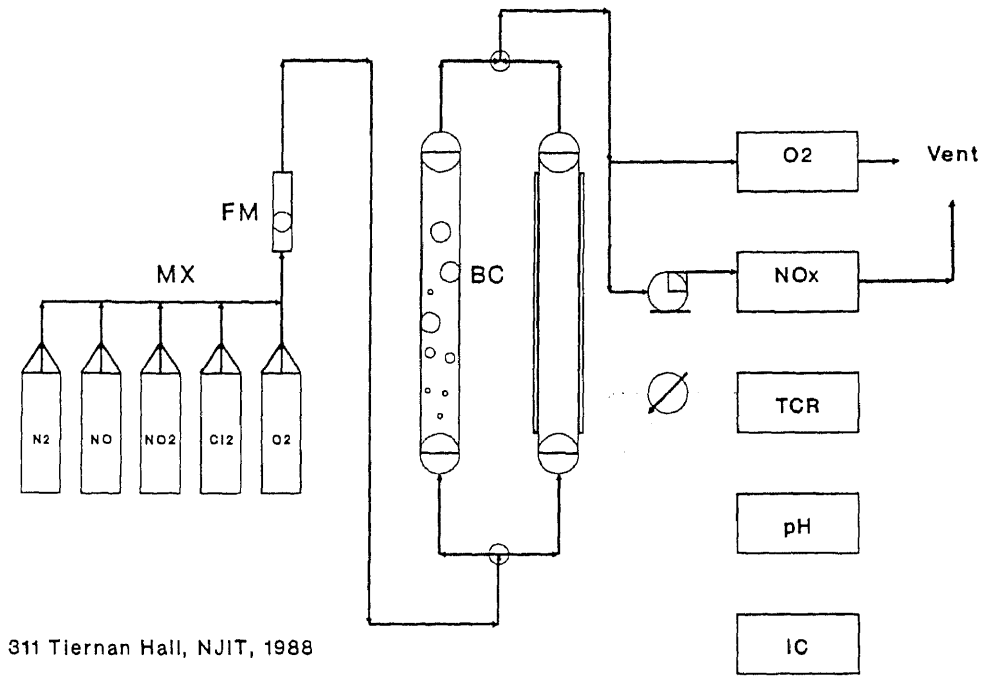

Nomenclature and Symbols

MX Mixer
BC Bubble Column
pH pH Meter
FM Rotameter
TCR Temperature Controller
IC Ion Chromatography

Valve
Heating Element
Pump
Cylinder
Gas/Liquid Stream
Cable

Figure 5.1 The bubble column scrubbing system

Sodium hydroxide shows no ability to oxidize NO to NO_2, but it absorbs equal molar quantities of NO and NO_2 from a gas stream. The result were reported in a previous study [Yang, 1990].

In a batch contactor, hydrogen peroxide removes 10,000 ppm NO in two to five minutes and produce 14,727 ppm O_2 at the same time. Without a stabilizer, hydrogen peroxide decomposes much more faster than it reacts with NO.

Sodium chlorate is a poor absorbent of NO. Tests of sodium chlorate in both acidic and alkaline aqueous solutions show no more than 10% removal on NO. With SO_2 in gas stream, the removal of NO increased up to 25%. The improved removal could be due to the formation of ClO_2 [White, 1986].

Sodium chlorite containing aqueous solutions quantitatively absorb NO from gas stream. It must be noted that due to the presence of Na_2CO_3 (18%) and Na_2SO_4 (2%) in $NaClO_2$, the initial pH of these solutions was 10. Under the same conditions, 90% removal is achieved by both chlorine and sodium hypochlorite aqueous solution. Results are presented in following sections.

5.1 Apparatus

The other scrubbing equipment evaluated in this study consisted of a flue gas blending system, a set of gas scrubbers and an analytical train which is shown in Figure 5.2. The blending system is capable of producing a mixture of nitrogen, oxygen, nitric oxide, nitrogen dioxide, and sulfur dioxide in order to simulate a wide variety of flue gas compositions by mixing pure gases components and blends in different proportions. This was done by feeding the individual gaseous components through rotameters into a manifold where they mixed. The gaseous mixture which was representative of a flue gas without components such as CO_2, CO, H_2O and particulate was then passed through another rotameter and fed to the scrubber. The composition of the flue gas was measured by analyzers described in chapter 4.

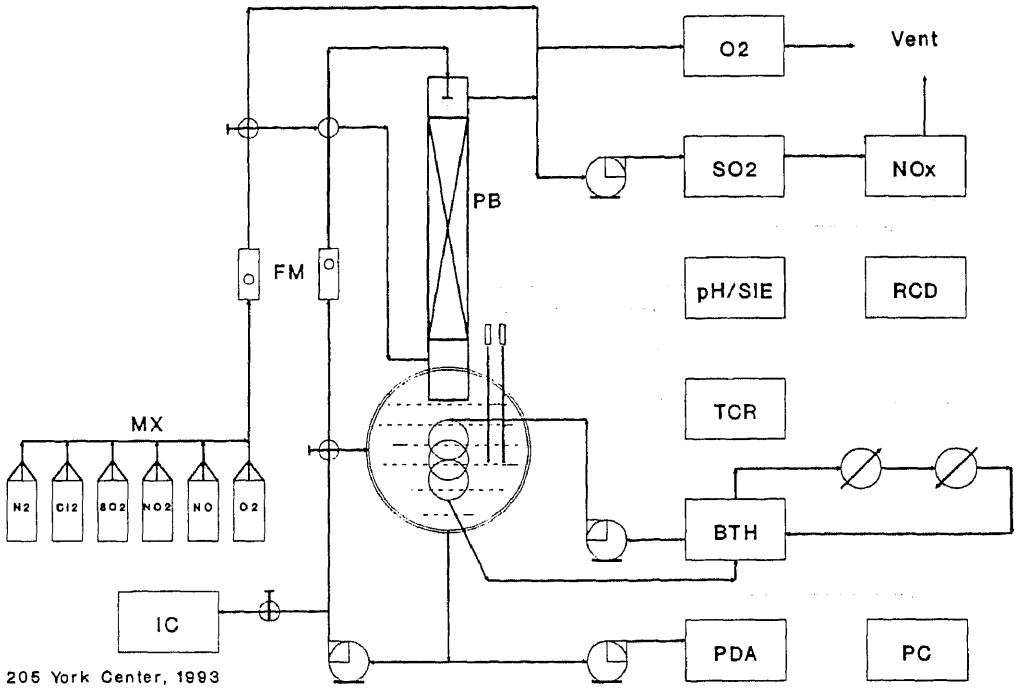

Nomenclature and Symbols

MX Mixer
PB Packed bed
pH pH Meter
FM Rotameter
TCR Temperature Controller
IC Ion Chromatography
PC Data Acquisition
PDA Photodiode Array
Heating Element

Valve
Heat Exchanger
Pump
Cylinder
Gas/Liquid Stream
Cable
Analyzer

Figure 5.2 The schematic diagram of a packed bed flue gas scrubbing system

The synthetic flue gas is introduced into the scrubber where the gas-liquid reaction occurs. The input and effluent gases were allowed to flow to the gas analyzers as required to allow the determination of NO, NO_2, O_2, and SO_2 concentrations. The different components of the total scrubbing system are described in greater detail below.

Flue Gas Blending System

The flue gas blending system is designed to provide synthetic flue gas from high pressure gas cylinders. The blending system is constructed out of 0.63 cm (1/4 inch OD.)) diameter by 60 cm long stainless steel type 316 tubing. Each component gas is delivered through a 0.63 cm diameter polyethylene tubing to a calibrated rotameter to the blending manifold. Characteristics of each rotameter are listed in Table 5.1. After blending, the entire mixture pass through a large calibrated rotameter to determine the total flow rate. The total flow rate from the blending system ranged from 1 to 40 standard liters per minute. The composition of a typical blend was 300 ppm NO, 300 ppm NO_2, 500 ppm SO_2, and 4% O_2 balanced with N_2. The flue gas blending system functioned satisfactorily.

Table 5.1 Tube Selection Table for Gas Scrubbing System

Placement Tube	Float Material	Nitrogen (Lpm)	Air (Lpm)	Water (cm^3/min)	Producer
FM4333	Sapphire 316 Stn Stl	0.5265 0.846	0.487 0.791	10.5 20.8	Linde
FM4334	Sapphire 316 Stn Stl	3.14 4.77	3.05 4.62	79.8 133.4	Linde
FM4335	Sapphire 316 Stn Stl	11.5 16.85	11.3 16.5	304 502	Linde
R-2-15-AAA	Sapphire 316 Stn Stl	0.5265 0.846	0.487 0.791	10.5 20.8	Brooks
E1-4C401-E700	Glass 316 Stn Stl		9.0 16.9		Matheson
E1-4C401-E800	Glass 316 Stn Stl		24.7 49.3	 1300	Matheson

Flue Gas Scrubbers

A review of Figure 3.1 and Table 3.1 leads to the conclusions that spray or packed column should be efficient devices for systems with fast reaction, while bubble contactors should be more efficient for slow reactions. Therefore, three 5.1 cm in diameter by 61 cm long Pyrex glass columns are used to build a bubble column, spray absorber, and packed bed scrubber.

For the bubble column scrubber, a polyethylene sparger was inserted into the bottom of the capped glass column. The flue gas is introduced into the scrubbing solution through the sparger and dispersed evenly in bubbles.

For the spray chamber absorber, a 2.8 dm^3 storage vessel was attached to the bottom of the glass column. The scrubbing solution is pumped through the sprayer, on the top of glass column, into the empty chamber where absorption occurred.

For the packed bed scrubber, the column was made of Pyrex glass consisting of different sections. These sections and a 2.8 dm^3 plastic reservoir were put together with plastic flanges. The bottom section of the column is equipped with the gas inlet and the liquid outlet to the reservoir. The section containing the tower packing was placed above the bottom section. The tower packing consisted of 6.35 mm (1/4 inch) ceramic Raschig rings. The randomly dumped packing height in the column could be easily varied from 10 cm (4 inches) to 38 cm (15 inches) by adding or subtracting Raschig rings. A Teflon grating is made to prevent the Raschig ring from falling down into the bottom section. The section, including the liquid inlet and gas outlet was placed on top of the packing section. The liquid was distributed evenly with a shower sprayer.

The column has a diameter of 5.1 cm (2 inch) and is packed with 0.64 cm (1/4 inch) ceramic Raschig rings. Raschig rings are chosen as packing material due to the substantial amount of data on Raschig rings available in the literature. Ceramic Raschig rings have the following characteristics:

Approximate surface area = 710 (m^2/m^3)

Percent void space = 62%

Packing factor = 5250 (m^{-1})

With these data, the equation of the Lobo curve [Figure 3.4] can be used to calculate flooding values. The agreement between experimental and calculated flooding points for the column is shown in Figure 5.3.

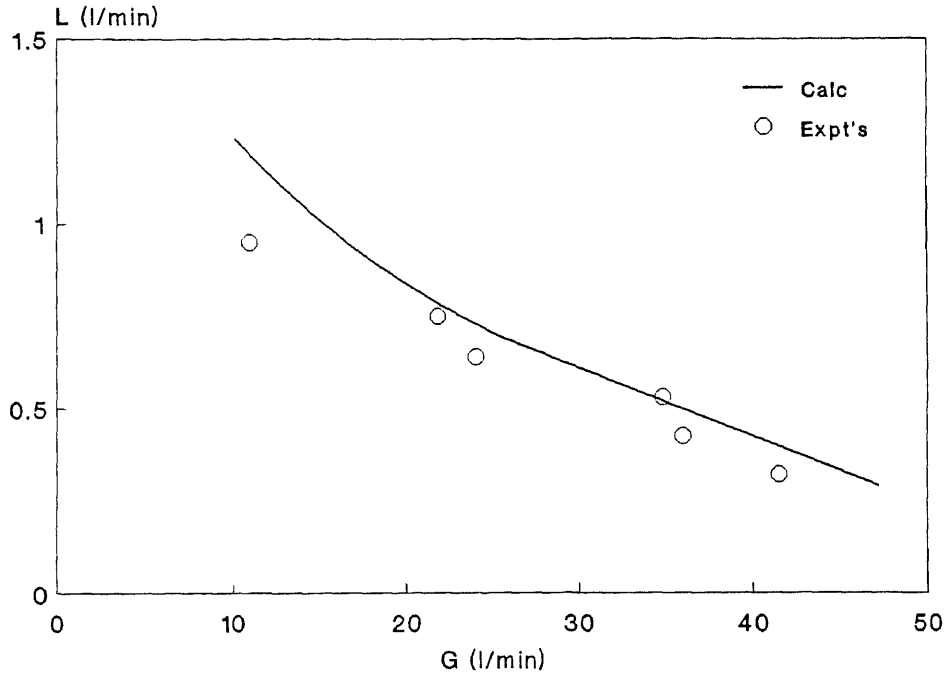

Figure 5.3 Calculated and experimental flooding points

The liquid hold-up was measured at different gas and liquid flow rates. The liquid hold-up increases with increasing liquid flow rate while the gas flow rate does not affect the liquid hold-up as long as the bed does not flood. Figure 5.4 shows the agreement between experimental values on the liquid hold-up and the calculated values from Buchanan's correlation [Equation 3.1].

Since experimental values on both flooding and liquid hold-up are in good agreement with calculated values, it is assumed that this is an ideal packed bed to take absorption data.

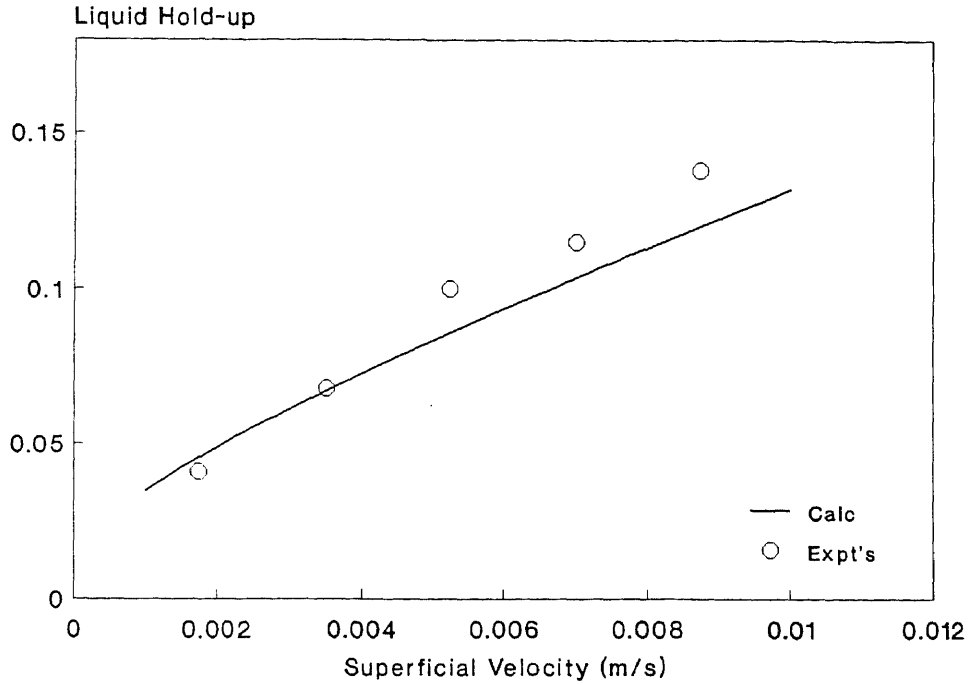

Figure 5.4 Calculated and experimental values on liquid hold-up versus liquid superficial velocity

When conducting a scrubbing experiment in a bubble column, one liter of scrubbing solution is generally used to run the experiment as semibatch process with continuous flue gas injection.

A 2.5 liter batch of scrubbing solution was generally used to run the experiments in the spray chamber and packed bed scrubbers. The scrubbing solution was circulating from reservoir through a shower sprayer and absorption chamber by a 1/3 horsepower pump. The flue gas was injected countercurrently into the absorption chamber where gas-liquid reaction and absorption occurred.

Analysis

The exiting gas was carried to an oxygen monitor, SO_2 analyzer, and NO_x analyzer from the top of the glass column by a 0.64 cm polyethylene tubing after removal of moisture.

During the scrubbing, the depletion of reactants and formation of intermediates are monitored continuously with Waters LC/PDA system described in Chapter 4. The pH value was measured and recorded by a Jenco model 7609 pH meter.

After breakthrough, samples of the solution were injected into a Waters ion chromatography to determine the anion concentrations of products, Cl^-, NO_3^-, and/or SO_4^{-2}.

When conducting a scrubbing experiment in a bubble column, the following sequence was followed:

1. Set the flue gas composition and flow rate while flowing through the reference scrubber.

2. Switch flue gas through the main scrubber (prefilled with the desire solution).

3. Monitor pH, temperature, and intermediates.

4. Check inlet flue gas composition using the oxygen monitor, NO_X analyzer, and SO_2 analyzer.

5. Measure outlet composition as a function of run time.

6. Take liquid samples after NO breakthrough.

7. Analyze liquid samples in ion chromatography.

The following steps were followed in order to perform experiments in a spray chamber or packed bed scrubber:

1. Set the flue gas composition and flow rate while flowing through empty chamber or dry bed.

2. Switch the gas stream to bypass.

3. Turn on the circulating system.

4. Turn on the temperature control system.

5. Switch back the gas stream to the scrubber.

6. Measure inlet composition and flow rate.

7. Monitor pH and temperature.

8. Measure concentration of reactants and intermediates using LC/PDA system.

9. Measure and record outlet composition using NO_x, SO_2, and O_2 analyzer.

10. Change liquid flow rate as required by experimental objective.

11. Record outlet composition as a function of liquid to gas ratio.

12. Analyze liquid samples by ion chromatography.

Temperature control is critical in this experiment. Normally, the 1/3 hp pump causes an increase in liquid temperature from room temperature (18 ^oC) to 55 ^oC after circulating the solution for one hour. The heat exchanger allowed us to maintain temperature constant as required. In most experiments, temperature was maintained at 25 ^oC. The outlet composition changes with operating temperature as well.

5.2 The Aqueous Equilibrium of Oxychlorine Compounds

Aqueous solutions of chlorine gas and oxychlorine compounds have been effectively used to remove NO_x from flue gas in a bubble column. The technique was transferred successfully to spray chamber and packed bed scrubbers in all aspects except for the unpredictable outlet composition. Without pH control, the absorption efficiency increases with run time. At the same time, pH drops as a result of the formation of nitric acid. It is believed that pH changes the equilibrium of oxychlorine compounds in aqueous solution and the concentration of active ingredient in the system. In order to estimate the mass transfer coefficient promoted by the chemical reaction of nitric oxide with oxychlorine compounds, it becomes important to determine the distribution of active components in the scrubbing solution as a function of time, pH, temperature, and concentration of oxychlorine compounds.

Chlorine, Hypochlorite and Hpochlorous Acid System

Chlorine gas, when dissolved in water, it hydrolyzes rapidly according to the following equation:

$$Cl_2 + H_2O \rightarrow HOCl + H^+ + Cl^- \qquad (5.1)$$

The rapidity of this reaction has been studied by many investigators. Complete hydrolysis occurs in a few tenths of a second at 18 ^{o}C, while at 0 ^{o}C only a few seconds are needed. At 2 psig and a temperature of 20 ^{o}C, the solubility of chlorine in water is only about 7.5 g/dm^3.

To demonstrate the relationship of the molecular chlorine-hypochlorous acid equilibrium for both buffered and unbuffered water, Figure 5.5 is made from a computer printout provided by the Bioengineering Research and Development Laboratory, US. Army, Fort Derrick, Maryland [White 1986]. The result of HClO and ClO^- has been confirmed by the LC/PDA system in our laboratory.

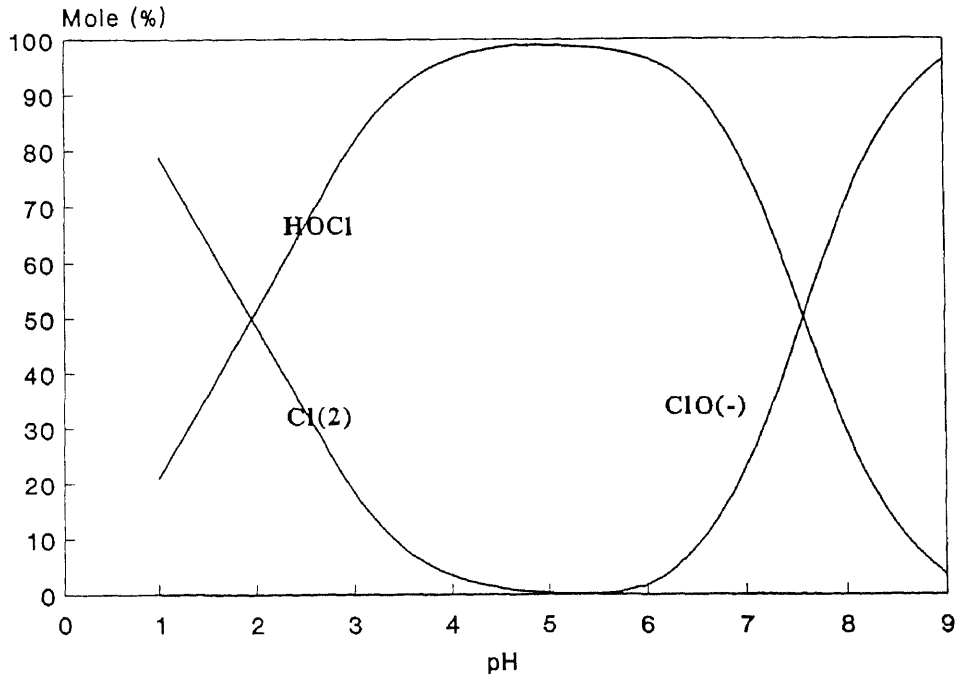

Figure 5.5 Equilibrium concentrations of Cl_2, HClO and ClO^- in aqueous solution as a function of pH.

In this system, the active ingredient is always the hypochlorous acid [White, 1986]. The low pH part of Figure 5.5 illustrates the equilibrium in the chlorine solution discharge from a sparger. In this pH range, solubility of chlorine is 3.5 g/dm^3. The high pH part of Figure 5.5 demonstrates the stability of a chlorine water solution buffered with sodium

hydroxide. Under this condition, the maximum solubility of chlorine can be as high as 7.4 g/dm^3 due to the reaction of

$$Cl_2 + OH^- \Leftrightarrow HOCl + Cl^- \quad (5.2)$$

If the scrubbing solution is prepared from sodium hypochlorite, the dominating ingredient is the hypochlorite ion (OCl^-) which hydrolyzes to form hypochlorous acid.

$$NaClO + H_2O \rightarrow HOCl + Na^+ + OH^- \quad (5.3)$$

The only difference between the reactions of hypochlorites and chlorine gas is the side reaction of the end products. The reaction with the hypochlorite increases the hydroxyl ions by the formation of sodium hydroxide according to Equation 5.3, the reaction with chlorine gas and water increases the H+ ion concentration by the formation of hydrochloric acid. There are strong indications that both systems have highest NO_x removal efficiency in pH range of 4 to 6, simply because there is more of the active ingredient HOCl in the aqueous solution.

Sodium Chlorite and Chlorine Dioxide System

When a mixture of $NaClO_2$ and NaOH aqueous solution is used to remove NO from flue gas, NO is always observed in the effluent in first few minutes [see Figure 4.1]. We observe with either 100% absorption, or no absorption at all in ten minutes. These results depend on the ratio of sodium chlorite to sodium hydroxide and whether the greenish yellow color appeared or not. The results have been reported in a previous study [Yang, 1990].

A Waters LC/PDA system is therefore used to identify the formation of ClO_2, the gas with the greenish yellow color, in $NaClO_2$ aqueous solutions. A 4 dm^3 $NaClO_2$ aqueous solution was titrated with HCl under real time monitoring of pH and wavelength with the LC/PDA system at 358 nm, the characteristic absorption wavelength of ClO_2. Figure 5.6 shows the equilibrium relationship of ClO_2 as a function of pH.

The stoichiometry from hydrochloric acid activation of sodium chlorite is as follows:

$$5NaClO_2 + 4HCl \Leftrightarrow 4ClO_2 + 5NaCl + 2H_2O \quad (5.4)$$

NO, when oxidized and dissolved in water, produces nitric acid. This explains why the pH of scrubbing solution drops from 10 to 2.5 in first ten minutes. Under this condition, $NaClO_2$ in the solution reacts with nitric acid to form ClO_2. Which reacts with NO rapidly and accelerates the absorption rate.

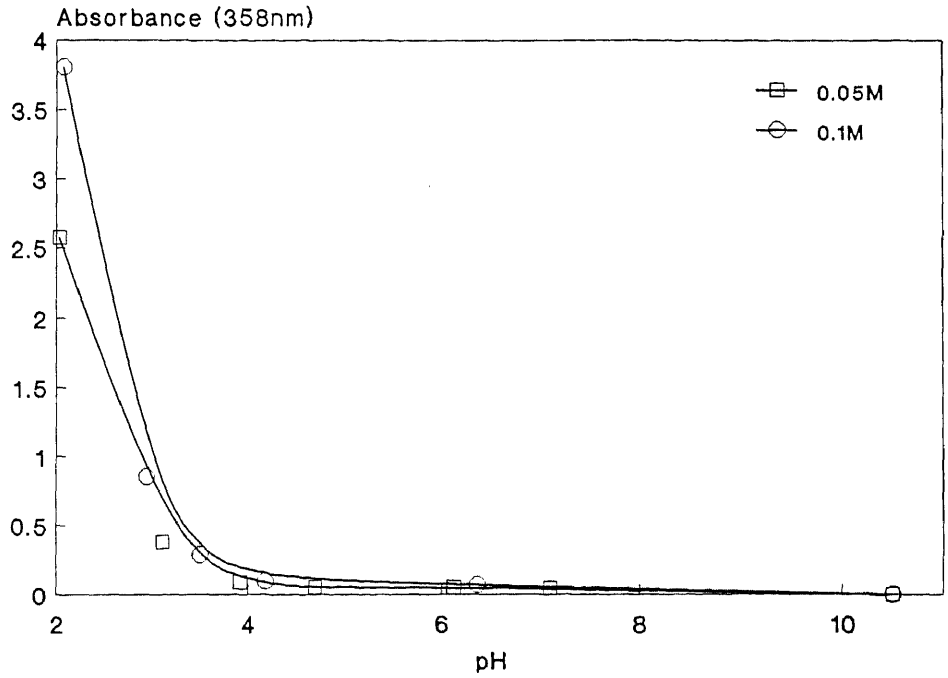

Figure 5.6 The effect of pH on chlorine dioxide formation

5.3 NO_x Absorption Induced by Cl_2 Oxidation

The removal of nitric oxide from flue gas via chlorine injection was studied by Hixson [1990]. In 1981, the Dow Chemical Company was issued a patent for this process. The Dow experimental results were presented in 1990 AFRC International Symposium, just after our results with this system were completed in our laboratory. Both studies have very similar results except for the NO_2 breakthrough which we observed.

Effects of pH

Chlorine, when dissolved in water, equilibrates with HClO and ClO^- in aqueous solution [see Figure 5.4]. The NO absorption induced by chlorine injection is a result of gas phase reaction of NO and Cl_2, and gas-liquid reaction of NO with Cl_2, HClO, and ClO^-. A gas phase reaction test was conducted by mixing 1000 ppm NO with 1000 ppm Cl_2 at room temperature. More than 95% of NO injected is detected by the NO_x analyzer after passing through the blending system. Assuming a minor gas phase reaction, pH control of scrubbing solution is the best way to separate NO absorption promoted by Cl_2, HClO or ClO^-.

The first series of runs used HCl aqueous solution as the scrubbing solution. experiments are conducted under the following conditions:

Flue gas: 1000 ppm NO, 1000 ppm Cl_2, and balance N_2

Flow rate: 1000 cm^3/min

Scrubbing solution: HCl aqueous solution

Volume: 500 cm^3

Ranges of pH: 1.5 to 6.5

At room temperature and ambient pressure.

Figure 5.7 shows the removal percentages of NO as a function of run time under different initial pH value.

Equilibrium concentration of HClO needs to be built up by either Reaction 5.1 or 5.2. Acidic solution takes only 20 minutes to reach equilibrium while higher pH solution needs 80 minutes. Chlorine has a lower solubility in low pH solution which reflects the lower NO removal in Figure 5.7. After two hours running, H^+ produced from Reaction 5.1 consumes all of the OH^- in the scrubbing solution, resulting in initial pH not affecting NO removal any more.

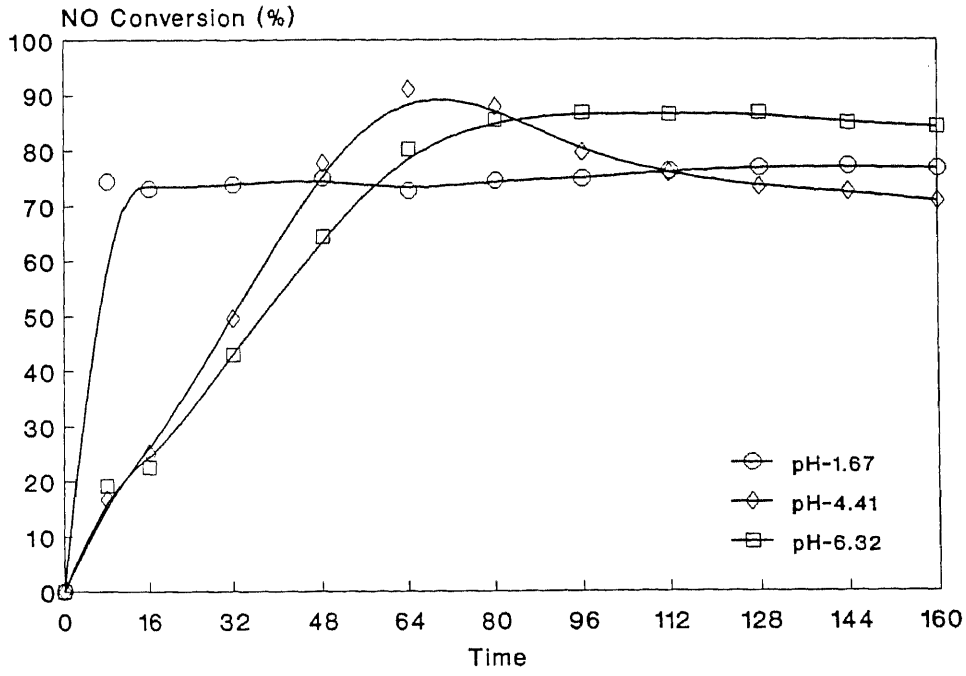

Figure 5.7 The effect of initial pH on NO absorption with chlorine injection.

NO_2 Breakthrough

Hixson [1990] studied the NO removal at various Cl_2/NO molar ratios, initial pH, ionic strength, and temperatures. In the range of Cl_2/NO molar ratio from 2.5 to 7.5, NO removal increases with Cl_2/NO ratio from 50% to 95%. When pH, due to the concentration of HCl, decreases from 6.5 to 0.5, NO removal increases from 50% to 99%. In our study, 80% NO removal is achieved with Cl_2/NO molar ratio of one. Which is in good agreement, except for the NO_2 breakthrough we observed. Experiments were conducted under following conditions:

Flue gas: 1000 ppm NO and 1000 ppm Cl_2 in nitrogen

Flow rate: 1000 cm^3/min

Scrubbing solution: water and water pretreated with chlorine for one hour

Volume: 500 cm^3

pH: 3.2

Room temperature and ambient pressure.

The exiting concentrations of NO and NO_2 are presented in Figure 5.8. With pretreated scrubbing solution, both exiting NO and NO_2 stabilize in 20 minutes while non-pretreated scrubbing solution takes 80 minutes to reach a steady state. After 80 minutes running, both scrubbing systems reach the same efficiency, which is 20% NO and 60% NO_2 breakthrough.

The pH of water, when treated with chlorine, drops from 6.5 to 2.7 in one hour. NO_2, an acid gas, has a very low solubility in acidic solution. We measure the production of only 25% NO_2 from NO scrubbing dissolved in the solution.

Without any improvement, this system can only be used as a prescrubber. Excess chlorine is another concern for scaling up this process.

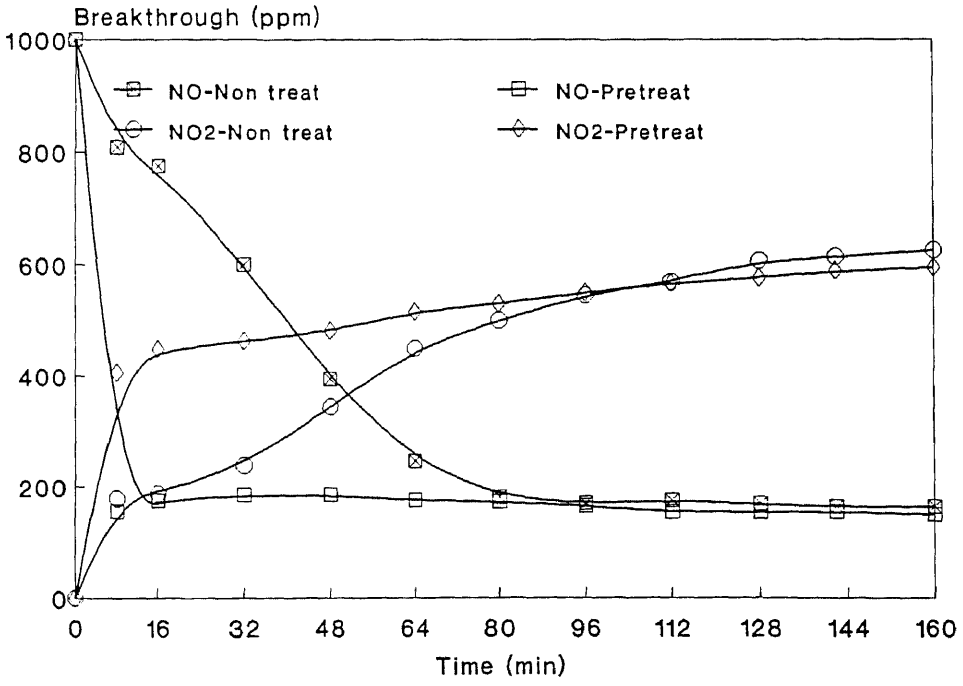

Figure 5.8 NO and NO_2 Breakthrough from a NO scrubbing induced by Cl_2 oxidation.

Bubble Column vs. Packed Bed Scrubber

Because of the highest volume of liquid to volume of film ratio, bubble columns always have the best efficiency for slow gas-liquid reactions. As long as the reaction is fast enough, commercial process tends to use packed beds for flue gas treatment. Not only because bubble column have relative high pressure drop, which increases operating cost, but also because it is difficult to handle particulate in the gas stream or suspended precipitates in liquid. A packed bed therefore is used to confirm the promising result from previous work. Experiments were conducted under the following conditions in both bubble columns and packed bed scrubbers:

Flue gas: 1000 ppm NO and 1000 ppm Cl_2 in nitrogen

Flow rate: 1000 cm^3/min in bubble column, 2000 cm^3/min in packed bed scrubber

Scrubber: bubble column and packed bed scrubber

Scrubbing solution: distilled water.

Volume: 500 cm^3 for bubble column, 2500 cm^3 for packed bed scrubber

pH: neutral

Room temperature and pressure.

Figure 5.9 shows the comparison of a bubble column and a packed bed scrubber for NO removal.

In the packed bed, the first data point taken was in eight minutes. NO removal is almost 80% already and the efficiency remains fairly constant for the whole experiment. While the NO removal in bubble column needs 80 minutes to climb up to 85%. That is because the relative high HClO concentration in packed bed due the relative low volume of liquid to volume of film ratio.

The differences of NO removal between the bubble column and packed bed are shown in Figure 5.9. This difference is attributable to the different gas phase flow rate.

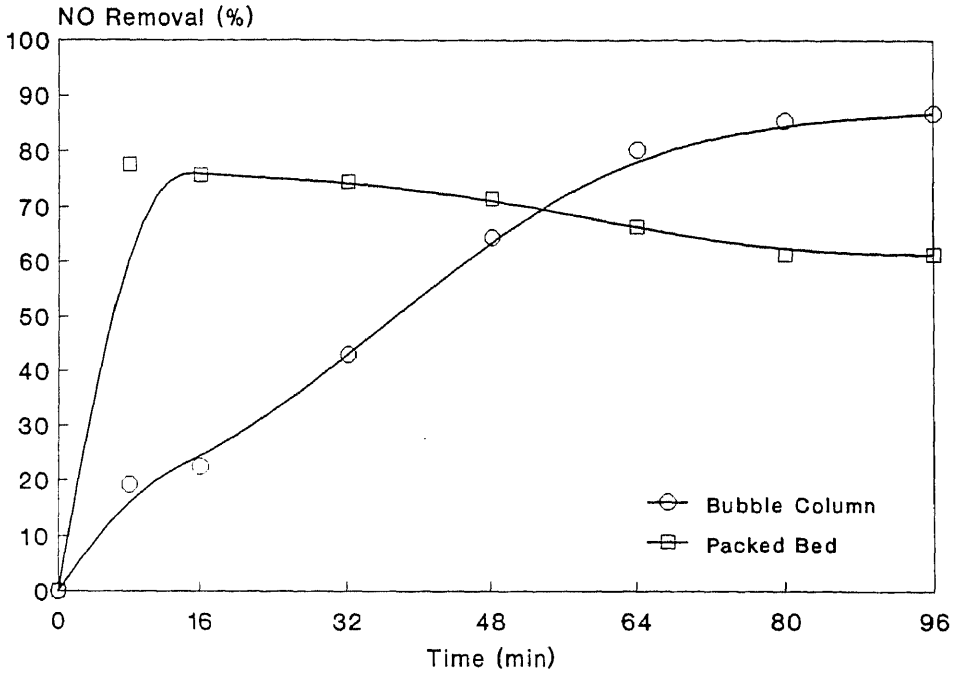

Figure 5.9 A comparison of bubble column and packed bed scrubber systems for NO absorption.

5.4 NO_X Absorption Induced by NaClO Oxidation

Aqueous solution of chlorine gas can be used to remove NO from gas stream. Due to the limitation of solubility, only 80% removal is achieved. Sodium hypochlorite is another option to prepare the scrubbing solution with higher chlorine concentration. Consequently, commercial bleach was investigated for its scrubbing potentials.

Concentration Effects

In order to study the concentration effect of NaClO on NO removal, commercial bleach containing 5.25% NaClO is used to prepare various concentrations of scrubbing solutions. Experiments were performed with different concentrations of NaClO aqueous solutions as follows:

Flue gas: 1000 ppm NO and balance nitrogen

Flow rate: 1000 cm^3/min

Scrubbing solution: 1.25, 0.63, 0.32, 0.2 0.15 W% NaClO

Volume: 1 dm^3

pH: 3.2

The result is shown in Figure 5.10. The NO removal reaches 90% at 0.6% NaClO aqueous solution and remained constant with concentration. Regardless of concentration, there is always 40% NO_2 breakthrough. Scrubbing converts more than 90% of incoming NO to NO_2, while only a half of that is dissolved in the solution due to the low solubility of NO_2 in acidic solution.

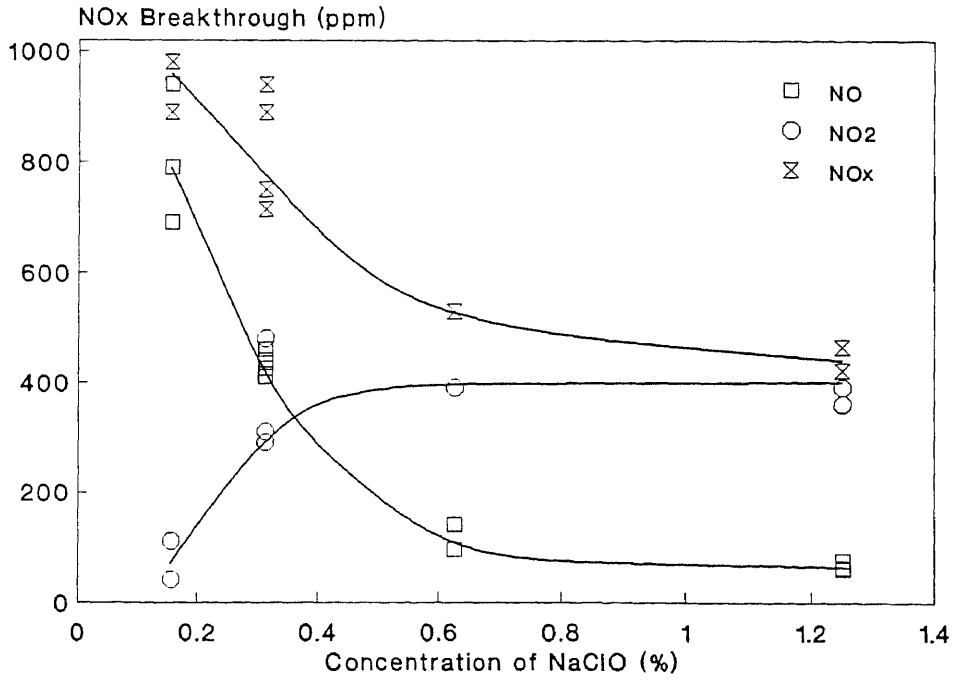

Figure 5.10 The effect of NaClO concentration on NO removal in an aqueous scrubbing.

pH Effect

Previous studies show the ability of NaClO aqueous solution for NO oxidation but not absorption. Large amount of NO_2, the product of NO oxidation, is observed due to its low solubility in acidic solution. Since NO_2 has a relatively high solubility in alkaline solutions, the effect of increase pH in the scrubbing solution were then investigated.

Normally, commercial bleach is stored at pH 10 to prevent the decomposition of NaClO. Even with 4 time dilution, the pH is still more than 9. Under this condition, ClO^- is the dominating ion in the solution. If ClO^- is the active ingredient, NO can be oxidized and absorbed in the scrubbing solution at the same time.

Figure 5.11 shows the results of NO removal under the following conditions:

Flue gas: 1000 ppm NO in nitrogen

Flow rate: 1000 cm^3/min.

Scrubbing Solution: 1.25 W% NaClO

Volume: 500 cm^3

pH: 1.7, 2.7, 3.2, 5.2 (adjusted with HNO_3), 6.7, 7.7, 11.6 (adjusted with NaOH)

At room temperature and pressure.

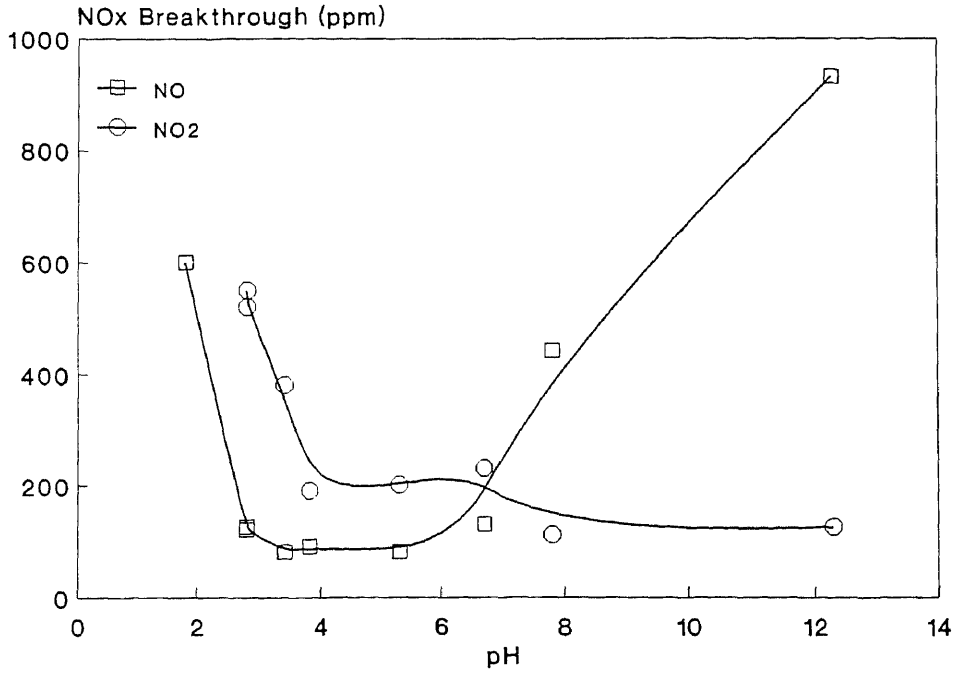

Figure 5.11 The NO breakthrough from NaClO aqueous scrubbing as a function of pH.

After scrubbing, the outlet concentrations of NO and NO_2 are measured carefully with the chemiluminescent NO_X analyzer.

The NO_2 evolution is reduced significantly under alkaline scrubbing. This is not a consequence of absorption of NO_2 but because NO does not react with ClO^-. Figure 5.12 shows the comparison of NO conversion based on the results shown in Figure 5.11 and equilibrium concentration of oxychlorine compounds in aqueous solution according to Figure 5.3. Instead of ClO^-, HClO is believed to be the active agent in this system. This is in agreement with the disinfecting ability of chlorination in water.

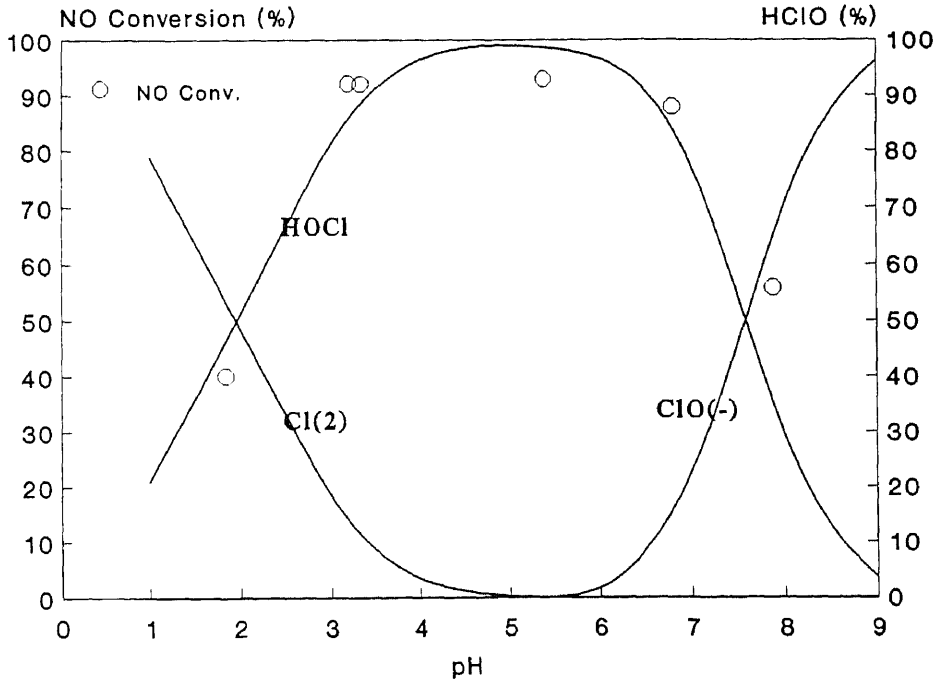

Figure 5.12 The equilibrium concentration of HClO in aqueous solution versus NO conversion in scrubbing.

Temperature Effect

Normally, flue gas enters a scrubber at a temperature of 70 ^oC after heat recovery. Thus, a series of runs is made to determine the effect of temperature on NO conversion.

Experiments are conducted under the following conditions:

Flue gas: 1000 ppm NO and balance N_2

Flow rate: 1000 cm^3/min

Scrubbing solution: 0.25, 0.5, and 1.25 W% NaClO

Temperature: 20 and 60 ^{o}C

Volume: 500 cm^3.

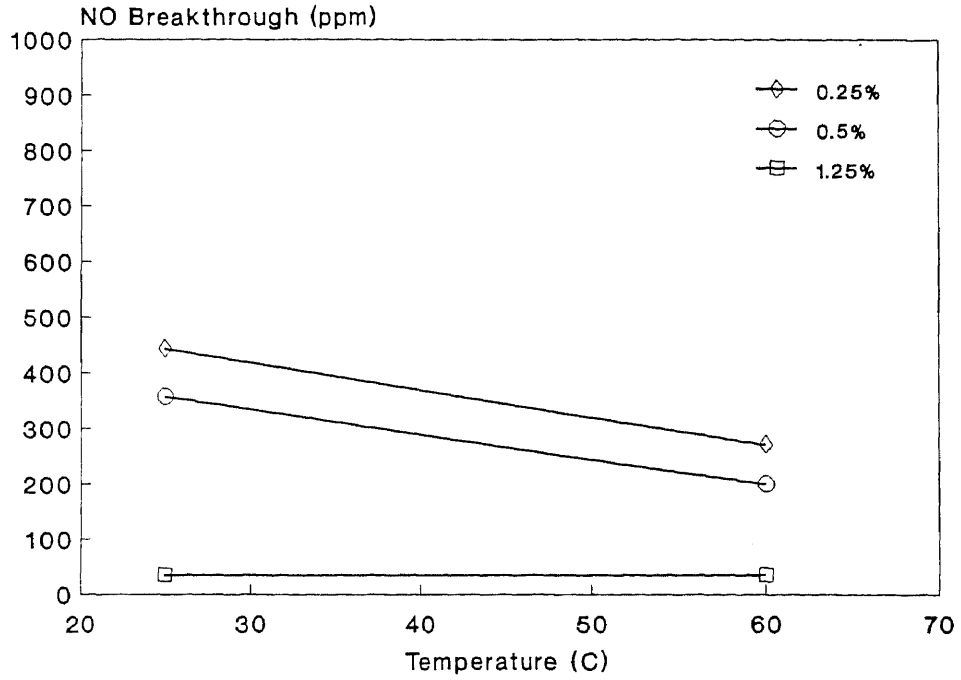

Figure 5.13 Effect of temperature on NO effluent concentration in NaClO scrubbing.

The results in Figure 5.13 show that the lower concentrations of ClO^- are more effectively utilized as the operating temperature is increased.

5.5 NO_x Absorption Induced by $NaClO_2$ Oxidation

Aqueous alkaline solution of sodium chlorite were found to be a good absorbents for flue gas NO. The following reaction was considered to take place in a stirred vessel during the absorption by Sada et. al. [1978].

$$4NO + 3ClO_2^- + 4OH \rightarrow 4NO_3^- + 3Cl^- + 2H_2O \qquad (5.5)$$

At low pH values, $NaClO_2$ produces ClO_2, which can be stripped out from the liquid and contributes to the oxidation of NO to NO_2 in gas phase.

$$4ClO_2^- + 2H^+ \rightarrow 2ClO_2 + ClO_3^- + Cl^- + H_2O \qquad (5.6)$$

A number of experiments were conducted to evaluate the ability of sodium chlorite to oxidize and absorb NO in aqueous solutions. Good results were reported in the patent literature by Senjo [1976] and Shibata [1977], but little information is available in the technical literature. Consequently, we conduct a number of experiments to determine the effectiveness of $NaClO_2$ as an oxidation agent of NO in nitric acid. It must be noted that sodium chlorite must be handled with great care.

Effect of pH

Due to the impurities in $NaClO_2$, the scrubbing solution has an initial pH of 10.0. The actual measurement shows that NO is quantitatively oxidized to NO_3^- during scrubbing. The increase in nitrate ion causes a decrease in pH to 3 after the first few minutes [Yang, 1990].

In an acidic aqueous solution, $NaClO_2$ equilibrate with ClO_2, Cl^-, and ClO_3^-. For safety consideration and scientific understanding, ClO_2 formation, desorption and reaction with NO was investigated at different pH values. Therefore, the first set of experiments was made to evaluate the effect of pH on the oxidation and absorption of NO in $NaClO_2$ aqueous scrubbing. Experiments are conducted at room temperature and pressure under the following conditions:

Flue gas: 2000 ppm NO balanced with N_2

Flow rate: 1 dm^3/min

Scrubbing solution: 0.0008, 0.008 and 0.08 M $NaClO_2$

0.0001, 0.001, 0.005, 0.01, 0.1 and 1 M NaOH

Volume: 1 dm^3

The results are shown in Figure 5.14. Low concentrations of NaOH, provided there is sufficient $NaClO_2$, does not inhibit the NO removal effectiveness. High concentrations of NaOH appears to inhibit the absorption. The upper limit for NaOH concentration necessary to completely absorb NO in $NaClO_2$ aqueous solution depends on the concentration of $NaClO_2$. NO is absorbed quantitatively in 0.008 molar $NaClO_2$ aqueous

solution when the concentration of NaOH is equal to, or lower than, 0.001 molar. The upper limit of NaOH in 0.08 molar $NaClO_2$ aqueous solution is 0.1 molar. The inhibiting effect may be due to the high pH rather than specifically to NaOH.

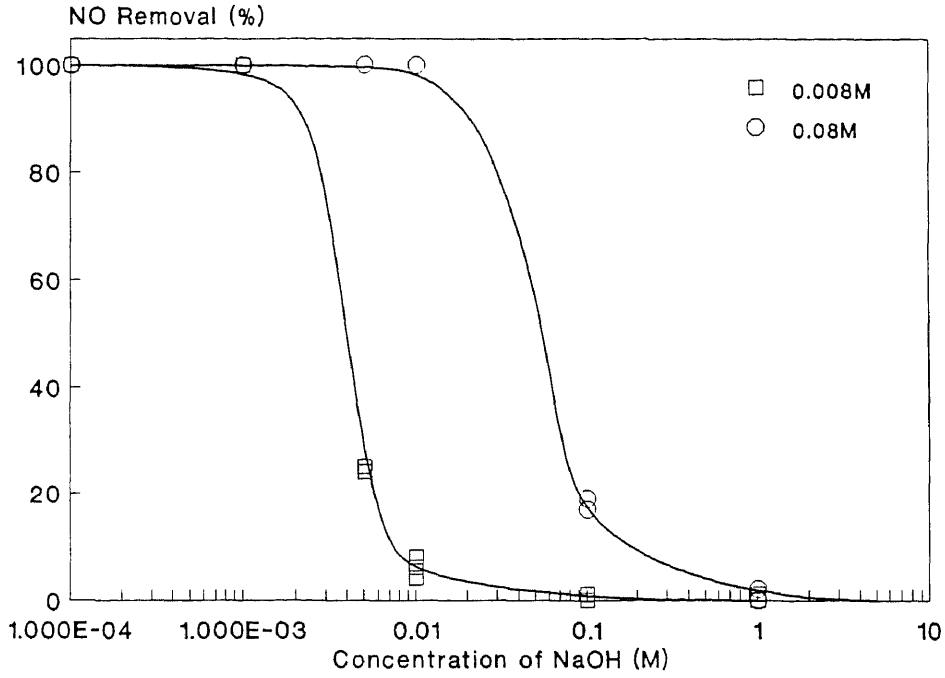

Figure 5.14 Effect of pH on NO absorption in $NaClO_2$ scrubbing.

ClO_2 Formation

At the upper limit concentration of NaOH, absorption can not reach 100% within the first few minutes, see Figure 4.2. If the NaOH concentration is a little higher than upper limit, absorption goes to zero after a few minutes of running time. Without pH control, a greenish yellow color in the solution is found after three minutes of operation and disappear right before NO breakthrough. A buffered solution delays appearance of the color. It is assumed that the color represents an active intermediate in the absorption of NO, apparently ClO_2.

A set of experiments was performed to identify the colored compound. Scrubbing solution were monitored with a LC/PDA system. Experiments are conducted in a packed bed scrubber at the following conditions:

Flue gas: 1000 ppm NO in N_2

Flow rate: 6 dm^3/min

Scrubbing solution: 0.008 M $NaClO_2$

volume: 2.5 dm^3

The original output from the LC/PDA system was a three dimensional plot of intensity, wavelength and time. ClO_2^- has a maximum absorbance at 259 nm while ClO_2 has an absorbance at 358 nm. Monitoring these two wavelength, ClO_2^- depletion and ClO_2 formation were determined in Figure 4.2. Quantitative results, which are shown in Figure 5.15, is calculated from calibration curves developed in Chapter 4.

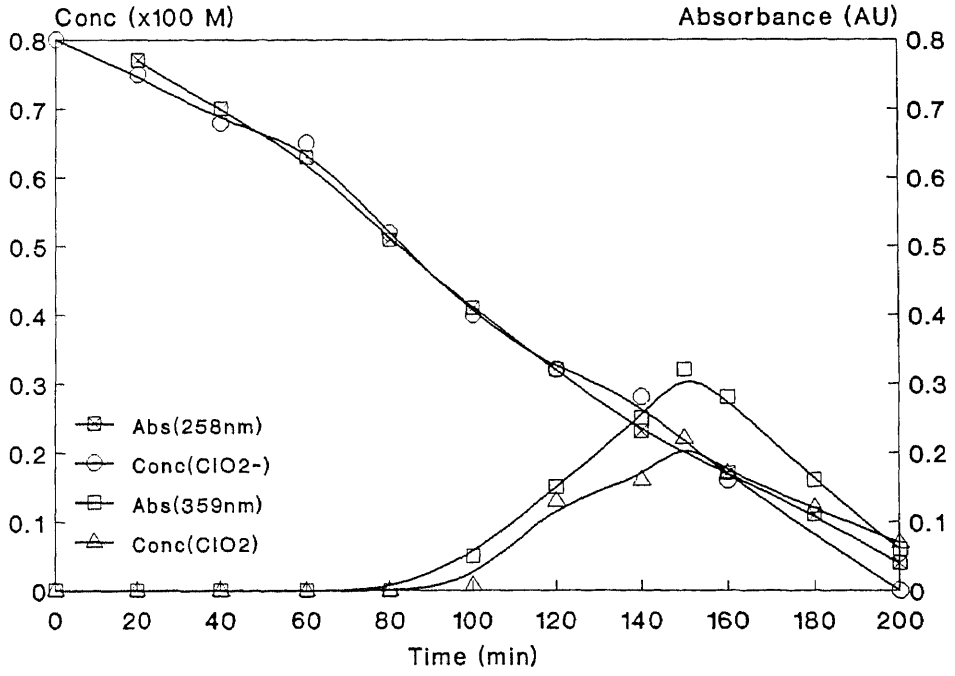

Figure 5.15 $NaClO_2$ depletion and ClO_2 formation during the NO scrubbing.

During scrubbing, $NaClO_2$ is consumed along with the formation of Cl^- and NO_3^- in the solution which have been reported in a previous study [Yang, 1990]. The production of NO_3^- causes the pH drop in the solution which increases the equilibrium concentration of ClO_2. This also helps explain why high pH instead of specifically high NaOH concentrations inhibit the NO removal.

Salt Bed Adsorption

Spent scrubbing solutions containing Cl^- and NO_3^- are considered as wastewater. There is an attempt to understand the process so that the wastewater problem can be taken care. Salt bed adsorption is an approach design to help explain the role water plays in NO absorption. Figure 5.16 shows the schematic diagram of NO adsorption system.

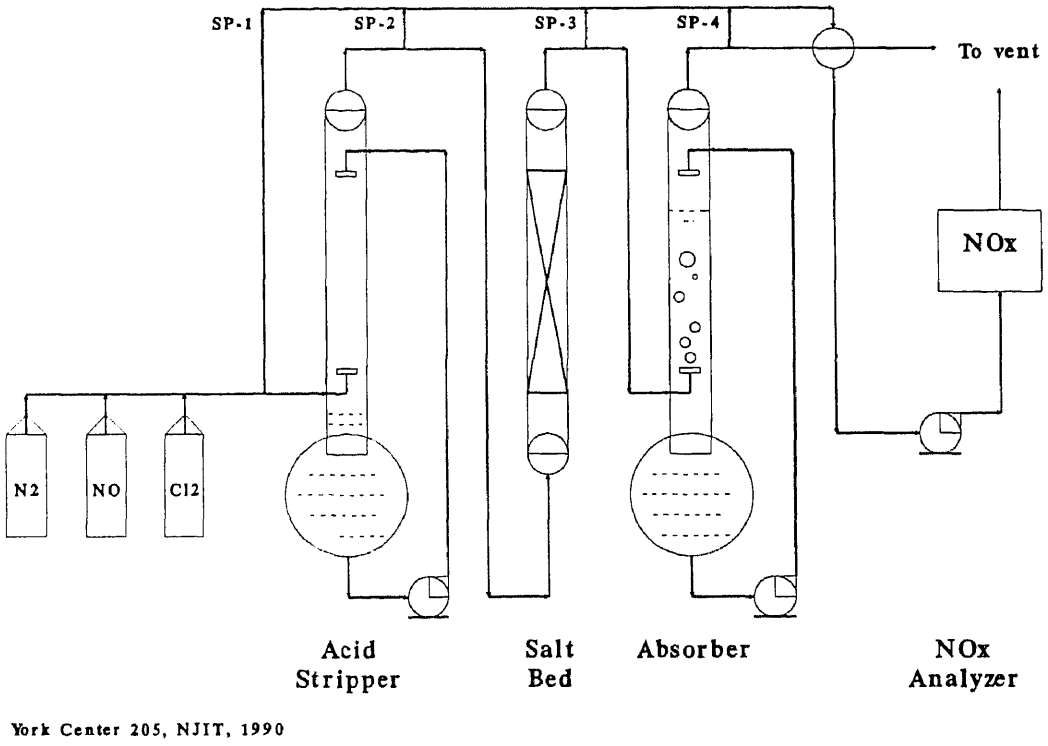

Figure 5.16 Schematic diagram of salt bed adsorption system

A set of experiment were constructed to illustrate NO adsorption in the absence of a solution. The process consists of a spray chamber as acid stripper or water saturator, a salt

bed of $NaClO_2$ particle, and a bubble column absorber. Flue gas from gas cylinders was injected into the spray chamber to carry out a small portion of acid or water and then introduced into the salt bed where reaction of NO with $NaClO_2$ or even with water or acid is expected. To prevent any poison gases breakthrough, the exiting flue gas is carried into a cold caustic water absorber. Where ClO_2 is expected to be collected, when acid was used in the process instead of water. Four sampling points were installed right after the mixer, acid stripper, salt bed and absorber. The objectives of this test were to determine the step by which NO was removed and the possibility of producing 2 grams of solid waste instead of 2.5 liter wastewater. Experiments are conducted at room temperature and pressure at the following conditions:

Flue gas: 600 ppm NO in N_2

Flow rate: 1 dm^3/min

Solution in stripper: Water or HCl aqueous solution

Salt bed: 2 gram $NaClO_2$ about 6 to 12 mesh

Solution in Absorber: Water or NaOH aqueous solution.

Table 5.2 NO Removal with $NaClO_2$ Oxidation in an Adsorption Bed

$NO + NaClO_{2(s)}$	Concentration(ppm)			
	SP-1	SP-2	SP-3	SP-4
NO	600	600	510	--
NO_2	0	0	90	--
$NO + H_2O + NaClO_2$				
NO	650	638	0	--
NO_2	0	0	128	--
$NO + HCl + NaClO_2$				
NO	590	570	0	0
NO_2	0	0	126	67

Table 5.2 presents the result of NO removal with $NaClO_2$ oxidation in an adsorption bed. Without moisture, 15% NO is converted to NO_2 by $NaClO_2$ and comes out with the gas stream. With moisture, NO is totally converted to NO_2 and more than 80% of NO_2 is

adsorbed in the salt bed. With acid, the same results are observed except for the large amount of ClO_2 collected in the absorber. The result shows that without moisture, $NaClO_2$ can not be used to removal NO from gas stream and acid is not required in this process. The salt bed is a way of avoiding waste water problem.

Operating Window

Inspection of Figure 5.6 shows that no significant ClO_2 is stripped out from the scrubbing solution, provided the pH is higher than 4.3. The experimental result of NaOH inhibition in Figure 5.14 shows that 100% removal of NO is a function of $NaClO_2$ to NaOH ratio. There is an operating window between these two conditions where the system can be operated at 100% NO removal without ClO_2 breakthrough.

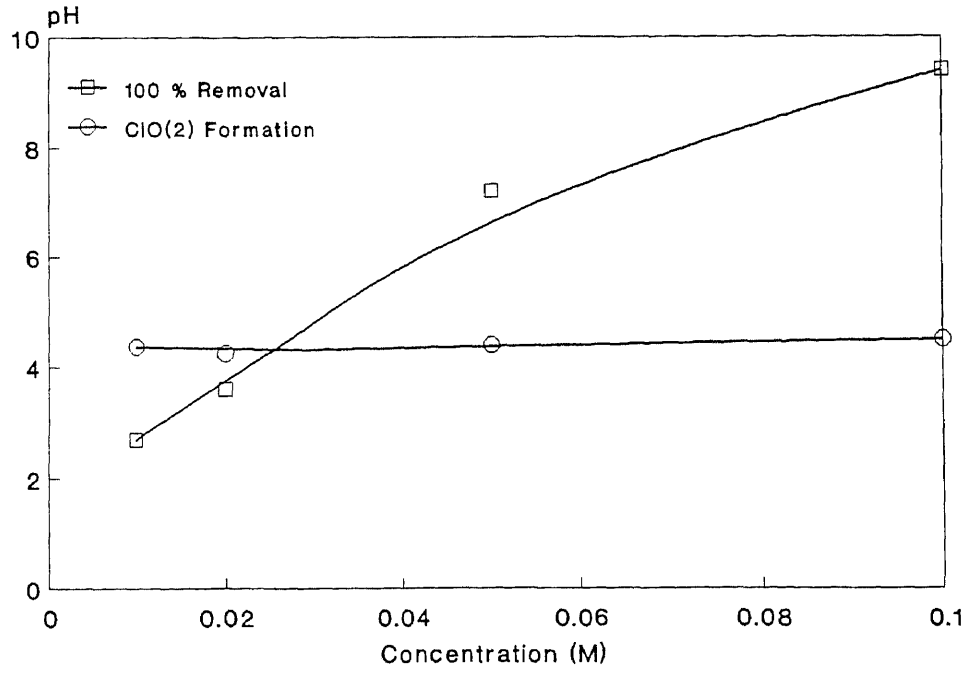

Figure 5.17 The operating window of NO removal with $NaClO_2$ oxidation.

A set of experiments were conducted to confirm this concept under the following conditions:

Scrubber: Packed bed

Flue gas: 300 ppm NO in air

Flow rate: 15 dm^3/min

Scrubbing solution: 0.01, 0.02, 0.05 and 0.1 M $NaClO_2$

pH: 2.7, 3.6, 7.2, and 9.4

Volume: 2.5 dm^3

L/G: 30

Figure 5.17 indicates that between the 100% removal line and ClO_2 formation line, there is an operating window. Note that the ClO_2 formation line is fixed there while the 100% removal line may shift up or down by changing L/G ratio, different type of absorber, or packing.

5.6 Utilization and Material Balance

In the previous study, aqueous solution of $NaClO_2$ was found to be the best oxidizing agent for NO removal. Before any further engineering investigation, it is necessary to obtain utilization information in order to conduct preliminary cost estimation and obtain material balances for safety and secondary pollution consideration.

Parameters in this study are NO, $NaClO_2$, NO_3^-, and Cl^-. NO is calculated from the flow rate, breakthrough time and concentration changes from the NO_x analyzer. Ion concentrations of NO_3^- and Cl^- are determined quantitatively using Waters Ion Chromatography System with UV and conductivity detectors. Results are presented in the following sections.

Utilization

For flue gas denitrification processes, catalyst might be the biggest investment of selective catalytic reduction (SCR), fuels can have more than 50% of thermal $DeNO_x$ costs. But for a wet process, chemicals are the major portion of total cost. Efficient utilization of chemicals is therefore a very important issue for a new process development.

Utilization is defined as the amount of NO removed by one unit of $NaClO_2$. experimental data is presented as molar ratio of NO and $NaClO_2$. According to the following equation, more than 100% of utilization can be obtained some conditions.

$$4\ NO + 3\ NaClO_2 + 2\ H_2O \rightarrow 4\ HNO_3 + 3\ NaCl \qquad (5.7)$$

Experiments were conducted at room temperature and pressure under the following conditions:

Scrubber: Bubble column

Flue gas: 2000 ppm NO in N_2

2000 ppm NO, 1000 ppm SO_2 in N_2

Flow rate: 1 dm^3/min

Scrubbing solution: 0.53 to 2 gram $NaClO_2$ per dm^3

pH: Uncontrolled and buffered at 6.7 and 9.6

Volume: 0.5 to 1 dm^3.

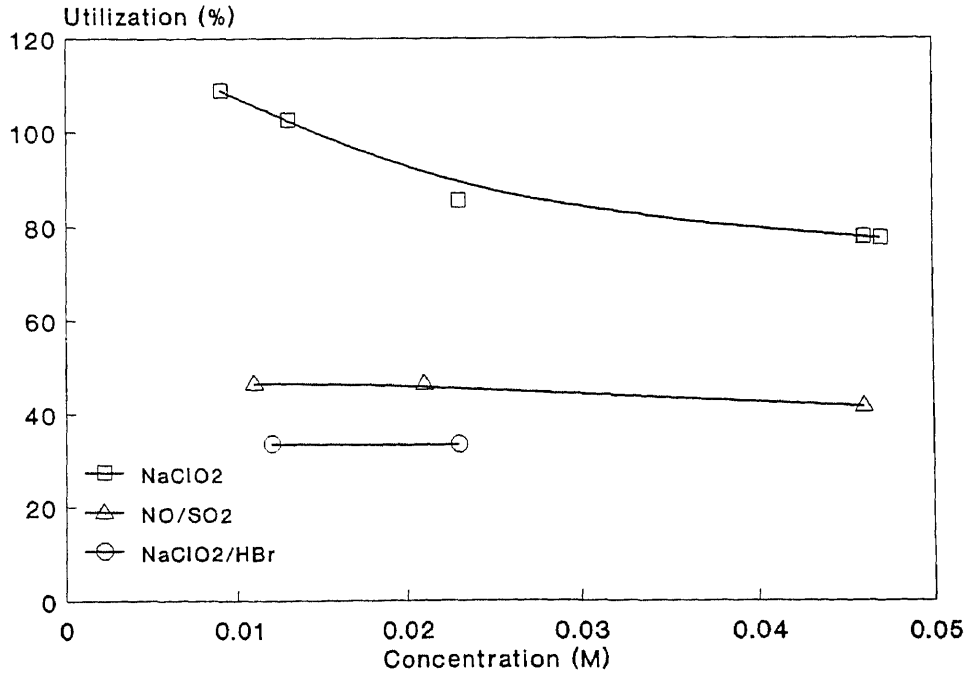

Figure 5.18 The utilization of $NaClO_2$ for NO removal without a pH control in scrubbing solution.

Figure 5.18 shows that without pH control, the higher the concentration of $NaClO_2$, the lower the utilization. Scrubbing solution with higher concentration of $NaClO_2$ ends up with higher NO_3^- concentration and lower pH. Equation 5.4 indicates that the formation of ClO_2 from $NaClO_2$ in acidic solution can be expressed as:

$$5\ ClO_2^- + 5\ H^+ \rightarrow 4\ ClO_2 + HCl + 2\ H_2O \qquad (5.8)$$

When converting $NaClO_2$ to Cl^-, its capacity for NO removal decreases. Under the same pH, the higher the concentration of ClO_2^-, the higher the equilibrium concentration of Cl^-, therefore a lower utilization can be expected.

The injection of SO_2 in the flue gas reduces the utilization to a half. Because of the higher solubility, SO_2 is dominating in the competition with NO for $NaClO_2$ consumption in aqueous solution.

With SO_2 in gas phase and HBr in scrubbing solution, the utilization is lower than 40%. Under this condition utilization lost by both Cl^- formation and SO_2 consumption mechanisms.

For process design consideration, SO_2 can be removed by a separate caustic scrubbing before the NO_x absorption. A well buffered scrubbing solution is studied to solve the second problem. Experiments were conducted under the same conditions except for the pH control. Potassium dihydrogen phosphate was used to keep the scrubbing solution at pH 6.7 and the pH change within one unit through out the experiment.

Results in Figure 5.19 show that the assumption is right and the buffered solution works. Without SO_2 in gas stream, the utilization is always more than 90%. Besides that, both uncontrolled and buffered scrubbing have the same trend on the effects of $NaClO_2$ concentration , SO_2 in gas phase, and HBr in the scrubbing solution.

Figure 5.20 indicates that alkaline scrubbing solution has the highest average utilization. The result can be easily explained that NO_2 has a higher solubility in alkaline aqueous solution.

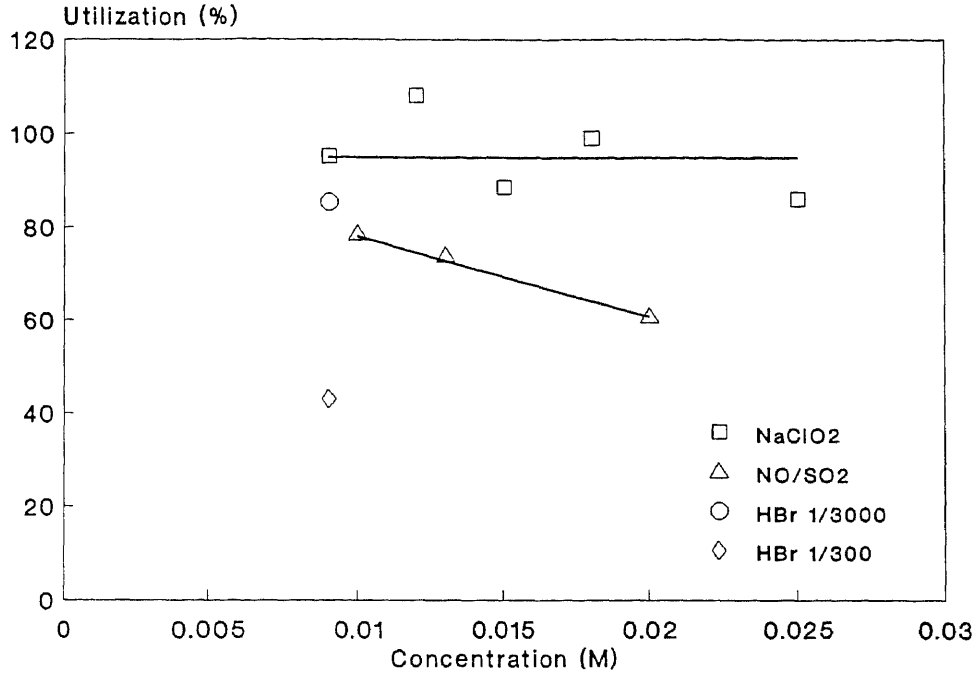

Figure 5.19 The utilization of $NaClO_2$ for NO removal in a buffered scrubbing solution at pH 6.7.

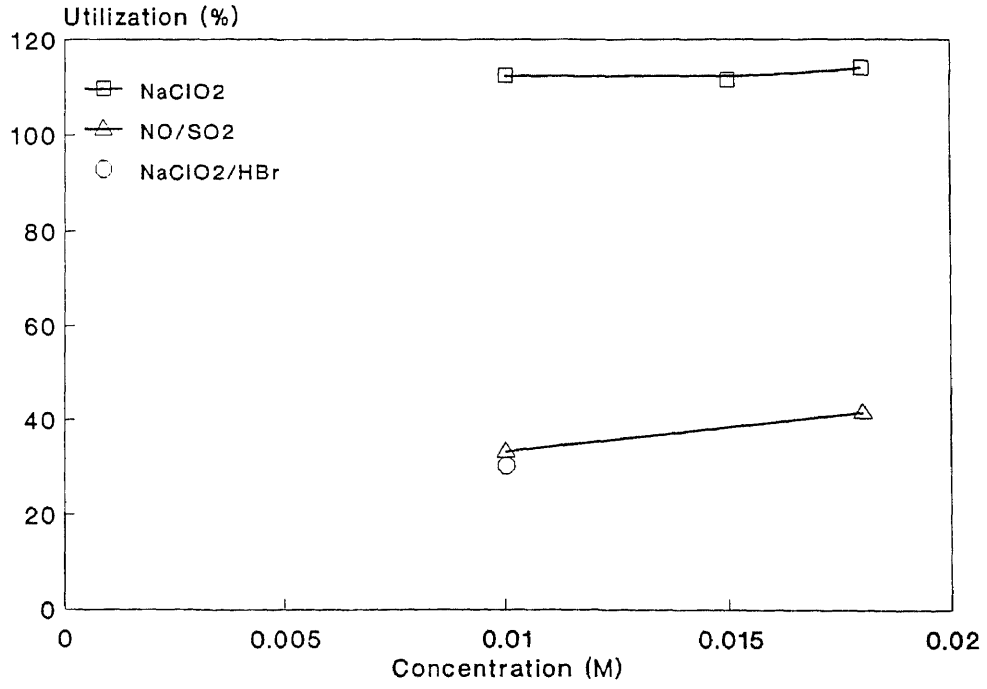

Figure 5.20 The utilization of $NaClO_2$ for NO removal in a buffered scrubbing solution at pH 9.6.

Material balances

The final step of this preliminary development were material balances. The fate of reactants, NO and $NaClO_2$, were studied in order to evaluate or prevent the problem of secondary pollution. According to Equation 5.7, NO_3^- and Cl^- are expected to be the only products in the system. Experiments were conducted at room temperature and pressure under the following conditions:

Scrubber: Bubble column

Flue gas: 2000 ppm NO in N_2

2000 ppm NO, 1000 ppm SO_2 in N_2

Flow rate: 1 dm^3/min

Scrubbing solution: 0.53 to 2 gram $NaClO_2$ per dm^3

Volume: 0.5 to 1 dm^3

pH: Uncontrolled and Buffered at pH 6.7 and 9.6.

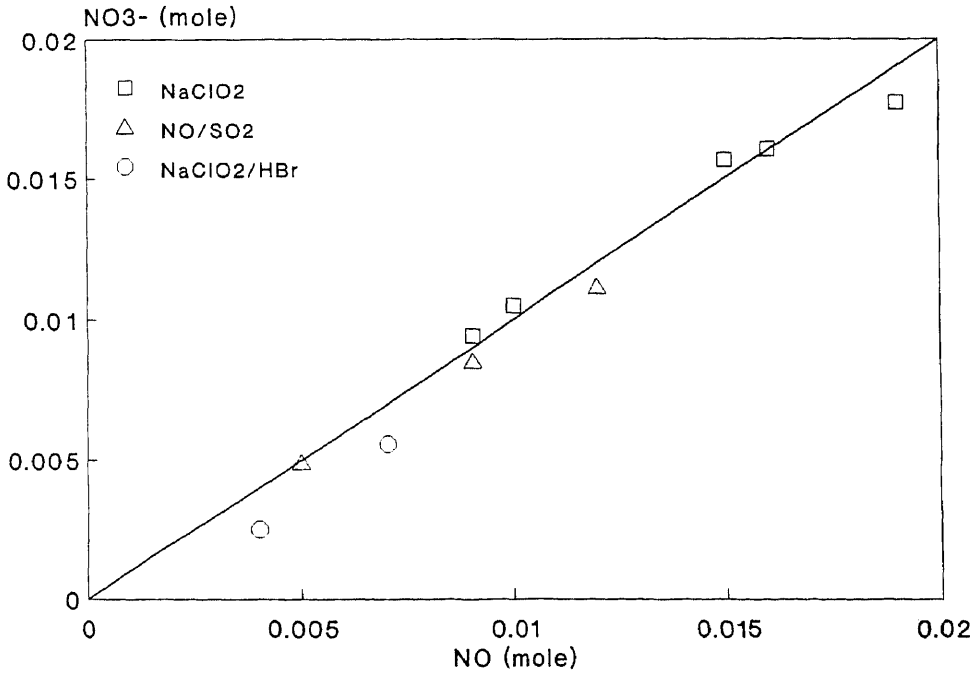

Figure 5.21 Nitrogen balance of $NaClO_2$ aqueous scrubbing for NO removal without pH control.

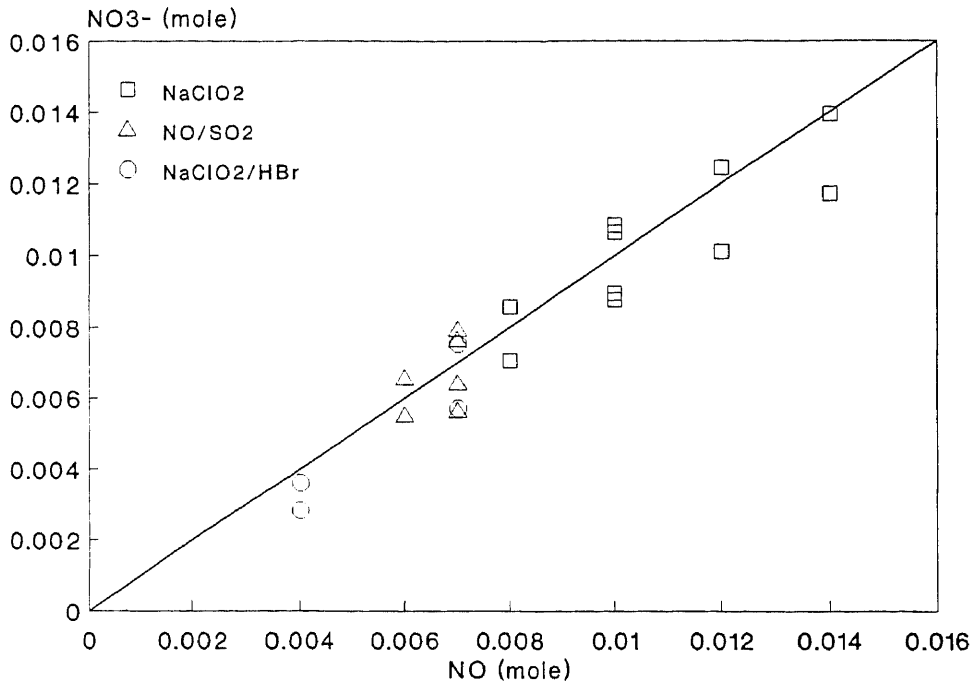

Figure 5.22 Nitrogen Balance of $NaClO_2$ aqueous scrubbing for NO removal at pH 6.7

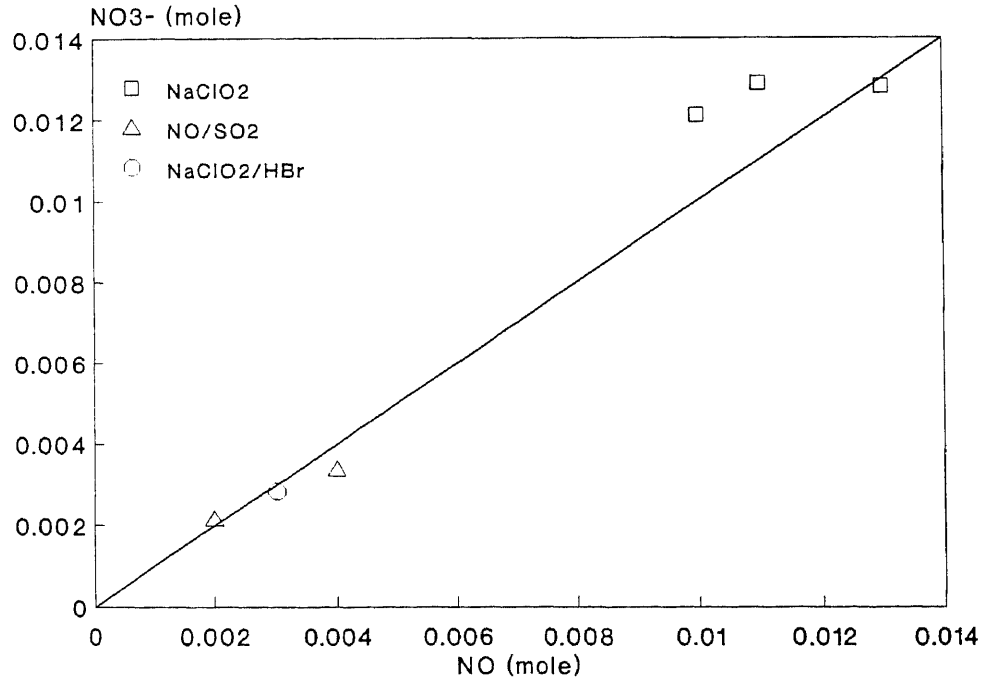

Figure 5.23 Nitrogen balance of $NaClO_2$ aqueous scrubbing for NO removal at pH 9.6.

Figures 5.21, 5.22 and 5.23 are the nitrogen balances in uncontrolled and buffered scrubbing solutions respectively. Values of NO were calculated from the flow rate, breakthrough time and concentration change using the NO_x analyzer while that of NO_3^- is determined by ion chromatography. All three scrubbing systems have good nitrogen recovery.

Figures 5.24, 5.25 and 5.26 show good balances of chlorine in both uncontrolled and buffered scrubbing. Values of $NaClO_2$ were calculated from the weight of commercial $NaClO_2$ powder with 80% purity and Cl^- values are determined by ion chromatography.

The lower Cl^- recovery, about 95%, from uncontrolled scrubbing is explained by Equation 5.4. Under low pH, ClO_2 is produced from $NaClO_2$ in the aqueous solution. A small portion, say 5%, of ClO_2 can be stripped out from the liquid. Which is also consistent with previous statement that the higher the concentration of $NaClO_2$ the lower the utilization.

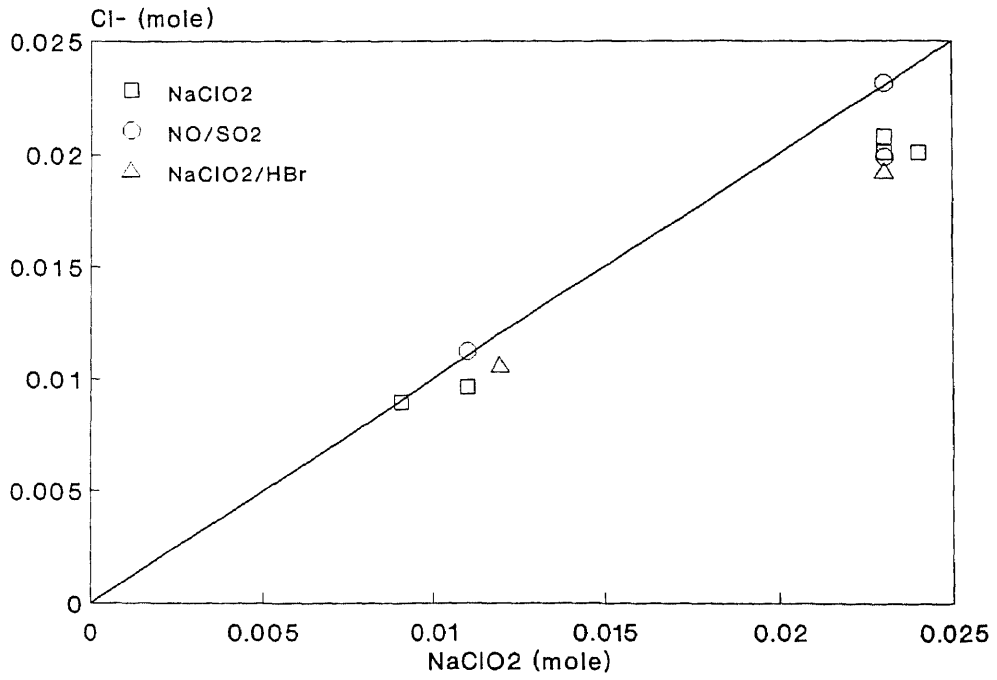

Figure 5.24 Chlorine recovery in $NaClO_2$ aqueous scrubbing for NO removal without pH control.

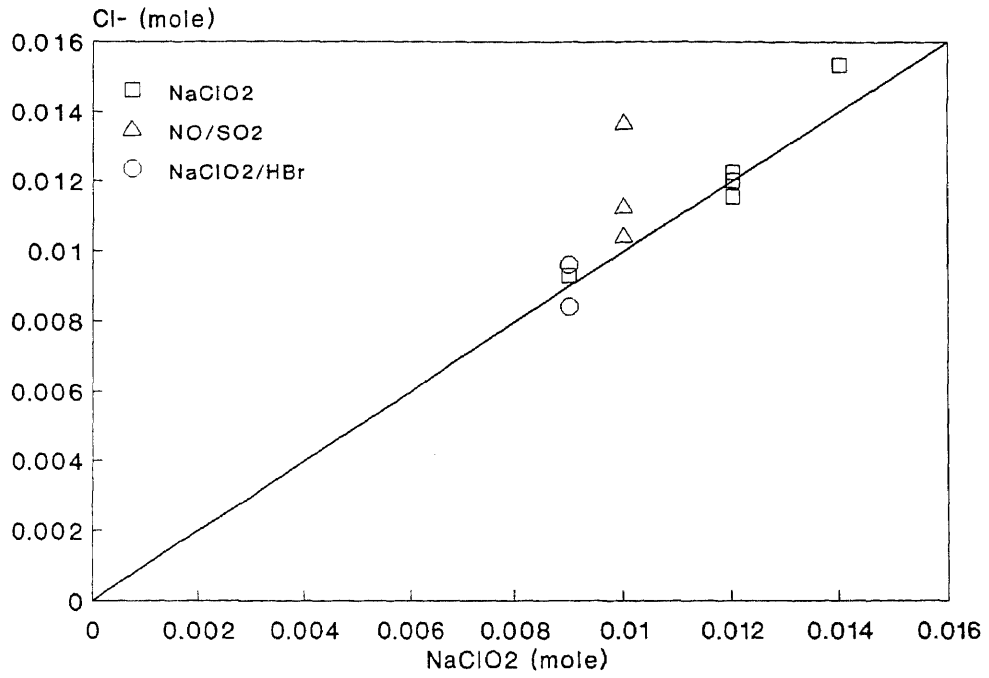

Figure 5.25 Chlorine recovery in $NaClO_2$ buffered aqueous scrubbing for NO removal at pH 6.7

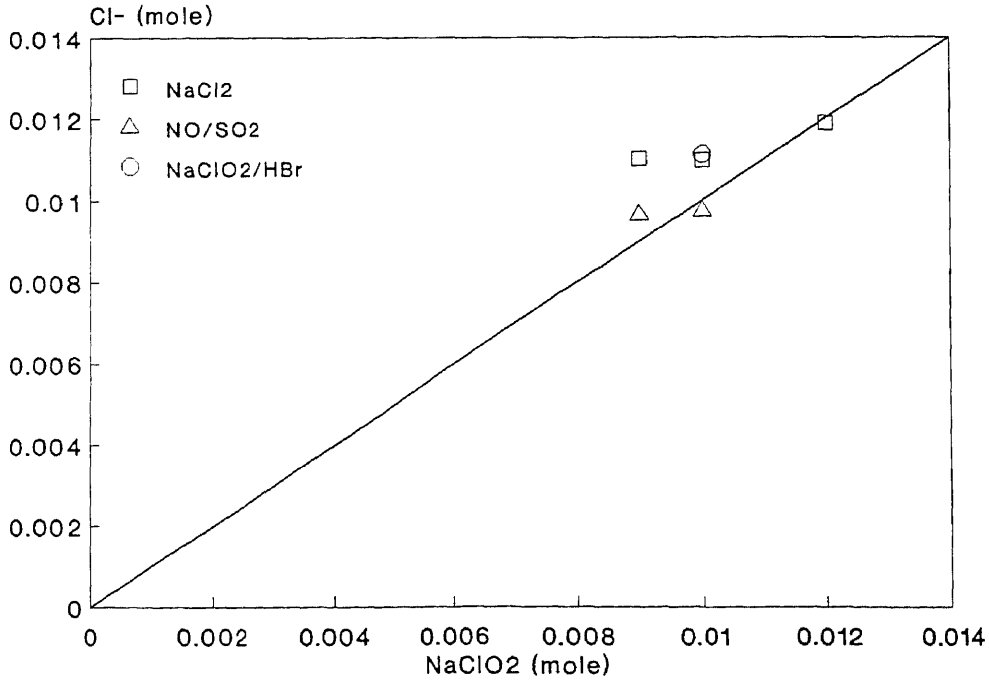

Figure 5.26 Chlorine recovery in $NaClO_2$ buffered aqueous scrubbing for NO removal at pH 9.6.

CHAPTER 6

THE OXIDATION AND ABSORPTION OF NO_x IN A SPRAY CHAMBER

6.0 Scope

A review of previous study leads to the conclusions that first, the reaction of NO to NO_2 is promoted by $NaClO_2$ concentration but inhibited by high pH. Second, the utilization of $NaClO_2$ for NO removal increases with high pH and low concentration. Third, Solubility of NO_2 in alkaline solution is much higher than that in acidic solution. NO removal from gas stream is a combined result of oxidation and absorption. The contradictions reveal that a two steps process might be the only solution.

Equal molar quantities of NO and NO_2 in gas stream can be removed quantitatively by NaOH aqueous scrubbing [Yang, 1990]. A spray chamber is studied as a prescrubber to convert 50% of incoming NO into NO_2. The outlet flue gas is than introduced into a NaOH aqueous scrubber where both NO and NO_2, and SO_2 if any, can be removed simultaneously. The spray chamber scrubber is chosen as a prescrubber because of its low capital and operating costs. Both savings are due to its simplicity and low pressure drop during the operation.

6.1 The Mathematical Correlations

Two mathematical equations are derived from the correlation of surface area for a shower sprayer [Mehta, 1970]. If the reaction of NO with $NaClO_2$ is first order in NO, the conversion of NO can be predicted by Equation 3.36 and experimental data is expected to fall on lines in Figure 3.7. If the reaction is so fast that the controlling factor is the interfacial surface area, then the mass flux is zero order with respect to NO concentration. NO conversion can be expressed by Equation 3.40 and experimental result are expected to fit lines in Figure 3.8.

In order to determine the better correlation between these two equations, several runs are made with NaOH under the following conditions:

Scrubber: Spray chamber scrubber

Flue gas: 300 ppm NO in N_2

Flue gas flow rate: 5, 10, 15, and 20 dm^3/min

Scrubbing solution: 0.037, 0.05, 0.073, 0.1, and 0.15 M $NaClO_2$

pH: 8.0

Scrubbing solution circulating rate: 200, 350, 500, 630, and 800 cm^3/min.

All experiments are conducted at room temperature and ambient pressure.

Figures 6.1 and 6.2 show a good agreement between experimental values and the curves calculated from Equation 3.36.

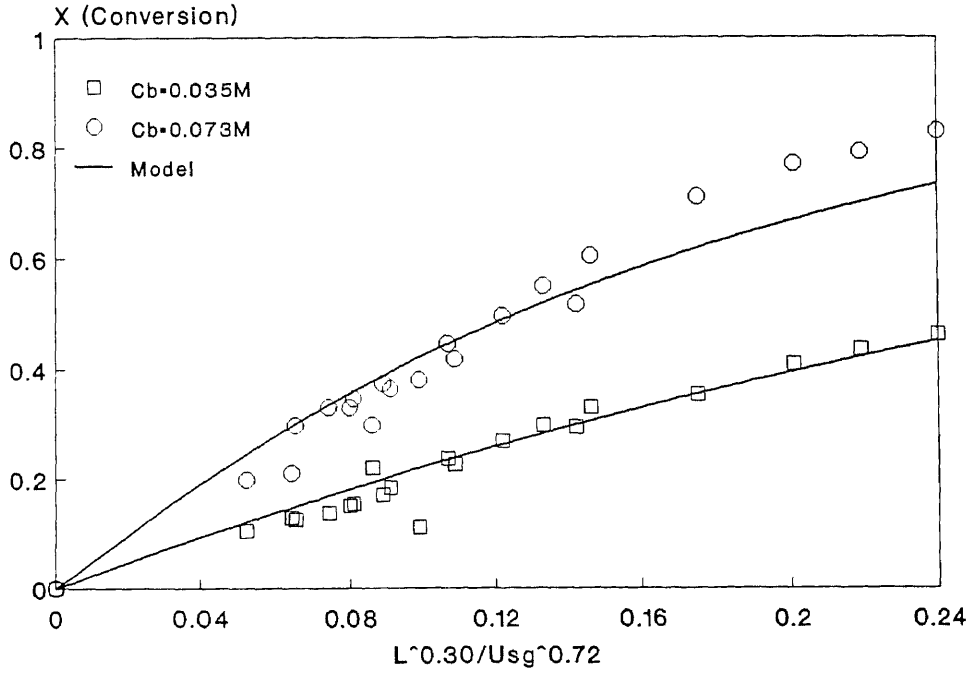

Figure 6.1 A comparison between the model (curves) and the experimental data used in the correlation (symbols) with first order in NO at low $NaClO_2$ concentration.

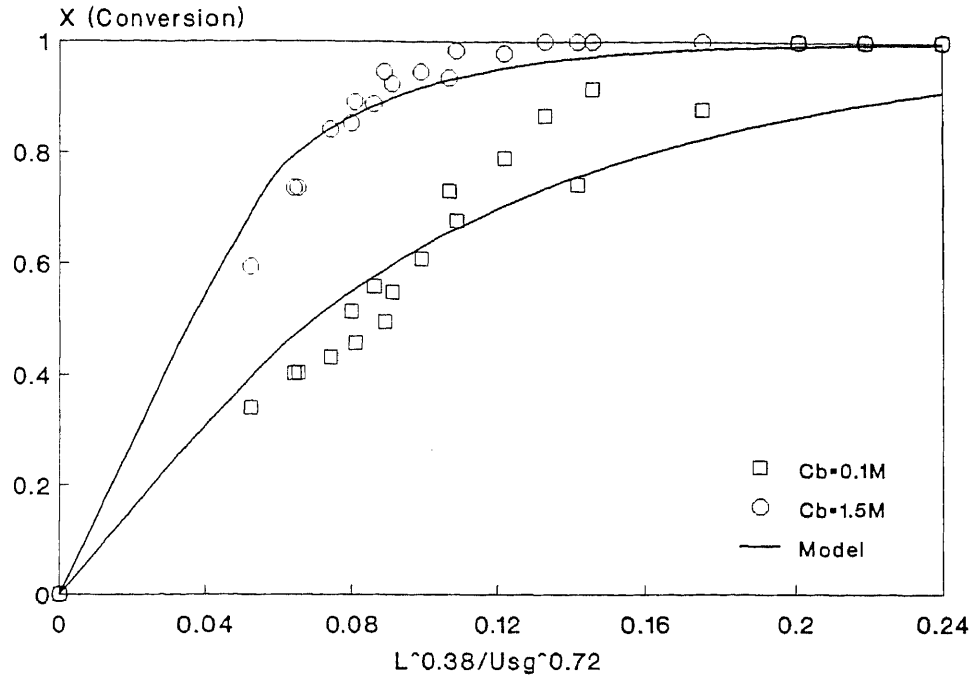

Figure 6.2 A comparison between the model (curves) and the experimental data used in the correlation (symbols) with first order in NO at high $NaClO_2$ concentration.

The good agreement is not surprising, since these experimental values have been used to estimate the pseudo rate constants. Model predictions are found to be always lower than experimental values at high liquid to gas ratio (L/G) and higher than experimental values at low L/G ratio. Therefore the data sets were tried to fit Equation 3.40.

Figure 6.3 shows that Equation 3.40 is the better correlation. The agreement between the experimental values and the model calculation is very good for both high and low L/G ratios. The model is ready to be used to evaluate the effects of $NaClO_2$ concentration, pH and temperature, etc. with great confidence. On the interfacial surface, NO is oxidized to NO_2. With the highest concentration on the interfacial surface, NO_2 can diffuse into both liquid and gas phase. In liquid phase, NO_2 is further oxidized to NO_3^- by $NaClO_2$. In gas phase, NO_2 is carried out of the scrubber and detected with NO_x analyzer. A simultaneous NO_2 absorption model is required to fully develop the spray chamber as a prescrubber.

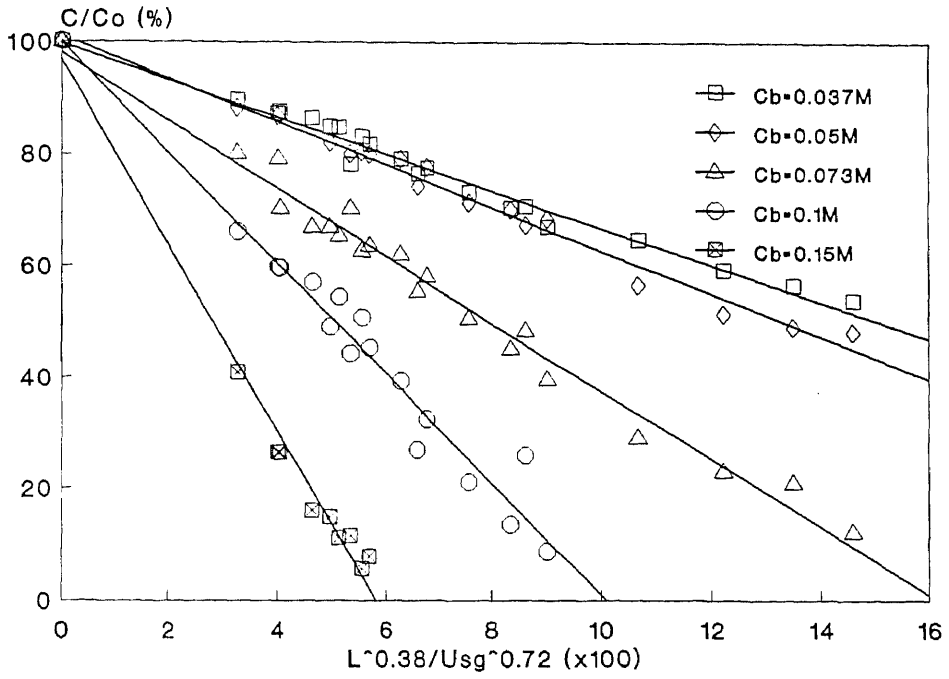

Figure 6.3 A comparison between the model (curves) and the experimental data used in the correlation (symbols) with zero order in NO.

6.2 NO Oxidation in a Spray Chamber Scrubber

In Equation 3.40, parameters can be categorized into two groups they are physical parameters and chemical parameters. The effects of physical parameters, such as cross section area, Ω, and density, ρ_l, on interfacial area in the literature [Mehta, 1970] are accepted as the same effects on NO removal. Further investigation is focused on the effects of chemical parameters such as concentration, temperature, and pH, etc. Liquid phase flow rate and superficial gas velocity are taken as independent parameters for the scale-up study.

6.2.1 Concentration Effect of $NaClO_2$ on NO Oxidation

To study the effect of $NaClO_2$ concentration on NO oxidation in a spray chamber scrubber, pseudo rate constants, the slopes, are carefully taken from previous data sets in

Figure 6.3. Figure 6.4 shows good linearity between the logarithms of rate constants and concentrations of $NaClO_2$. The slope is 1.2 which is considered as the order of $NaClO_2$ in the gas liquid reaction.

Flue gas flow rate: 5, 10, 15, and 20 dm^3/min

Scrubbing solution: 0.037, 0.05, 0.073, 0.1, and 0.15 M $NaClO_2$

pH: 8.0

Scrubbing solution circulating rate: 200, 350, 500, 630, and 800 cm^3/min.

All experiments are conducted at room temperature and ambient pressure.

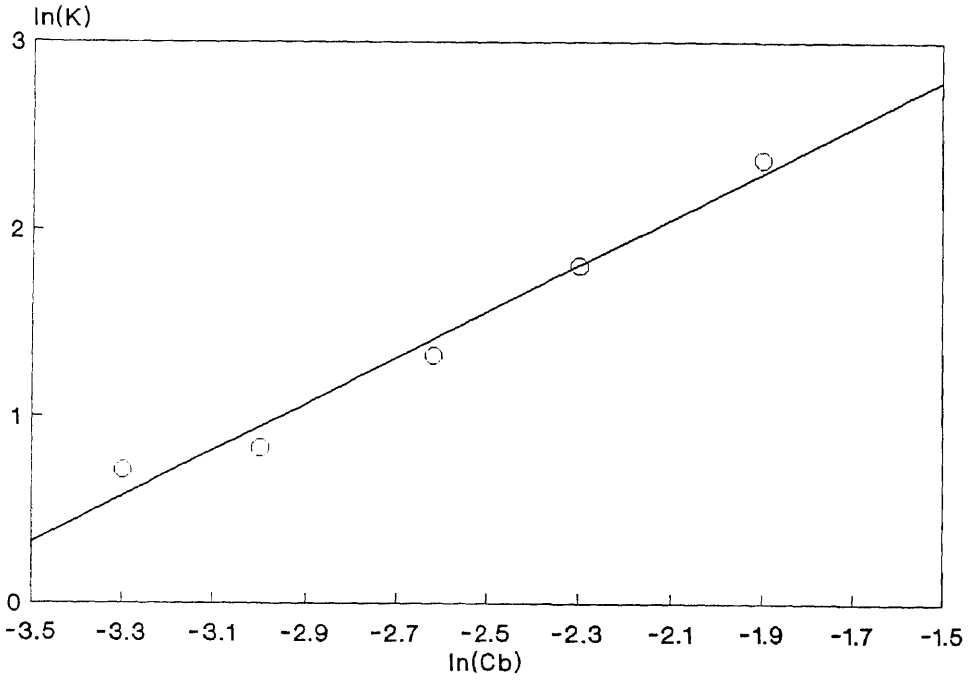

Figure 6.4 Order estimation of $NaClO_2$ for NO oxidation in a spray chamber scrubber.

6.2.2 The Effect of pH on NO Oxidation

Figure 5.14 indicates that high concentrations of NaOH inhibit NO absorption in $NaClO_2$ aqueous scrubbing. Absorption of NO consists of the oxidation of NO to NO_2 and the diffusion of NO_2 into the solution. Base on the results reported above, a certain amount of NO_x breaks through from $NaClO_2$ scrubbing in NaOH aqueous solution. NaOH may

inhibit the oxidation or lower the mass transfer coefficient of this process. Most likely, the high pH inhibit the oxidation of NO to NO_2 because high pH is in favor of NO_2 absorption [Yang, 1990].

The spray chamber scrubber is used to study the inhibition of NaOH for NO oxidation for its limitation of interfacial surface. Under this condition, NO conversion instead of NO_2 breakthrough can be determined. In order to determine if this effect actually takes place, a number of experiments are performed under the following conditions:

Scrubber: Spray chamber

Flue gas: 300 ppm NO in N_2

Flue gas flow rate: 5, 10, 15, and 20 dm^3/min

Scrubbing solution: 0.05 M $NaClO_2$

pH: 3.6, 4.8, 5.9, and 7.9 with NaOH and HCl

Circulating rate of scrubbing solution: 200, 350, 500, 630, and 800 cm^3/min

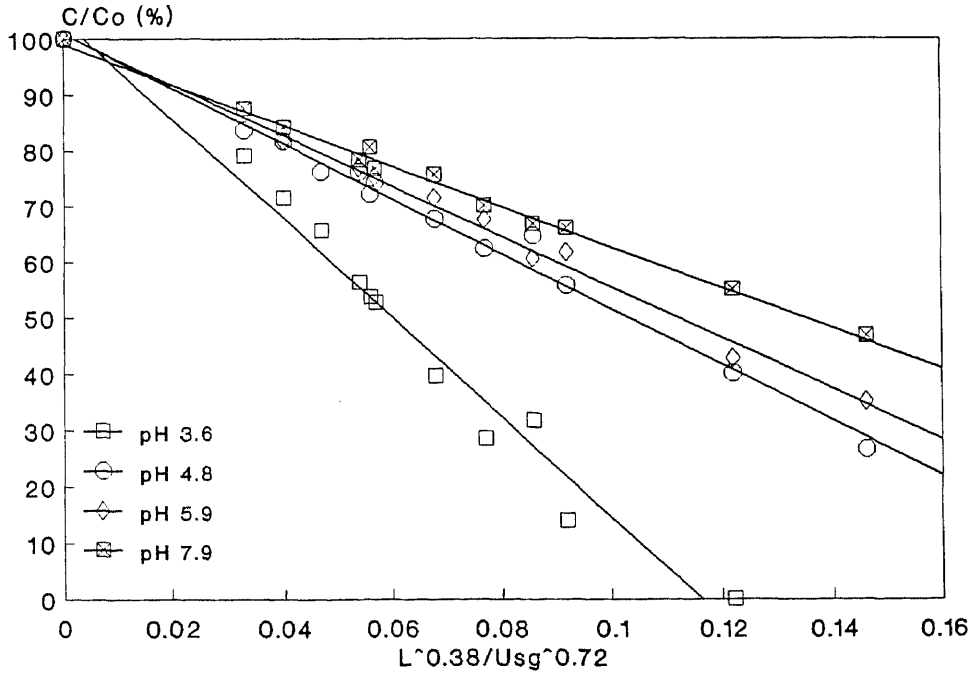

Figure 6.5 The effect of pH on NO oxidation in $NaClO_2$ aqueous scrubbing

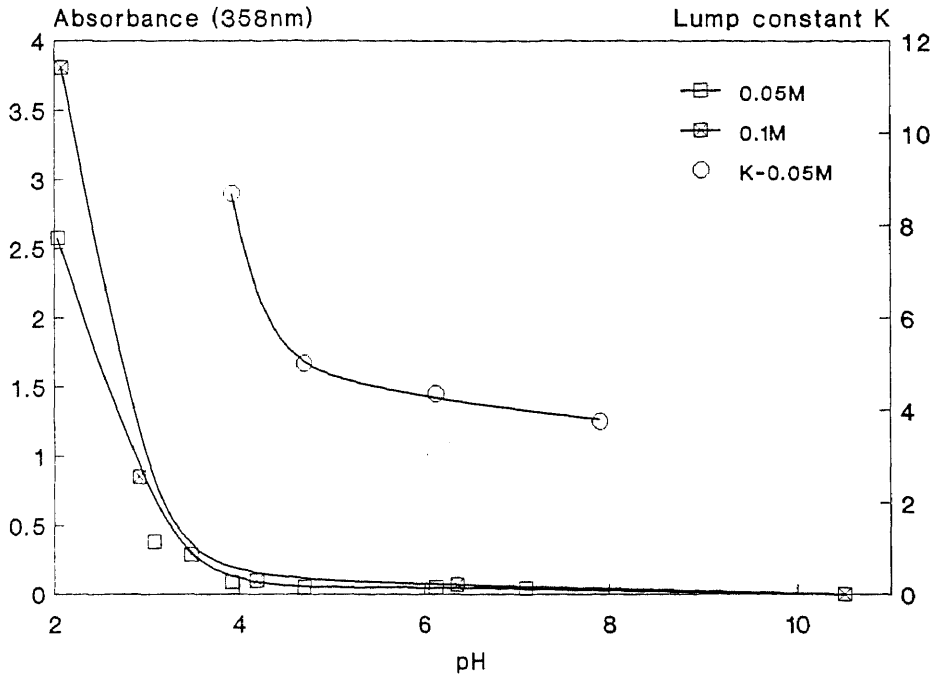

Figure 6.6 A comparison of pseudo rate constant versus the equilibrium concentration of ClO_2 in $NaClO_2$ aqueous solution.

All runs are conducted at room temperature and atmospheric pressure. Figure 6.5 shows that the rate constant increases with the decreasing of pH. It is consistent in the inhibition of NaOH on NO absorption. A comparison of rate constants and equilibrium concentrations of ClO_2 in $NaClO_2$ aqueous solution at different pH is plotted in Figure 6.6. These results reveal that the effect of $NaClO_2$ concentration on NO oxidation depends on the equilibrium concentration of ClO_2. ClO_2 is the active intermediate in the scrubbing solution.

6.2.3 The Effect of Temperature on NO Oxidation

Normally, flue gas enters a scrubber at a temperature of 70 ^{o}C after heat recovery. Thus, a series of runs is made to determine the effect of temperature on NO conversion in a $NaClO_2$ aqueous scrubbing. Experiments are conducted under the following conditions:

Scrubber: spray chamber

Flue gas: 300 ppm NO in N_2

Flue gas flow rate: 5, 10, 15, and 20 dm^3/min

Scrubbing solution: 0.05 M $NaClO_2$

Circulating rate of scrubbing solution: 200, 350, 500, 630 and 800 cm^3/min

pH: 8.0

Temperature: 25, 40, and 60 ^oC.

Generally, high temperature enhances a reaction rate and retards a mass transfer process due to the low solubility of a gas at high temperature. Figure 6.7 shows that the lower temperatures are more efficient as the same concentration of $NaClO_2$ in scrubbing solution.

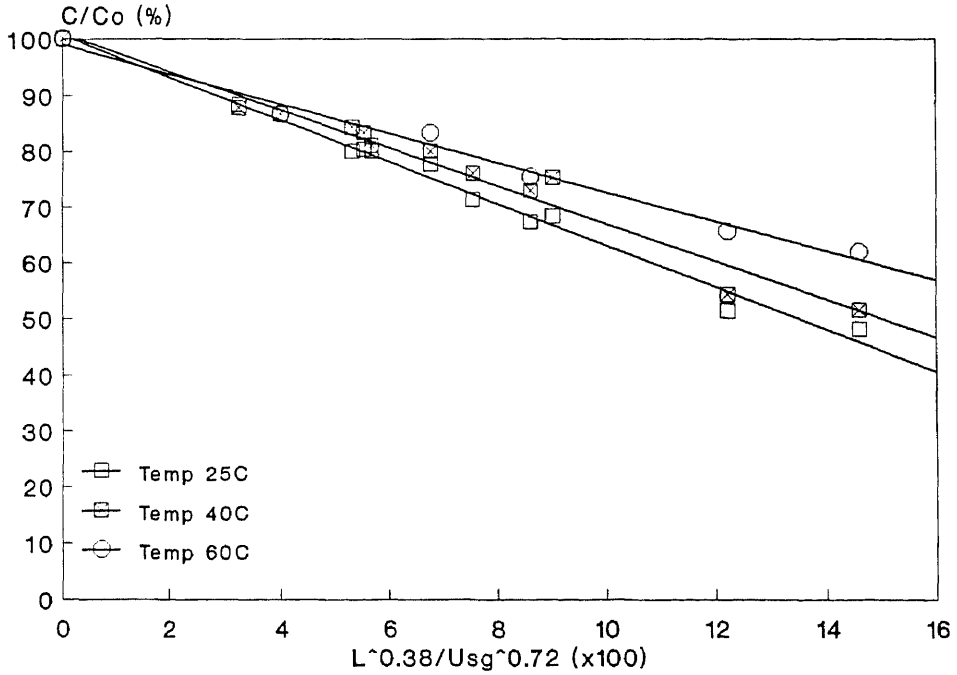

Figure 6.7 Effect of temperature on NO oxidation in $NaClO_2$ aqueous scrubbing.

CHAPTER 7

THE OXIDATION AND ABSORPTION OF NO_X IN A PACKED BED

7.0 Scope

Absorption with chemical reaction systems have been studied for different purposes in different fields using different approaches for over fifty years. The operation is used commercially for one of the three reasons. First, the product of an absorption reaction is a desired material. Chlorination of liquid benzene or other hydrocarbons with gaseous chlorine is an example of the first case. The second reason for using this operation is to obtain an improvement in product distribution and yield. A good example of the second case is the emulsion polymerization which is an industrially important reaction where these principles are used. This operation is used to remove an unwanted component from a fluid. Table 7.1 shows some of the well known reagents used to absorb various gases. Current results specifically for NO_X absorption with various reagents are summarized in Chapter Two. This technique has been widely used in pollution control applications.

In kinetic studies, absorption with chemical reactions are categorized as heterogeneous fluid-fluid reactions. In terms of the two film theory of Lewis and Whitman (1924), eight kinetic regimes were defined as the relative rates of reaction and mass transfer vary from one extreme to the other. Figure 3.5 shows what may occur in the interfacial film [Levenspiel, 1972]. Enhancement factor, which is defined by Equation 3.19, is used to correlate the experimental data and evaluate the effect of reaction on absorption.

In unit operation studies, chemical absorption is defined as absorption promoted by a chemical reaction. Without a chemical reaction, the relationship between height of packed bed and absorption can be expressed by Equation 3.48. The height of transfer unit (HTU) can be used to evaluate the efficiency of a system. If an irreversible reaction is involved in

the system, the equilibrium partial pressure of solute gas is zero. The HTU in Equation 3.49 can be used to correlate experimental data and evaluate the effects of other parameters in the system.

Table 7.1 Absorption Systems with Chemical Reaction.

Solute Gas	Reagent
CO_2	Carbonates
CO_2	Hydroxides
CO_2	Ethanolamines
CO	Cuprous amine Complexes
CO	Cuprous ammonium chloride
SO_2	$Ca(OH)_2$
SO_2	Ozone-H_2O
SO_2	H_2CrO_4
SO_2	KOH
Cl_2	H_2O
Cl_2	$FeCl_2$
H_2S	Ethanolamines
H_2S	$Fe(OH)_3$
SO_3	H_2SO_4
C_2H_4	KOH
C_2H_4	Trialkyl phosphates
Olefins	Cuprous ammonium complexes
NO	$FeSO_4$
NO	$Ca(OH)_2$
NO	H_2SO_4
NO_2	H_2O

[Levenspeil, 1972].

The HTU is closely related to the mass transfer coefficient. The HTU is simpler to use because it has the units of length. Usually the order of magnitude of HTU is 0.15 to 1.5 m (0.5 to 5 ft). H_{ox} and H_{oy} tend to be independent of the liquid phase circulation rate.

Most experimental data on packed beds are given in HTUs rather than in terms of mass transfer coefficients.

7.1 The Effect of Liquid Rate on HTU

The overall height of a transfer unit in gas phase (H_{oy}) is defined as

$$H_{oy} = \frac{\frac{F}{\Omega}}{K_y a} \tag{7.1}$$

If G_y/M or Gm is substituted for F/Ω in Equation 7.1, the equation of H_{oy} may be written

$$H_{oy} = \frac{\frac{G_y}{M}}{K_y a} \tag{7.2}$$

Ideally, H_{oy} is a function of G_y, the mass velocity of gas stream, only. To place a strong basis for this statement, a series of experiments were made to determine the effect of liquid phase circulating rate on H_{oy} under the following conditions:

Scrubber: 2 inch diameter packed bed with 1/4 inch ceramic Raschig rings

Flue gas: 300 ppm NO in N_2

Flue gas flow rate: 8, 10, and 15 dm^3/min

Scrubbing solution: 0.08 M $NaClO_2$

pH: 5.4

Temperature: 10 ^oC

Circulating rate: 70 to 800 ml/min

Figure 7.1 shows that in reality HTU is a weak function of liquid circulating rate. At low liquid rates much of the packing is dry. The wetted surface decreases with decreasing liquid rate. Therefore a higher HTU can be excepted from Equation 7.2 and is indeed observed in Figure 7.1. As the liquid rate increased, the wetted fraction of the packing increases until a point at which almost all of the packing becomes completely wet. This

critical liquid flow rate is called the minimum wetting rate. In this study, the minimum wetting rate is determined as 7200 kg/m^2-h (1800 lb/ft^2-h) based on the empty cross section of the bed. Which is 300 cm^3/min in the 5 cm diameter packed bed in the laboratory. Results in following sections are based on this criteria.

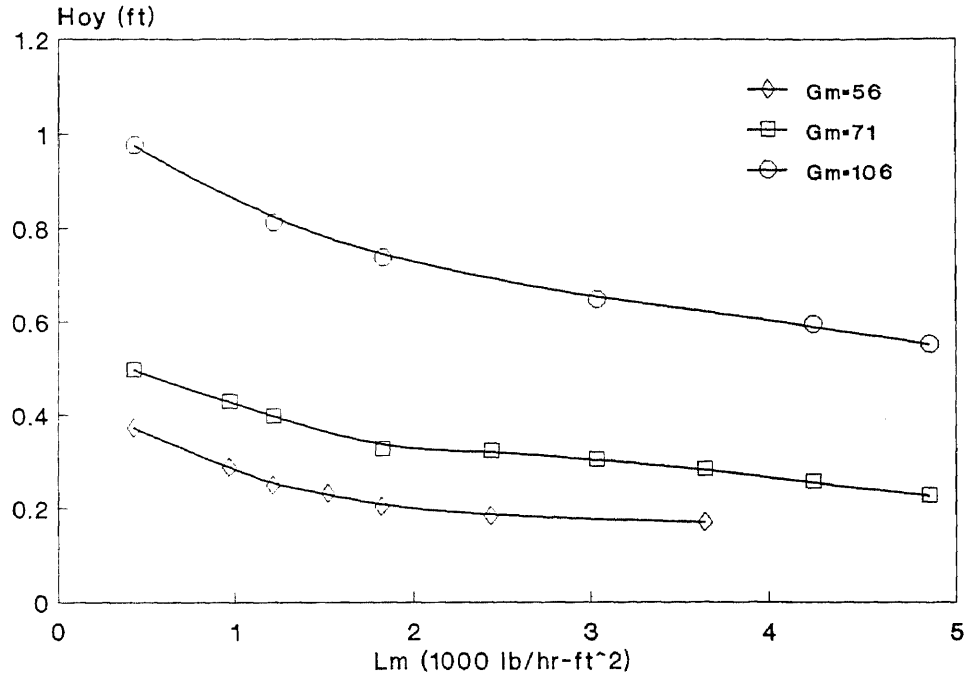

Figure 7.1 The effect of liquid phase circulating rate on the height of a transfer unit base on gas phase resistance

7.2 The HTU for NO Oxidation, NO Absorption with Oxidation, NO_2 Absorption, and NO_2 Absorption with Oxidation

When conducting an experiment of NO absorption with $NaClO_2$ oxidation in a packed bed, both NO and NO_2 can breakthrough under certain conditions. Figure 7.2 presents the results from a series of experiments to determine the impact of SO_2 on NO_x absorption. Consider a single run at pH 10, 300 ppm NO in N_2 is injected into the scrubber. With 300 ppm SO_2 present, more than 80% NO goes through the packed bed unreacted and no NO_2 is detected. Without SO_2 injection , 38% NO_2 and no NO are detected in the

effluent. HTU for NO oxidation, for NO absorption with oxidation, for NO_2 absorption, and for NO_2 absorption with oxidation are defined as follows:

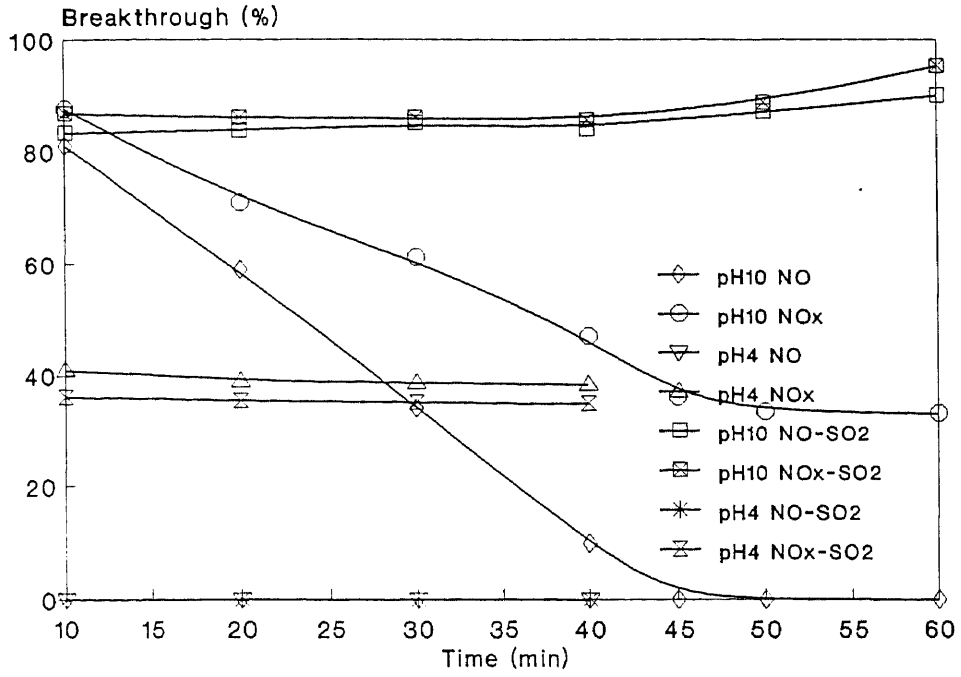

Figure 7.2 The breakthrough of NO_X from $NaClO_2$ aqueous scrubbing.

HTU calculated from NO injection and NO breakthrough is the HTU for NO oxidation.

HTU calculated from NO injection and NO_X breakthrough is the HTU for NO absorption with oxidation.

HTU calculated from NO_2 injection and NO_2 breakthrough without an oxidizing agent in the scrubbing solution is the HTU for NO_2 absorption.

HTU calculated from NO_2 injection and NO_2 breakthrough with an oxidizing agent in the scrubbing solution is the HTU for NO_2 absorption with oxidation.

7.3 The Effect of Temperature on HTU for NO Oxidation

Flue gas generally enters a scrubber at a temperature of approximately 70 ^{o}C after heat recovery. Chemical reactions, especially oxidation, are enhanced by high temperature but not gas absorption. Normally, solubility of a gas decreases with the increasing temperature. Therefore, temperature effect on NO oxidation and absorption is one of the uncertainties in the design of a scrubber. Experiments were conducted at four different temperatures under the following conditions:

Scrubber: 5 cm packed bed with 0.64 cm ceramic Raschig rings

Flue gas: 300 ppm NO in N_2

Flow rate: 8, 10, 15, 20, 25, 30, and 35 dm^3/min

Scrubbing solution: 0.08 M $NaClO_2$

pH: 5.4

Temperature: 10, 20, 30, and 40 ^{o}C

Circulating rate: 300 to 800 cm^3/min

Figure 7.3 shows that at room temperature, HTU for NO oxidation is a linear function of gas mass velocity. Which is consistent in Equation 7.2. The slope is the ratio of average molecular weight of gas stream and the product of the mass transfer coefficient and effective interfacial area ($K_y a$). A good straight line in Figure 7.3 indicates that within the experimental range, both the mass transfer coefficient and interfacial area are not a function of the gas mass velocity. A comparison of HTU for NO oxidation shows that as temperature increases efficiency decreases, measured in an increase in HTU height without changing the mass transfer coefficient.

7.4 The Effect of pH on HTU for NO Oxidation

pH is the key parameter for $NaClO_2$ aqueous scrubbing system. The inhibition of NO oxidation by $NaClO_2$ at high pH was observed in bubble column and confirmed in a spray chamber scrubbing system. In a packed bed, HTU is used to estimate the extend of

inhibition that can be achieved due to pH change. Experiments were conducted at room temperature, 20 ^{o}C, and ambient pressure under the following conditions:

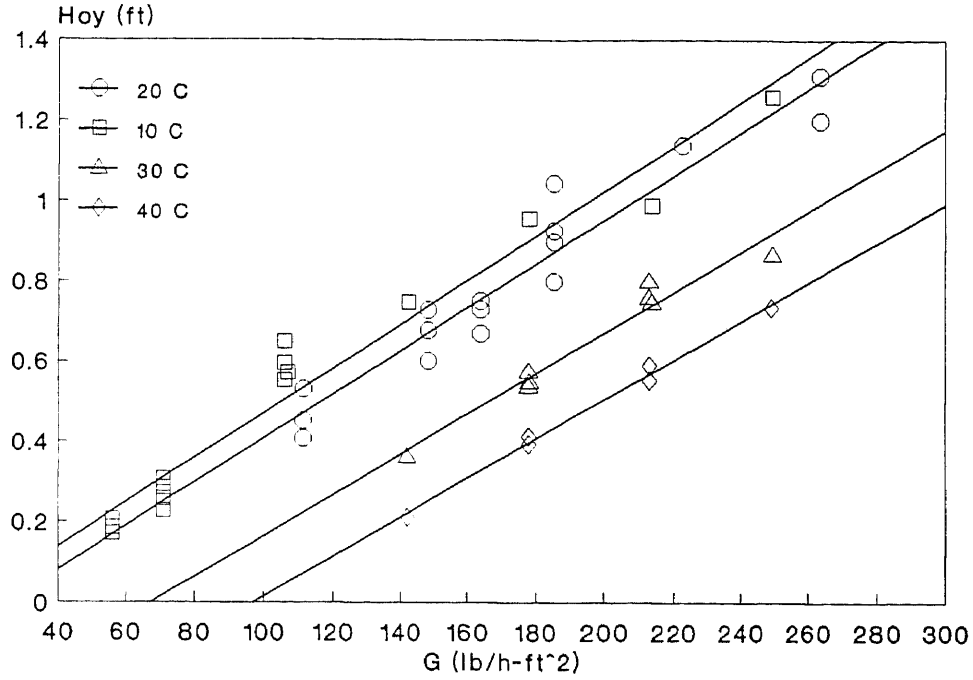

Figure 7.3 The effect of temperature on height of a transfer unit for NO oxidation.

Scrubber: 5 cm packed bed with 0.64 cm ceramic Raschig rings

Flue gas: 300 ppm NO in N_2

Flow rate: 10, 15, 20, 25, 30, and 35 dm^3/min

Scrubbing solution: 0.08 M $NaClO_2$

pH: 4, 5.3, 7.4, 8.2, and 10.2

Circulating rate: 450 cm^3/min

Figure 7.4 shows that HTU for NO oxidation is a linear function of gas mass velocity at different pH values. At pH 5, 7, and 8, the efficiencies are almost the same. When pH drops to 4, the efficiency, in terms of HTU for NO oxidation, increases significantly. This is no surprising since ClO_2, the actual oxidizing agent, is liberated at low pH in the

scrubbing system. Attention must be drawn to the unexpected experimental result at pH 10.2. As expected, the efficiency at this pH started low (high H_{oy}) in this series, but it kept increasing with run time under the same pH. This could be a very useful observation for process design, although it is not fully understand at this point.

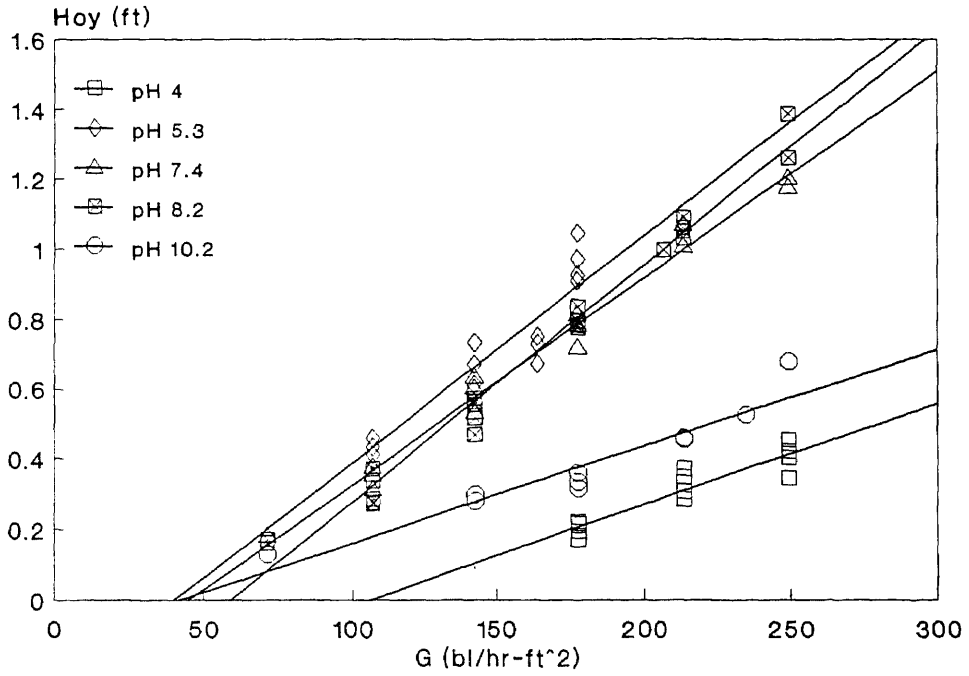

Figure 7.4 The effect of pH on the HTU for NO oxidation in $NaClO_2$ aqueous scrubbing.

Figure 7.5 indicates that the product of gas phase mass transfer coefficient and interfacial area (K_ya) is a function of pH. This result is in agreement with the anticipated trends of equilibrium concentration of ClO_2 in $NaClO_2$ aqueous solution and pseudo zero order rate constant in spray chamber scrubbing.

7.5 The Effect of Concentration on HTU for NO Oxidation and K_ya

The effect of $NaClO_2$ concentration on NO oxidation was studied in order to better understand operating costs for process design consideration. High concentration gives

high removal efficiency which means a lower HTU or Z_T, the total height of a packed tower. However high concentration scrubbing solutions have lower utilization efficiency and end up with high concentrations of NO_3^- and Cl^- in spent solution which may need further treatment before discharge.

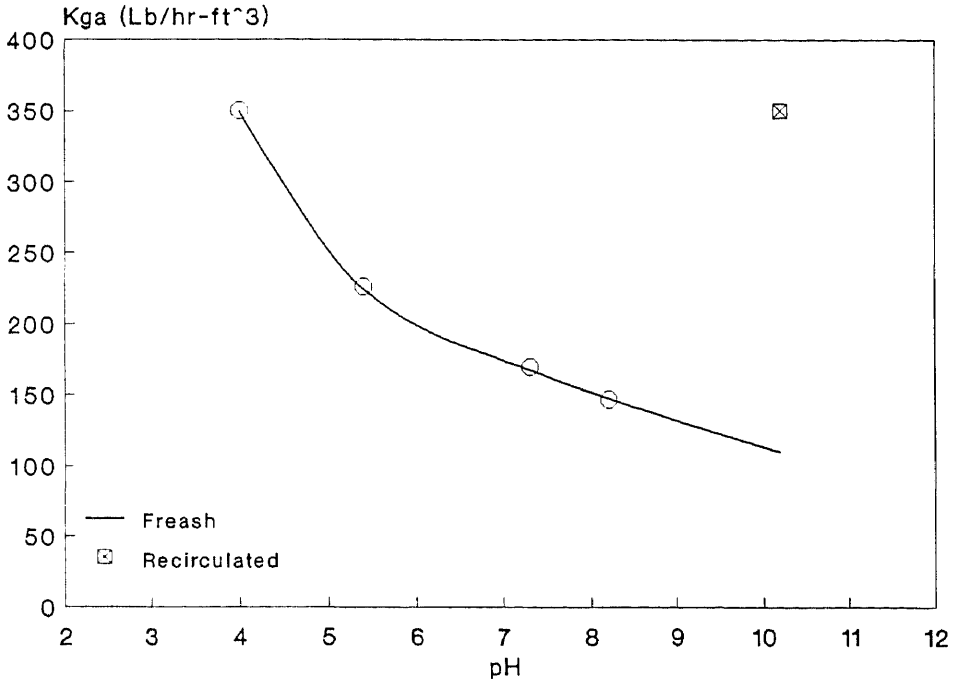

Figure 7.5 The effect of pH on overall mass transfer coefficients

Another concern is that for a certain removal efficiency, a packed bed with lower HTU will allow a higher concentration of the spent solution. Emitting $NaClO_2$ is not only a cost problem, but also an environmental problem. All these considerations are quantified in this part of the research. Experiments were conducted at room temperature and pressure under the following conditions:

Scrubber: 5 cm packed bed with 0.64 cm ceramic Raschig ring

Flue gas: 300 ppm NO in N_2

Flow rate: 5, 10, 15, 20, 25, 30, and 35 dm^3/min

Scrubbing solution: 0.02, 0.04, 0.05, 0.06, 0.08, 0.1, and 0.12 M $NaClO_2$

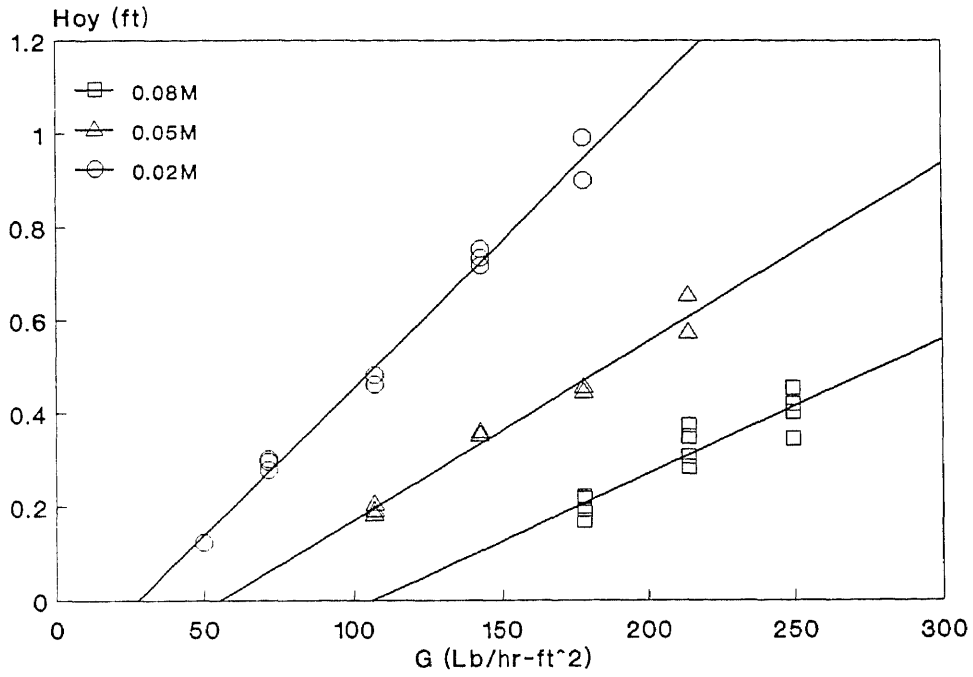

Figure 7.6 The effect of $NaClO_2$ concentration on HTU for NO oxidation at pH 4.0

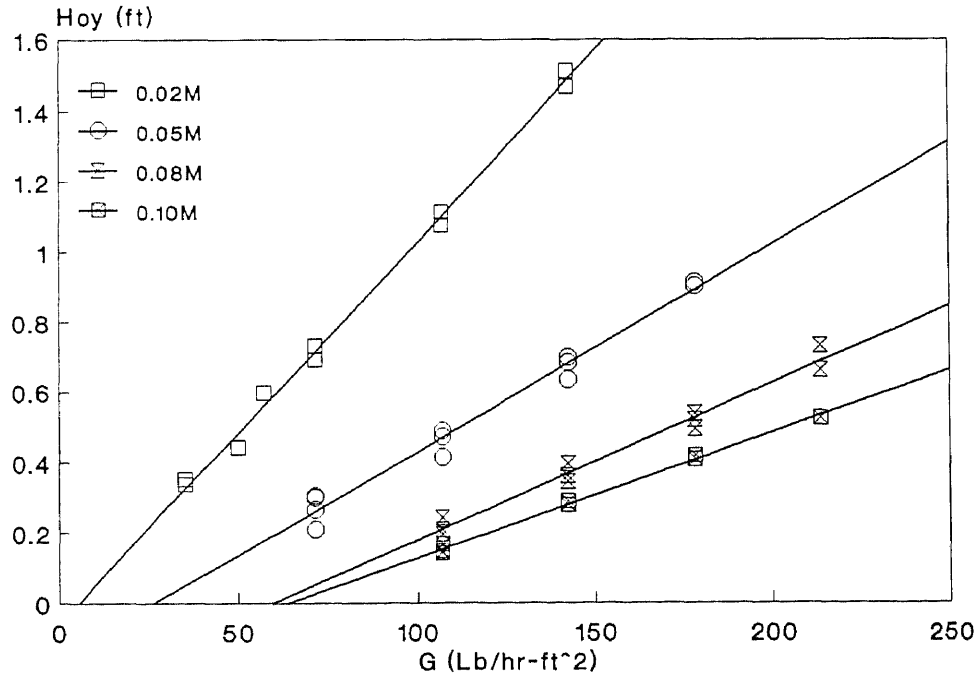

Figure 7.7 The effect of $NaClO_2$ concentration on HTU for NO oxidation at pH 5.4

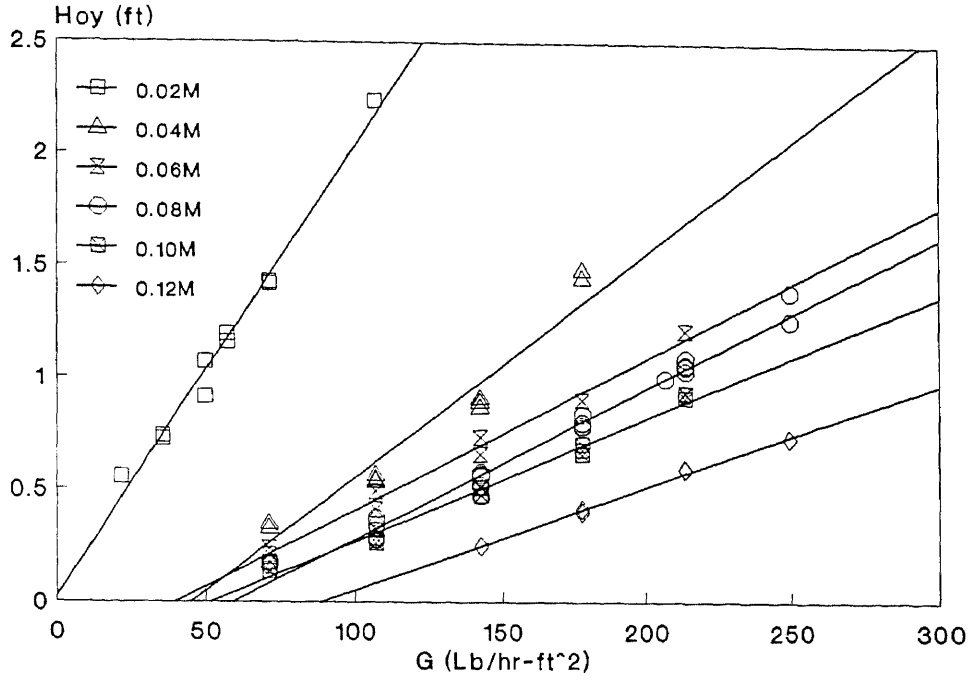

Figure 7.8 The effect of $NaClO_2$ concentration on HTU for NO oxidation at pH 8.2.

pH: 4.0, 5.4, and 8.2

Liquid rate: 300 to 800 cm^3/min

Figures 7.6, 7.7, and 7.8 show that regardless of pH, the higher the concentration of $NaClO_2$ the higher the efficiency, i.e. lower HTU for NO oxidation in a packed bed scrubbing.

Data in Figure 7.9 show the effect of $NaClO_2$ concentration on K_ya. These results were obtained from Figures 7.6, 7.7, and 7.8. These results show how high concentration of $NaClO_2$ enhances oxidation of NO, while high pH inhibits it. The relationship of K_ya and concentration is linear. A mathematic correlation of K_ya as a function of concentration and pH can be easily derived. These data are needed for pilot plant design and scale-up. It should be noted that due to the pressure drop and flooding limitations, this system is only capable to operate under 40 dm^3 per minute (280 lb/ft^2-hr) in gas flow and

800 ml per minute (4800 lb/ft^2-hr) in liquid flow. Therefore, any substantial extrapolation of gas flow must be checked experimentally.

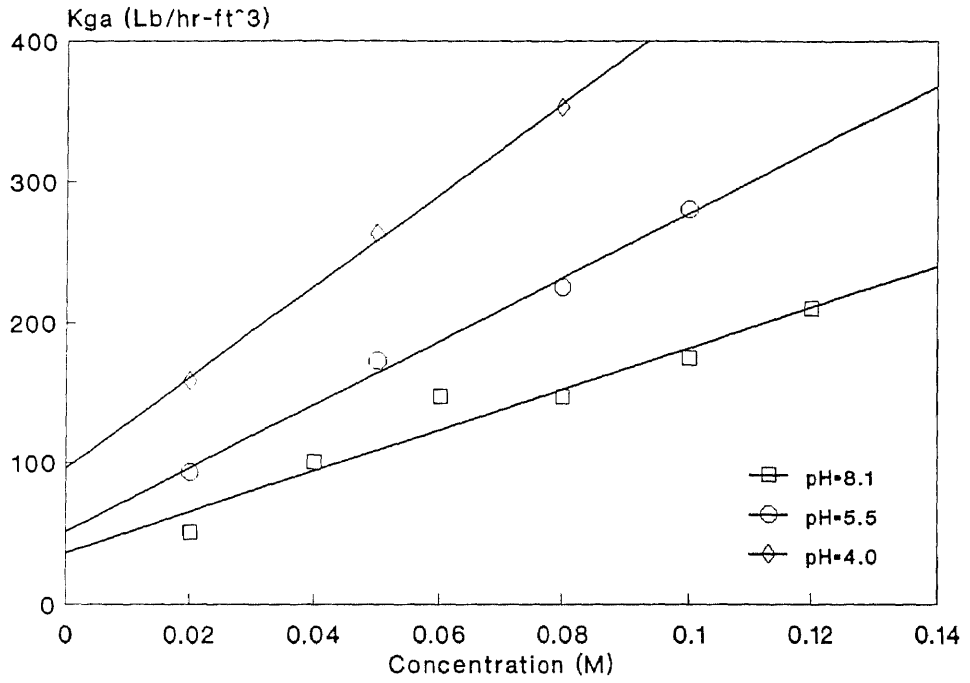

Figure 7.9 The concentration effect of $NaClO_2$ on overall mass transfer coefficient.

7.6 The Effect of SO_2 on HTU for NO Oxidation

A typical flue gas contains CO, CO_2, H_2O, O_2, SO_2, SO_3, VOCs, NO_x and N_2. The composition of different flue gases from the combustion of coal, oil and gas is shown in Table 7.2. Effects of O_2 and NO_2 on NO oxidation and absorption have been reported in a previous study [Yang, 1990]. CO_2 is considered as an inert gas in the scrubbing system, especially in acid solution.

The effect of SO_2 on NO oxidation and absorption in $NaClO_2$ aqueous scrubbing was studied extensively and is reported in this section. HTU for NO oxidation was used to measure the effect of SO_2. At pH 4.0, 7.9 and 10.3, NO oxidation was studied as a function of $NaClO_2$ concentrations and gas flow rate with and without SO_2 injection.

Experiments were conducted at room temperature and ambient pressure at the following conditions:

Scrubber: 5 cm ID by 10 cm packed bed with 0.64 cm ceramic Raschig rings

Flue gas: 300 ppm NO in N_2

Flow rate: 3 to 35 dm^3/min

Scrubbing Solution: 0.02, 0.03, 0.04, 005, 008, and 0.12M $NaClO_2$

pH: 4.0, 7.9, and 10.3

Liquid rate: 300 to 800 cm^3/min

Table 7.2 Typical Compositions of Flue Gases

	Volume % Combustion of		
Component	Coal	Oil	Gas
N_2	76.2	77.0	72.3
CO_2	14.2	12.0	9.1
H_2O	6.0	8.0	16.8
O_2	3.3	3.0	1.8
SO_2	0.2	0.15	--
NO_x	------- 0.01 to 0.15% -------		
Particulate (g/ft^3)	0.5(a)	0.01	--

(a) Assumes 90% particulate removal

Figures 7.10, and 7.11 present HTU data for NO oxidation with and without SO_2 injection at pH 4.0, and 7.9, respectively.

Figure 7.10 shows that SO_2 actually enhances the reaction of NO and $NaClO_2$ solution under acid condition. At various $NaClO_2$ concentrations, HTU decreases with 300 ppm SO_2 injection. Figure 7.11 shows that at pH 7.9, which is slightly alkaline, HTU increases with injection of 300 ppm SO_2.

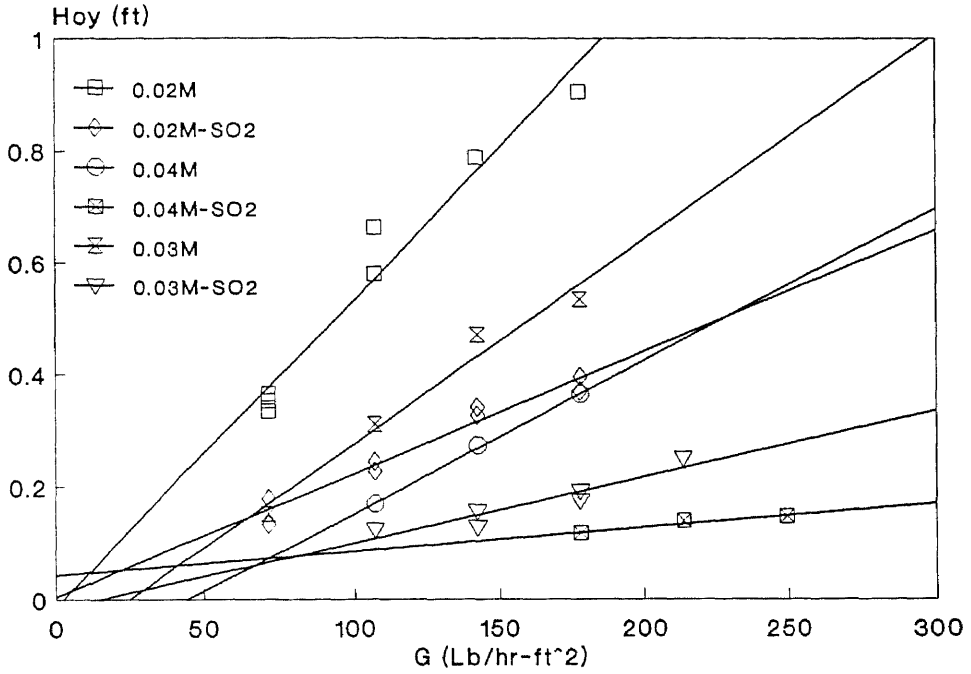

Figure 7.10 The effect of SO_2 on HTU for NO oxidation at pH 4.0

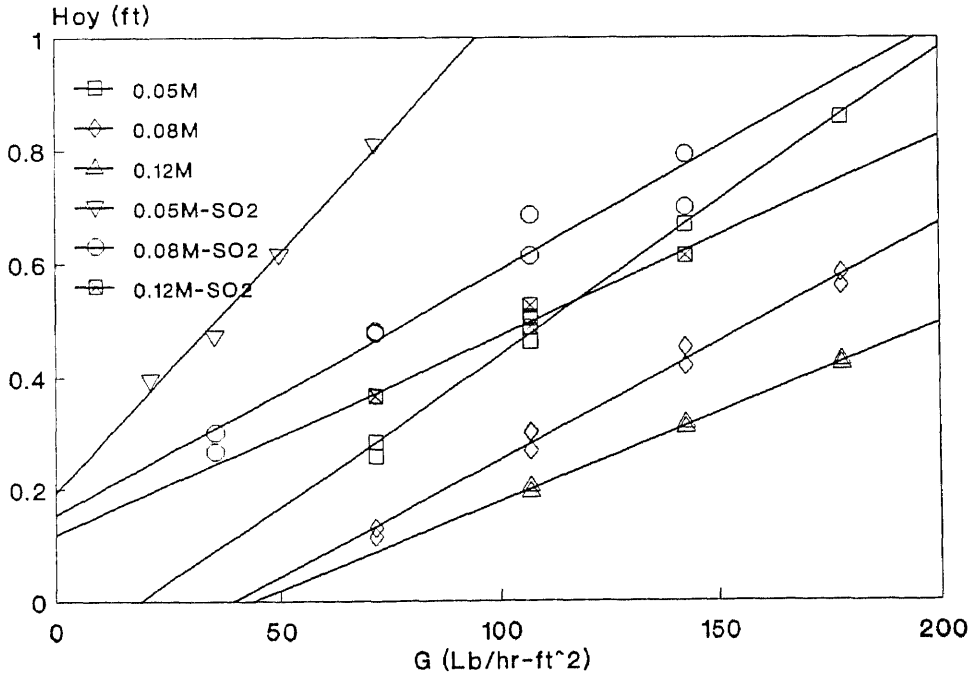

Figure 7.11 The effect of SO_2 on HTU for NO oxidation at pH 7.9

The measured HTU values for NO oxidation at different pH are summarized in Figure 7.12. Arrows indicate the direction of the effect of SO_2 on NO oxidation. Efficiency decreases with SO_2 injection at pH 7.9. In terms of HTU for NO oxidation, H_{oy} increases with SO_2 in alkaline scrubbing. In the scrubbing system, ClO_2 is the actual oxidizing agent, as indicated previously. When dissolved in water, SO_2 reacts with ClO_2 to form sulfates. In waste water treatment, this reaction is called dechlorination [White, 1986]. SO_2 consumes all of the ClO_2 in the water, and thus the disinfecting ability of ClO_2 in water treatment and NO removal in gas scrubbing is lost.

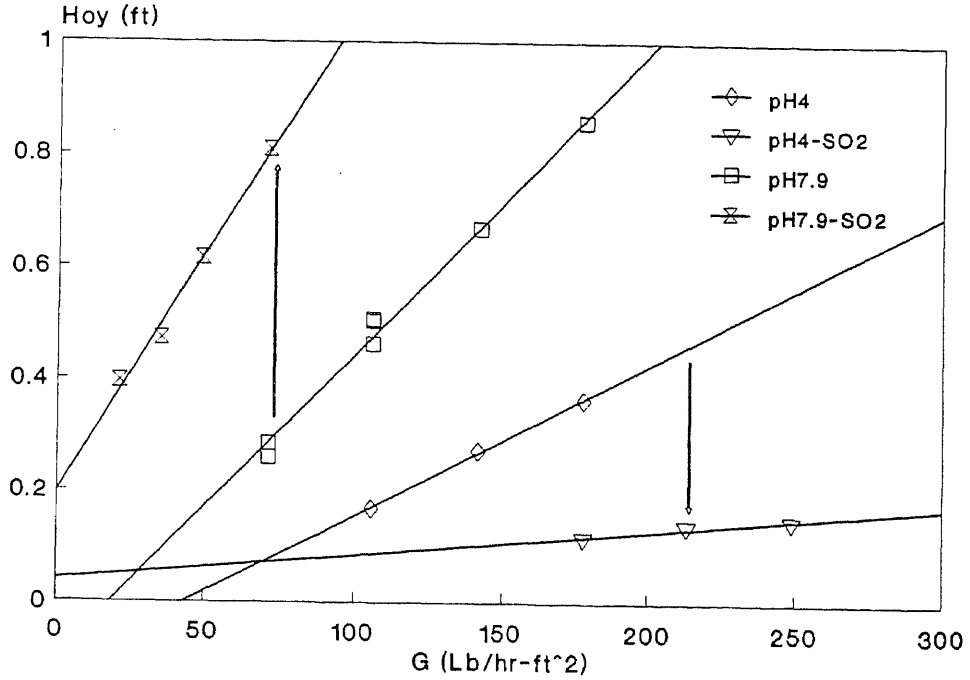

Figure 7.12 A comparison of the effect of SO_2 on HTU for NO oxidation in $NaClO_2$ alkaline and acidic scrubbing.

7.7 The HTU for NO_2 Absorption and NO_2 Absorption with Oxidation

NO_2 breakthrough was found in every scrubbing system tested, except for the NO absorption with $NaClO_2$ oxidation in a bubble column. To prevent breakthrough of NO_2, the HTU for NO_2 absorption, and absorption with oxidation, as defined in Section 7-2

were investigated. This research is designed to provide quantitative information for controlling both NO and NO_2 in one scrubber. Design considerations for a secondary caustic scrubber for NO_2 removal are expressed in terms of HTU for NO_2 absorption.

The absorption of NO_2 in NaOH aqueous solution was used to get data on HTU for NO_2 absorption. $NaClO_2$ aqueous solutions were prepared for the evaluation of HTU for NO_2 absorption with oxidation. Experiments were conducted at room temperature and ambient pressure under the following conditions:

Scrubber: 5 cm ID by 38 cm or 43 cm long packed bed with 0.64 cm ceramic Raschig rings

Flue gas: 300 ppm NO_2 in N_2

Flow rate: 3 to 20 dm^3/min

Scrubbing solution: 0 or 0.08M $NaClO_2$

pH: 4.0, 5.6, 7.9, and 10.4 (with HCl and NaOH)

Liquid rate: 300 to 800 cm^3/min.

HTU data for NO_2 absorption and absorption with oxidation are given in Figure 7.13. Absorption of NO_2, an acid gas, in NaOH aqueous solution is the absorption induced by neutralization. Oxidation provides a stronger driving force than neutralization for NO_2 absorption. The high HTU for NO_2 absorption confirms the low solubility of NO_2 in acidic solution.

7.8 The HTU for NO Absorption with Oxidation

An optimal design for NO_x control could encompass an acid prescrubber for NO control and a caustic main scrubber for SO_2 and NO_2 control. If a single scrubber control system were to be used, then the design would be based on the HTU for NO absorption with oxidation. According to the definition in Section 7.2, HTU for NO absorption with oxidation is calculated from the disappearance from the gas phase of NO_x instead of NO.

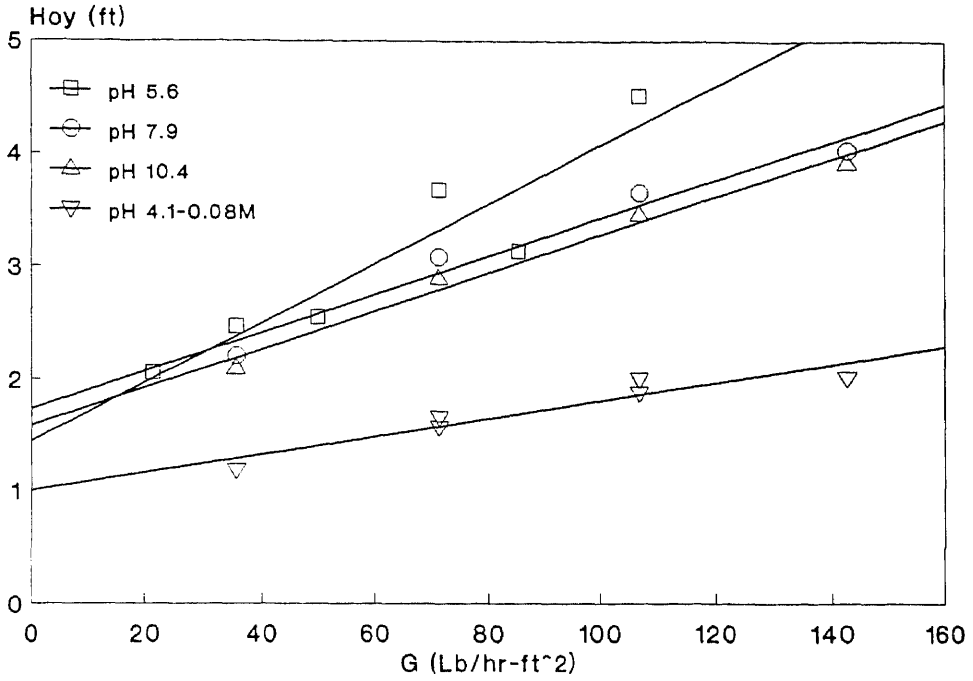

Figure 7.13 Heights of a transfer unit for NO_2 absorption and absorption with oxidation in NaOH and $NaClO_2$ aqueous solution with 0.64 cm ceramic Raschig rings.

Experiments are conducted at room temperature and ambient pressure under the following conditions:

Scrubber: 5 cm ID by 43 cm length packed bed with 0.64 ceramic Raschig rings

Flue gas: 300 ppm NO in N_2

Flow rate: 5 to 20 dm^3/min

Scrubbing solution: 0.04, 0.08, 0.12M $NaClO_2$

pH: 4.1, 6.2 and 10.3

Liquid rate: 300 to 800 cm^3/min

For gas mass flow rate up to 150 lb/hr-ft^2, data for HTU for NO absorption with oxidation are given in Figures 7.14, 7.15 and 7.16.

In both acidic cases, values of H_{oy} are between one and two feet which is the same to the HTU for NO_2 absorption with reaction in the previous section. HTU for NO oxidation is always very small compare to HTU for absorption. In the first few cm of a packed bed,

all NO has been oxidized to NO_2. The rest of the packed bed is needed to carry out the absorption of NO_2 with $NaClO_2$ oxidation. At pH 10, NaOH inhibits the reaction of NO to NO_2. Since the absorption of NO_2 is the rate limiting step, the values of HTU are still between one and two feet. But when SO_2 is present in the flue gas, dechlorination occurs in the scrubbing system, and the HTU for NO absorption with oxidation increases to 6.5 ft. Such a high HTU is considered not economically feasible.

Since the rate limiting step is the absorption of NO_2, and absorption of NO_2, induced by neutralization, is slower than oxidation, the only reason to go for a secondary caustic scrubber is economic.

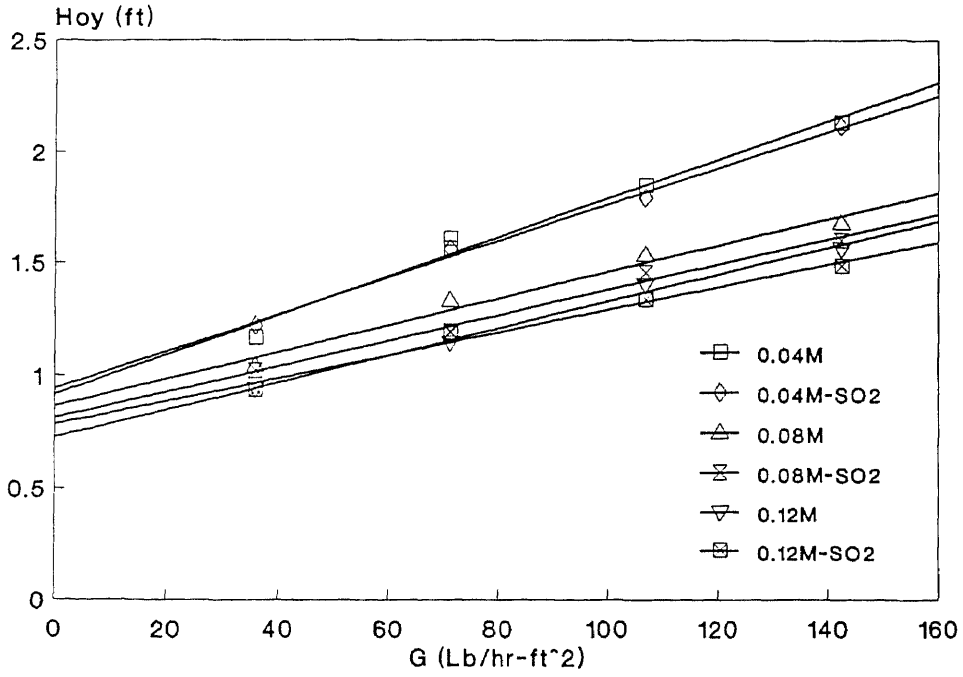

Figure 7.14 HTU for NO absorption with $NaClO_2$ oxidation at pH 4.1

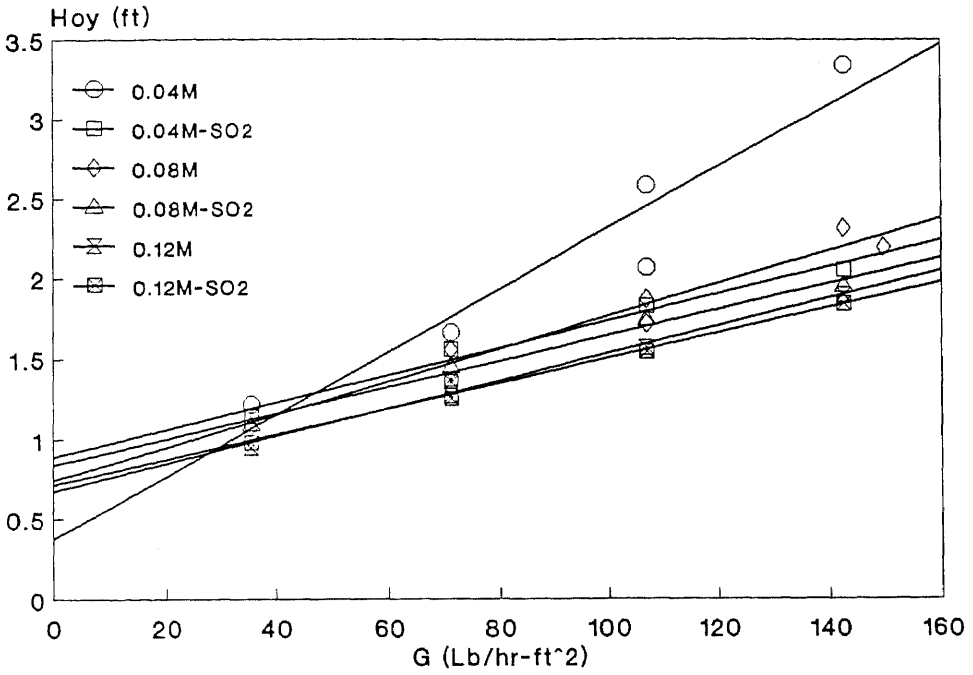

Figure 7.15 HTU for NO absorption with $NaClO_2$ oxidation at pH 6.2

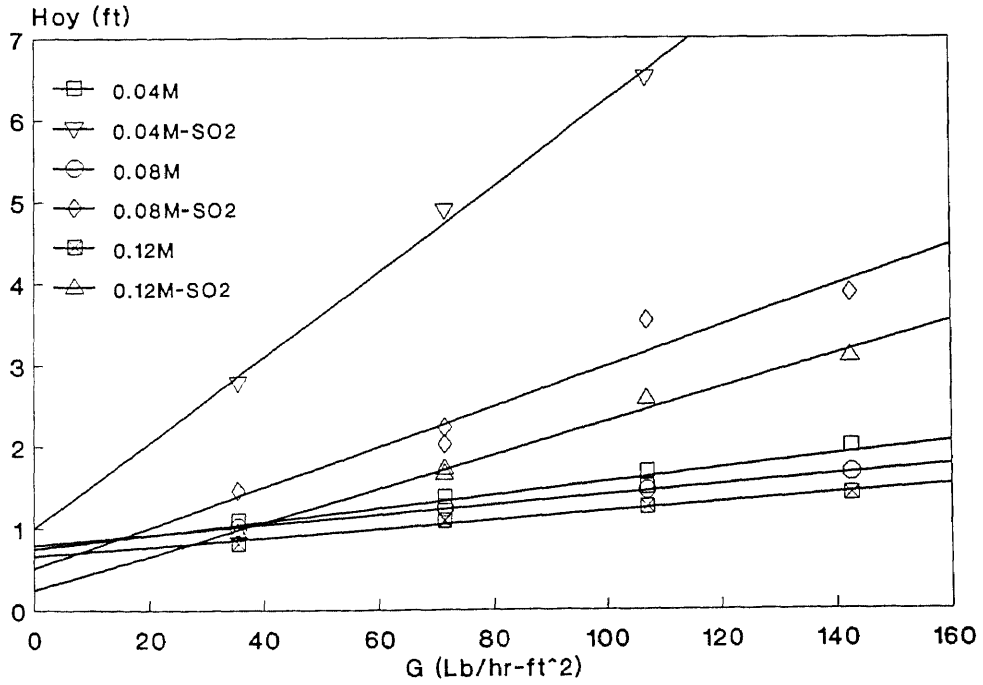

Figure 7.16 HTU for NO absorption with $NaClO_2$ oxidation at pH 10.3

7.9 HTUs for NO_x Aqueous Scrubbing

For pilot plant design and scale-up study, it is important to define the rate limiting step in this system. Using the definitions from previous sections HTU for NO oxidation, NO absorption with oxidation, NO_2 absorption, and NO_2 absorption with oxidation are depicted together in Figures 7.17 and 7.18 for pH 4.1 and 10.3, respectively. Figure 7.17 shows that up to 300 lb/hr-ft^2, HTU for NO oxidation is less than 0.5 ft. HTU for NO absorption with oxidation and HTU for NO_2 absorption with oxidation are identically between 1 to 3.5 ft. Absorption of low concentration NO_2 in acidic solution is very slow. Figure 7.18 shows similar result to Figure 7.17 except that with SO_2 in the gas stream, the absorption of NO with $NaClO_2$ oxidation at pH 10.3 is not feasible.

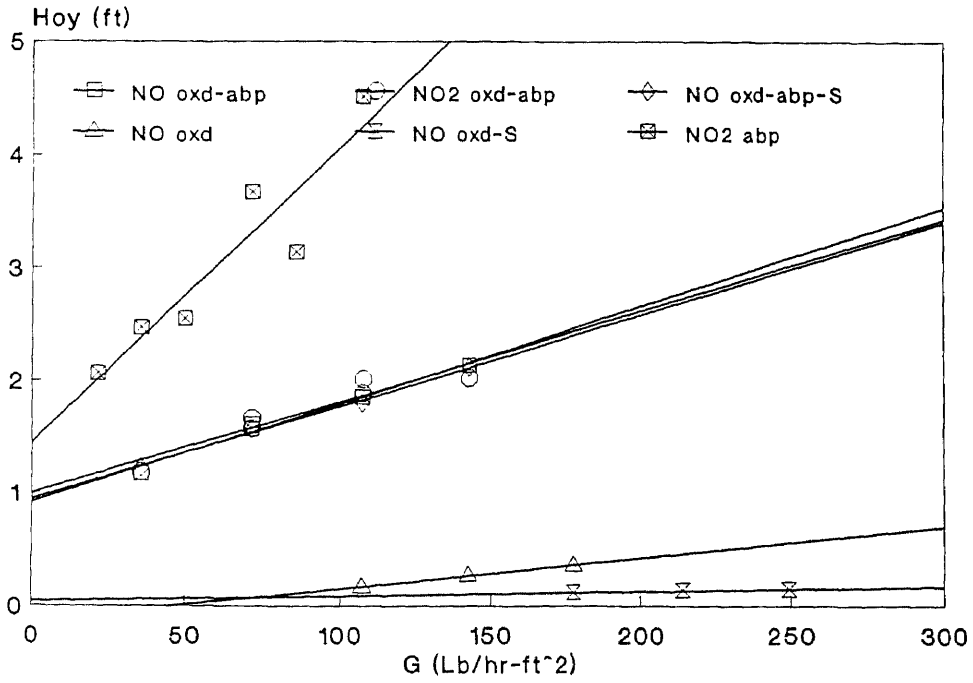

Figure 7.17 HTUs for NO_x aqueous scrubbing at pH 4.1

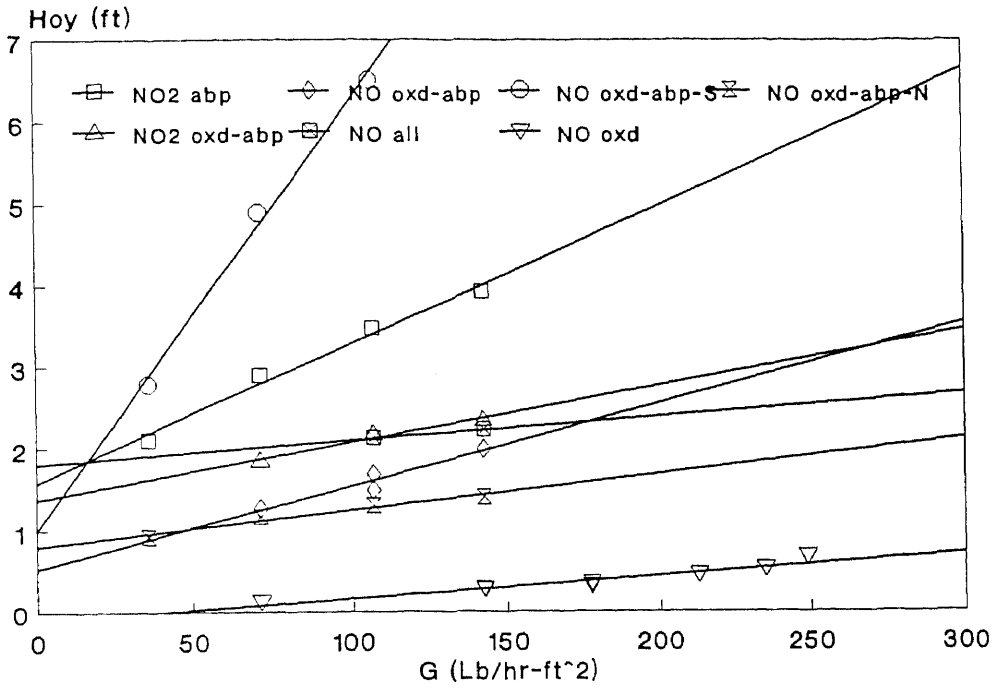

Figure 7.18 HTUs for NO_X aqueous scrubbing at pH 10.3

CHAPTER 8

DISCUSSION

A semibatch reactor was used to evaluate oxidation and absorption of NO with Cl_2, NaClO, and $NaClO_2$ in aqueous scrubbing solution. Synthetic flue gas was blended from compressed gas cylinders through rotameters into a manifold. The flow from the manifold continuously fed through rotameter to the scrubbing solution which was the stationary phase in the scrubber. The flue gas was introduced into the bubble column through a polyethylene sparger located at the bottom of the scrubber. Thus, the bubble size is influenced by sparger openings, and the viscosity of the scrubbing solution.

When Cl_2 and NO were injected into distilled water or NaOH scrubbing media, only 50% of the incoming amount of NO was absorbed within the first 30 minutes. It appeared that an intermediate, HClO, is formed during the first hour. To evaluate this effect, another series of experiments were performed by pretreating the scrubbing solution with chlorine for one hour before the NO is introduced. In this case, steady state absorption of over 80% is quickly established in nitric acid at pH 2.7. Tamony and Youngson [1981] pointed out that starting with hypochlorite in the scrubber is required to effectively use chlorine for NO_x control.

When using commercial bleach, where the active ingredients exist as 5 w% NaClO, it was found that when the pH of the solution dropped to 6 or lower, more than 90% of the active ingredient is converted to HClO. It is well known that HClO is a very active oxidizing compound. When the pH drops below 2, dissolved Cl_2 becomes the predominant oxidant. The results show that 40% conversion of NO is reached when the pH of the scrubbing solution is lower than 3, and 90% conversion of NO is achieved when pH is increased to between 3 and 6. Conversion of NO decreases from 89% to 9%, when pH is increased from 7 to 12. The pH affects the fraction of Cl_2, HClO and NaClO in

solution, while the fraction of HClO affects the oxidation reaction rate. When the operating temperature is increased to 60 ^{o}C, the absorption rate improved, but it appears that some ClO or ClO_2 may have been stripped from the solution. This observation is based on the increase in the order of these compounds.

In both NaClO and chlorine scrubbing systems, NO_2 breakthrough were found in the effluent. Water, when treated with chlorine, results in pH dropping from 6.5 to 2.7 in one hour. NO is oxidized to NO_2 on the interfacial film. With the high concentration in the film, NO_2 diffuses into both gas and liquid streams. In the solution, NO_2 is further oxidized to NO_3^-. In the gas phase, NO_2 is eluted and measured with the NO_x chemiluminescent analyzer. Because of its low solubility, NO_2 breakthrough may as high as 60% of incoming NO concentration.

The absorption of NO by an aqueous solution of alkaline $NaClO_2$ was accomplished at room temperature and atmospheric pressure. A greenish yellow color in the solution was found after three minutes of operation and disappeared right before NO breakthrough. The color represents an intermediate in the absorption of NO. The intermediate was identified as ClO_2. The mole ratio of the amount of NO that flowed through the scrubber to $NaClO_2$ is 0.95 at breakthrough. It should be emphasized that 80 w% $NaClO_2$ was used with the rest of the starting material in solution consisting of 18 w% Na_2CO_3 and 2 w% Na_2SO_4. Thus, the initial composition of the scrubbing solution was quite alkaline. Under all conditions when $NaClO_2$ was present, the other two reagents were also present.

Low concentrations of NaOH, provided there is sufficient $NaClO_2$, does not inhibit NO removal effectiveness. High concentrations of NaOH inhibit the absorption. The upper limit for NaOH concentration necessary to completely absorb NO in $NaClO_2$ aqueous solution depends on the concentration of $NaClO_2$. NO is absorbed quantitatively in 0.008 molar $NaClO_2$ aqueous solution when the concentration of NaOH is equal to, or lower than, 0.001 molar. The upper limit of NaOH in 0.08 molar $NaClO_2$ aqueous solution is 0.1 molar. At the upper limit concentration of NaOH, absorption can not reach 100%

within the first few minutes. If the NaOH concentration is a little higher than the upper limit, absorption goes to zero after a few minutes of running time. The inhibiting effect is due to high pH rather than specifically to NaOH.

The addition of NaOH to $NaClO_2$ in an aqueous solution allows the NO to $NaClO_2$ reactant ratio at breakthrough to approach unity (0.96 to 1.05), while 5% oxygen in the flue gas decreases this ratio to 0.84. Before saturation, concentration-time curves are straight lines with different slopes. The slope of NO_3^- is greater than that of Cl^-. Thus, the rate of formation of NO_3^- is faster than that of Cl^-. The time between their formation is the life time of ClO_2, the green intermediate.

The pH of the aqueous solution drops drastically from 10 to 3 within the first ten minutes. The solution was prepared with 0.008 molar of $NaClO_2$ and 0.0015 molar of Na_2CO_3 due to the 18% w% and 2 w% Na_2SO_4 impurity. The pH of this solution is 10. After three minutes running, the reaction was carried out under acidic condition.

After the $NaClO_2$ in the scrubbing solution is used up, only two products are found in the scrubbing solution, viz., NO_3^- and Cl^-. CO_3^{-2} is converted to H_2CO_3 when pH falls below 3. Under conditions of Waters ion chromatography method # A-102, bicarbonate is found at retention time of 3 minutes.

Without pH control, The utilization of $NaClO_2$ can be reduced from 110% to 80%. Utilization losses simply due to the formation of Cl^-. With SO_2 in gas stream, sulfur dioxide competes with NO to consume $NaClO_2$ in the scrubbing solution. In the scrubbing solution, NaOH inhibits the reaction rate but increases the utilization of $NaClO_2$ for NO absorption.

Salt bed adsorption provides an alternative for flue gas NO_x control. Efficiency, without optimization, can reach more than 80% of NO_x removal. The other 20% breakthrough from the bed is NO_2 which can be easily removed by NaOH aqueous scrubbing. Advantage of this process is that instead of producing 2.5 dm^3 waste water, 3

grams solid waste of a mixture of NaCl and $NaNO_3$ is produced. Further investigation is needed for scale-up and optimize.

Hypochlorous acid is found to be the active intermediate in both chlorine and sodium hypochlorite systems, while chlorine dioxide is the key oxidant for the sodium chlorite process.

Spectra of solutions of chlorine and oxychlorine compounds were obtained with a photodiode array detector (PDA) system. Except for Cl^- which has maximum absorbance in the cut off range, 190 nm, and Cl_2 which has relative low extinction coefficient at 330 nm, the other oxychlorine compounds were measured with great accuracy. It was found that HClO can be quantified by its absorbance at 238 nm, ClO^- at 293 nm, ClO_2^- at 258 nm, and ClO_2 at 358 nm.

Absorbance versus concentration curves were found to be linear when concentration was kept low enough so as not to exceed 2 absorbance units. To extend the range of oxychlorine compounds to higher concentrations, such as were used in the scrubbing work, the eluent pumping system of the prep. LC. was used to dilute the inlet sample. However, such samples were not pumped back into the process. The mixing did not cause any disturbance, if the flow rate was kept below 3 cm^3/min.

For free available chlorine measurements, the pH of incoming sample was controlled at 10.5 with a borax buffer solution that was mixed into the eluent pumping system of the prep. LC. As a function of pH, free available chlorine can be quantified by measuring the ClO^- at 293 nm.

For pH control, the background scan i.e., water or buffer solution without any oxychloride compounds, must be carefully determined by sending the buffer solution into the PDA system. If the background scan had an absorbance at 230 nm lower than 80% of full scale, sampling time would have to be adjusted to meet this criteria of increasing sampling time in order to increase the absorbance to at least 80% of full scale.

The reaction rate of $NaClO_2$ with HCl to produce ClO_2 is not instantaneous. When preparing a solution of ClO_2 for PDA calibration, it is recommended that a scan of the HCl solution be taken as background, and then run the titration with $NaClO_2$ aqueous solution.

The mathematical model for spray chamber scrubber was derived from the interfacial surface correlation in literature [Metha, 1970]. The result is no better than semiempirical correlation. Reaction rate of NO to NO_2 is proportional to interfacial surface area and concentration of sodium chlorite. The model can be used to predict NO conversion in a spray chamber. A model for simultaneous NO_2 absorption is required to develop the spray chamber for single unit NO_x (NO and NO_2) control.

Both zero order and first order models fit experimental data quite well. In the first order model, model predictions are found to be always lower than experimental values at high liquid to gas ratio (L/G) and higher than experimental values at low L/G ratio. A zero order model is believed to occur in the system for its random deviation. If it is true, interfacial surface area is the rate limiting step of NO oxidation by $NaClO_2$ in aqueous scrubbing.

A packed tower was used to confirm the experimental results from bubble column scrubber and derive design parameters for scale-up study. Channeling was avoided by using 0.64 cm ceramic Raschig rings to pack the 5 cm diameter tower. Generally, it is desirable to use a liquid mass velocity of at least 1.1 kg/m^2-s (800 lb/ft^2-h) based on the empty cross section of the tower. Through the study more than 1000 lb/ft^2-h were used to reduce the dry packing surface. Since experimental values on both flooding and liquid holdup were in good agreement with the theoretical values, it is assumed that other column characteristics also agree with theoretical values.

In the diagram of pH vs. $NaClO_2$ concentrations, there are lines of 100% NO removal and ClO_2 formation. The area between these two lines is defined as the operating window. Within the operating window, the system can be operated at 100% NO removal without

ClO_2 being stripped out. Relative concentration of ClO_2 is a weak function of $NaClO_2$ concentration while NO removal is a strong function of both $NaClO_2$ concentration and pH. The line for 100% NO removal may shifts up or down by changing L/G ratio, type of absorber or packing.

Theoretically, height of a transfer unit (HTU) is a function of gas phase mass velocity only. The statement is true only in dilute system and both K_y and a, the interfacial area per unit packed volume, are constants. For certain packing, dry packing surface area are always constants but the effective interfacial area depends on liquid phase mass velocity. At low liquid rates, the effective interface area may be as low as 30% of the dry packing surface. According to experimental results, the critical liquid rate is 1800 lb/hr-ft^2 in this system.

When switching to a packed bed scrubber, the breakthrough of NO_2 is always found, therefore four types of height of a transfer unit were defined in this research. HTU for NO oxidation is used to design a packed bed as a prescrubber to produce a fixed ratio of NO/NO_2 for the main scrubber. HTU for NO oxidation and absorption provides information to collect all kinds of pollutants in one scrubber. HTU for NO_2 absorption is used to design a main scrubber for NO_2 removal and HTU for NO_2 absorption with oxidation shows the effect of oxidizing agent on NO_2 absorption. The absorption of a mixture of NO and NO_2 was discussed in a previous study [Yang, 1990].

In terms of HTU for NO oxidation, the inhibition of NaOH can be quantified. When pH changes from 4.0 to 8.2, HTU for NO oxidation increases from 0.3 ft to 1.1 ft at gas phase mass velocity of 175 lb/hr-ft^2.

HTU for NO oxidation increases drastically due to the consumption of the active oxidants, ClO_2, in caustic scrubbing by sulfur dioxide [White, 1986]. In slightly acidic solution, SO_2 promotes the formation of ClO_2 and has a different effect on HTU for NO oxidation. Since NO can not be converted to NO_2 in a caustic scrubbing in the presence of SO_2, usually more than 90% of incoming NO breakthrough. Under this condition, the

system is totally useless for NO_x removal. In an acidic scrubbing system, HTU for NO oxidation is enhanced by the existence of SO_2 but not HTU for NO oxidation and absorption. In the process of NO oxidation and absorption, NO_2 absorption is the rate limiting step. Since SO_2 only enhance the NO oxidation, the HTU for NO oxidation and absorption is not affected.

CHAPTER 9

CONCLUSIONS AND RECOMMENDATIONS

9.1 Conclusions

Research was conducted to evaluate the ability of Cl_2, NaClO, and $NaClO_2$ in aqueous nitric acid solution to scrub NO by oxidizing it from synthetic flue gas. In some runs, NO_2, O_2 or SO_2 were mixed into the synthetic flue gas to simulate the flue gas emitted by municipal incinerators or stationary power plants. The conclusions from this investigation are summarized in this section.

An aqueous solution of chlorine can be used to oxidize and absorb NO from flue gas. More than 80% of NO conversion is achieved. Most of the NO is oxidized to NO_2. An alkaline scrubber would be needed to remove the NO_2.

Within pH 3 to 6, sodium hypochlorite is a good scrubbing medium. More than 90% of NO conversion is achieved. These results are consistent with HClO being the oxidizing agent in solution.

NO can be quantitatively oxidized by $NaClO_2$ in aqueous solution. During scrubbing, NO is oxidized to NO_3^-, and ClO_2^- is converted to Cl^-.

NaOH inhibits the NO oxidation but enhances the utilization of $NaClO_2$ for NO removal to more than 100%.

Due to the formation of HNO_3, NO enhances the production of ClO_2 in the scrubbing solution and accelerates its absorption. If the production of HNO_3 can not compensate NaOH in the scrubbing solution, absorption goes to zero.

Rates of Cl^- and NO_3^- formation in scrubbing solution are constants at the low concentration scrubbing process as the concentration of $NaClO_2$ changes from 0.008 molar to 0 molar.

Utilization decreases from 0.95 to 0.84 when 5% O_2 in present in the flue gas.

The existence of SO_2 increases the reaction rate of NO to NO_2 in acidic solution but decreases that in alkaline solution.

Increasing temperatures from 20 to 60 ^oC, slightly enhances the reaction rate of NO to NO_2 in both NaClO and $NaClO_2$ systems.

HTU for NO oxidation, HTU for NO oxidation and absorption, HTU for NO_2 absorption and HTU for NO_2 absorption with oxidation are linear functions to gas phase mass velocity in the range of 30 to 250 lb/hr-ft^2.

9.2 Recommendations for Future Work

The results from this research clearly indicate the utility of oxygen chlorine chemistry for NO_x emission control. The best conditions for chemical reaction of NO_x with these oxidizing agents and aqueous solution are reached as indicated in this thesis. Scale-up parameters in terms of HTUs are presented extensively in previous sections. However, some critical factors which need to be studied are listed below:

Effect of CO_2 on NO absorption in $NaClO_2$ aqueous scrubbing.

HTUs for NaClO scrubbing system.

A test in a two unit scrubbing process, oxidation prescrubber and caustic main scrubber.

An appropriate treatment method for the spent scrubbing solution.

REFERENCES

Anderson, I. C. and J. S. Levine, "Biogenic Production of Nitrogen Oxides," *Eos. Trans. Am. Geophys. Un.* 64, 195. 1983.

Andrew, S. P. S., and D. Hanson, *Chem. Eng. Sci.*, 14, 105, 1961.

Armor, J. N., *J. Chem. Eng. Data.*, 19, 82, 1974.

Baveja, K. K., D. Subba Rao, and M. K. Sarkar, *J. Chem. Eng. Japan*, 12, 322, 1979.

Beattie, I. R., *Dinitrogen Trioxide in Preogree in Inorganic Chemistry, Vol. 5*, Wiley, New York, 1963.

Bethea, R. M. *Air Pollution Control Technology*, Van Nostrand Reinhold, 1978.

Bhatia, S. C., J. H. Jr. Hall, *J. Phys. Chem.*, 84(24), 3255, 1980.

Bienstock, D. "Control of NO_X Emission in Coal Firing," Industrial Coal Conference, Purdue University, Oct., 1972.

Borders, R. A., "A Direct Determination of the Activation Energy for the Reaction of Nitric Oxide with Ozone," Univ. Microfilms Int., Order No. DA 8203409, Diss. Abstr. Int., B 42(9), 3674, 1982.

Bronsted, J. N., *Z. Phys. Chem.*, 102, 169, 1922.

Calvert, Jack G., James N. Pitts, Jr., *Photochemistry*, John Wiley and Sons, 1966.

Chang, S. G. "A Ferrous Cysteine Based Recyclable Process for the Combined Removal of NO_X and SO_2 from Flue Gas" *Environ. Sci. Technol.* Vol. 22, No. 2, 1988.

Chapman, S. "A Theory of Upper-Atmosphere Ozone," *Roy. Metero. Soc.*, 3, 103-125, 1930.

Charlson, R. J., and H. Rodhe, "Factors Controlling the Acidity of Nature Rainwater," *Nature*, 295, 683-685, 1982.

Chemical Week. "Electron Guns Clean Up SO_2 and NO_X," 133(21), November 23, 1983.

Cichanowicz, E., "Selective Catalytic Reduction Controls NO_X in Europe," *Power Engineering*, Aug. 1988.

REFERENCES
(Continued)

Colannino, Joseph "Low Cost Techniques Reduce Boiler NO_X," *Chemical Engineering*, Feb., 1993.

Cooper, C. David, and F. C. Alley, *Air Pollution Control- A Design Approach*, Waveland Press, 1986.

Cowling, E. B. "Acid Precipitation in Historical Perspective," *Environ. Sci. Technol.*, 16, 110A-123A, 1982.

Crawford, A. R., et. al. "Field Testing: Application of Combustion Modifications to Power Generating Combustion Sources," EPA-600/7-77-073b. Washington, D.C.: US. Environmental Protection Agency, 1977.

Danckwerts, P. V., *Gas-Liquid Reactions*, McGraw-Hill, New York, 1970.

Davenport, Gerald B. "Understand the Air Pollution Laws That Affect CPI Plants," *Chemical Engineering Progress*, Vol. 88, No. 4, April, 1992

Enger, Eldon D., Bradley F. Smith, "*Environmental Science: A Study of Interrelationships*," 4th ed. Wm. C. Brown Publishers, 1991.

Fenimore, C. P. "Formation of Nitric Oxide in Premixed Hydrocarbon Flames," 13th International Symposium on Combustion. Pittsburgh, PA, The Combustion Institute, 1971.

Fusselman, Deborah, Dan Lipsher, "Several Technologies Available to Cut Refinery NO_X," *Oil and Gas Journal*, Nov. 2, 1992.

Galbally, I. E. and C. R. Roy, "Loss of Fixed Nitrogen from Soils by NO Exhalation" *Nature*, Lond. 275, 734-735. 1978.

Galloway, J. N., et. al. "The Composition of Precipitation in Remote Areas of the World," *J. Geophys. Res.*, 87, 8771-8786, 1982.

Garedel, T. E., L. A. Farrow, and T. A. Weber, *Int. J. Chem. Kinetics Symposium*, 1, 581, 1975.

Gorham, E., et. al. "Acid Rain: Ionic Correlation in the Eastern United States, 1980-1981," *Science*, 225, 407-409, 1984.

Greenberg, Arnold E. editor, *Standard Methods for The Examination of Water and wastewater*, 18th edition, American Public Health Association, 1992.

REFERENCES
(Continued)

Haines, Terry A. "Fish Population Trends in Response to Surface Water Acidification," Chapter 8, *Acid Deposition: Long-term Trends*, National Academy Press, 1986.

Handbook of Chemistry and Physics, The Chemical Rubber Publishing Co., Clevland, 44th Ed., p2234, 1963.

Hanwant B. Singh "Reactive Nitrogen in The Troposphere," *Environ. Sci. Technol.*, Vol. 21, NO 4, 1987.

Harcourt, R.T., *J. Mol. Struct.*, 11(1), 1, 1972.

Hayashi, S., and T. Yamada, "Removal of Nitric Oxide from Refuse Incinerating Gas," *Japan Kokai*: 76, 57, 675(Cl. B01 D53/34), 20 may, 1976, CA-85: P181759c, 1976.

Hixson, Eric M. "Removal of Nitric Oxide from Gas Stream via Direct Chlorine Injection," AFRC Int'l Symposium, 1990.

Hollowell, David A. "Selective Chlorine Dioxide Determination Using Gas Diffusion Flow Injection Analysis With Chemiluminescent Detection," *Analytical Chemistry,* Vol. 58, No. 7, 1986.

International Critical Tables, E. W. Washburn (Ed.), Vol. III, Mcgraw Hill, New York, p. 259, 1928.

Jahnig, C. E. and Henry Shaw, "A Comparative Assessment of Flue Gas Treatment Process Part I- Status and Design Basis," *APCA Journal*, Vol. 31, April 1981.

Jahnig, C. E. and Henry Shaw, "A Comparative Assessment of Flue Gas Treatment Process Part II- Environmental and Cost Comparison," *Journal of the Air Pollution Control Association*, Vol. 31, No. 5, May 1981.

JANAF Thermochemical Tables, 2 edition, US NBS NSRDS-37, 1971.

Johnson, Arthur H. and Samuel B. McLaughlin, "The Nature and Timing of the Deterioration of Red Spruce in the Northern Appalachian Mountains," Chapter 6, *Acid Deposition: Long Term Trends*, National Academy Press, 1986.

Johnston, H. S. "Pollution of the Stratosphere," *Ann. Rev. Phys. Chem.*, 26, 315-338, 1975.

Joint Army, Navy, Air Force Thermochemical Tables, Dow Company, PB-168370. Washington, D.C., US. Government, 1965.

REFERENCES
(Continued)

Jones, D. G. et. al. "Two Stage DeNO_X Process Test Data from Switzerland's Largest Incineration Plant," Presented at the NO_X Symposium, April 1989.

Joshi, J. B. et. al. "Invited Review Absorption of NO_X Gases," *Chemical Engineering Communication*, Vol. 33 pp. 1-92, 1985.

Kane, John T. Jr. "NO_X Rules in 1990 Clean Air Act Amendments: Implications on Coke Industry," *Iron and Steel Engineer*, Dec., 1992.

Kann, J., et. al., "Oxidation of Nitric Oxide by Potassium Permanganate," Tr. Tallin. Polytecch. Inst., 402, 65, 1976, CA-86: 176358n, 1977.

Komiyama, H., and H. Inoue, *Chem. Eng. Sci.*, 35, 154, 1980.

Kramer, James R., et. al. "Streams and Lakes," Chapter 7, *Acid Deposition: Long-term trends*, National Academy Press, 1986.

Kushiro, J., T. Yamada, T. Kita, "Nitrogen Oxide Removal from Waste Gas," *Japan Kakai*: 76, 45, 673(Cl. B01 D53/35)19 April 1976, CA-85: P165956j, 1976.

Kustin, K., L. A. Taub, and E. Weinstock, *Inorg. Chem.*, 5, 1079, 1966.

Ladhabhoy, M. E., and M. M. Sharma, *J. Appl. Chem.*, 19, 267, 1969.

Lahari, R.N., *Indian Chemical Engineer*, 23(4), 44, 1981.

Levenspiel, Octave, *Chemical Reaction Engineering*, 2nd edition, John Wiley and Sons, 1972.

Levine, Joel S. et. al. "Tropospheric Sources of NO_X: Lightning and Biology," *Atmospheric Environment* Vol. 18, No. 9, pp. 1797-1804, 1984.

Lim, K. J., et. al. "Environmental Assessment of Utility Boiler Combustion Modification NO_X Controls- Vol. I: Technical Results," EPA-600/7-80-075a. Washington, D.C.: US. Environmental Protection Agency, 1980.

Mackinnon, D. J. "Nitric Oxide Formation at High Temperatures," *Journal of Air Pollution Control Association*, 24(3), March, 1974.

McCabe, Warren, Julian Smith, and Peter Harriott, *Unit Operations of Chemical Engineering*, 4th ed, McGraw-Hill, 1985.

REFERENCES
(Continued)

Moore, T. "The Retrofit Challenge in NO_X Control," *Electric Power Research Institute Journal*, Nov. pp. 26-33, 1984.

Parkinson, G. "NO_X Controls: Many New Systems Undergo Trials," *Chemical Engineering*, March 9, pp. 39-43, 1981.

Perlmutter, H. D., H. Ao, and H, Shaw, "Absorption of NO Promoted by Strong Oxidizing Agents: Organic Tertiary Hydroperoxide on n-Hexadecane," *Environ. Sci. Technol.*, Vol. 27, No. 1, 1993.

Perry, R. H., and D. Green, *Chemical Engineers' Handbook*, 60th ed., McGraw Hill, New York, 1984.

Pershing, D. W. "Nitrogen Oxide Formation in Pulverized Coal Flames," Ph.D. Dissertation, University of Arizona, 1976.

Pershing, D. W., et. al. "Influence of Design Variables on The Production of Thermal and Fuel NO From Residual Oil and Coal Combustion," American Institute of Chemical Engineers Symposium Series, 148(71), 1975.

Rhoads, T. W. et. al. "Overview of Industrial Source Control for Nitrogen Oxides," *Environmental Progress*, Vol. 9, No. 2, May, 1990.

Rittenhouse, R. C. "Action Builds on 1990 Clean Air Act Compliance," *Power Engineering*, May, 1992.

Rittenhouse, R. C. "Action Builds on the Road to CAA Compliance (Part II)," *Power Engineering*, June, 1992.

Robinson, Steve "Hydrogen Peroxide: First Aid for Air Pollution," *The National Environmental Journal*, May/June, 1993.

Sada, E., H. Kumazawa, and M. A. Butt, *J. Chem. Eng. Data.*, 23, 161, 1978.

Sada, E., H. Kumazawa, N. Hayakawa, I. Kudo, and T. Kondo, *Chem. Eng. Sci.*, 32, 1171, 1977.

Sada, E., H. Kumazawa, T. Kudo, and T. Konda, Ind. Eng. Chem. proc. Des. Develop., 20, 46, 1981.

Sada, E, and H. Kamazawa, "Absorption of NO in Aqueous Mixed Solutions of $NaClO_2$ and NaOH," *Chemical Engineering Science*, Vol. 33, pp. 315-318, 1977.

REFERENCES
(Continued)

Sada, Eizo, et. al. "Absorption of Lean NO_X in Aqueous Solutions of $NaClO_2$ and NaOH," Ind. Eng. Chem. Process Des., Vol. 18, No. 2, 1979.

Schwartz, S. E., W. H. White, "Solubility Equilibria of the Nitrogen Oxides and Oxyacids in Dilute Aqueous Solutions," in Advances in Environmental Science and Engineering, Vol. 4, Pfafflin, J. R. and Zeigler, E. N. (Eds.),Gordon and Breach Science Publishers, New York, 1981.

Seidell, A., and W. F. Linke, "Solubility of Inorganic and Metal Organic Compounds," Vol. II, 4th ed., American Chemical Society, Washington, D.C., p. 790, 1228, 1965.

Seinfeld, John H., *Atmospheric Chemistry and Physics of Air Pollution,* John Wiley and Sons, 1986.

Shaw, Henry "Aqueous Solution Scrubbing for NO_X Control in Munitions Incineration," ASME winter annual meeting, 1977.

Shaw, Henry "The Effect of Water on Nitric Oxide Production in Gas Turbine Combustors," ASME Conference & Products Show, Houston, Texas, March 2-6, 1975.

Shaw, Henry "The Effect of Water, Pressure, and Equivalence Ratio on Nitric Oxide Production in Gas Turbines," *Journal of Engineering for Power*, July 1974.

Sommerlad, R. S., et. al. "Nitrogen Oxides Emission: An Analytical Evaluation of Test Data," 33rd. Annual Meeting. The American Power Conference, Chicago, IL. 1971.

Takahashi, S., et. al., "Oxidation of Nitrogen Monoxide in a Waste Gas," *Japan Kokai*: 79,37,095(Cl.C01 B21/36), 19 March 1979, CA-91: p78463b, 1979.

Takeuchi, H., K. Takahashi, and N. Kizawa, *Ind. Eng. Chem. Proc. Des. Develop.*, 16, 303, 1977.

Teramoto, M., M. Ikeda, and H. Teranishi, *Kagaku Kogaku Ronbunshu*, 2, 86, 1976.

Thompson, R. E. and M. W. McElroy, "Effectiveness of Gas Recirculation and Staged Combustion in Reducing NO_X in a 560 MW Coal Fired Boiler," *Electric Power Research Institute* FP-257, National Technical Information Service PB 260582, 1976.

Topol, L.E., K. B. Oldham, and R. G. Adler, *J. Inorg. Chem.*, 30(11), 2977, 1968.

REFERENCES
(Continued)

Tsai, S. S. et. al. "Field Evaluation of Nitric Oxide Abatement with Ferrous Chelates," *Environmental Progress* 8, 2, May 1989.

US. Environmental Protect Agency "Control Techniques for Nitrogen Oxide Emissions from Stationary Sources, revised 2nd ed." EPA-450/3-83-002. US. Environmental Protect Agency, Research Triangle Park, NC, 1983.

US. Environmental Protect Agency "National Air Pollution Emission Estimation, 1970-1981," EPA-450/4-82-012. US. Environmental Protect Agency, Research Triangle Park, NC, 1982.

US. Environmental Protection Agency "Control Techniques for Nitrogen Oxides Emission from Stationary Sources," revised 2nd ed. EPA-450/3-83-..2. US. EPA, Research Triangle Park, NC, 1983.

US. Environmental Protection Agency "Control Techniques for Nitrogen Oxide Emissions from Stationary Sources," Pub. AP-67. Washington, D.C., National Air Pollution Control Administration, 1970.

US. Environmental Protection Agency "National Air Pollution Emission Estimates, 1970-1981," EPA-450/4-82-012. US. EPA, Research Triangle Park, NC, 1982.

US. EPA Method 300.0 (Revision) "The Determination of Inorganic Anions in Water by Ion Chromatography," US. EPA, 1984.

Uchida, S., K. Kobayashi, and S. Kageyama, *Ind. Eng. Chem. Process Des. Develop.*,22, 323, 1983.

Vicard J. F., US. Patent #5063034, Nov. 5, 1991.

Waters Ion Analysis Method "Method #A-119 Oxyhalide Analysis Using IC-Pak A HC Column Borate/Gluconate Eluent,".

White, Geo. Clifford "*The Handbook of Chlorination*," 2nd ed., Van Nostrand Reinholh, 1986.

Yang, C. L., H. D. Perlmutter, H. Shaw, "Absorption of NO_X Induced by Strong Oxidants," International Conference on Hazardous Waste Management: Technology, Perception and Reality, The Diplomat Hotel, Atlantic City, New Jersey U.S.A., May 5-7, 1992.

REFERENCES
(Continued)

Yang, Chen-Lu "Aqueous Absorption of NO_X Induced by Sodium Chlorite Oxidation," Master Thesis, NJIT, 1990.